A NOVEL INTELLIGENT FATIGUE SENSOR FOR MONITORING THE HEALTH STATE OF STRUCTURAL MEMBERS

2019
Ph.D. THESIS
METALLURGICAL AND MATERIALS ENGINEERING

AHMED EL BAROUNI HADYIA

A NOVEL INTELLIGENT FATIGUE SENSOR FOR MONITORING THE HEALTH STATE OF STRUCTURAL MEMBERS

A THESIS SUBMITTED TO
THE GRADUATE SCHOOL OF NATURAL AND APPLIED SCIENCES OF KARABUK UNIVERSITY

BY

AHMED EL BAROUNI HADYIA

IN PARTIAL FULFILLMENT OF THE REQUIREMENTS FOR THE DEGREE OF DOCTOR OF PHILOSOPHY OF SCIENCE IN DEPARTMENT OF METALLURGICAL AND MATERIALS ENGINEERING

February 2019

I certify that in my opinion the thesis submitted by Ahmed El barouni HADYIA titled "A NOVEL INTELLIGENT FATIGUE SENSOR FOR MONITORING THE HEALTH STATE OF STRUCTURAL MEMBERS" is fully adequate in scope and quality as a thesis for the degree of Doctor of Philosophy.

Prof. Dr. Ali GÜNGÖR
Thesis Advisor, Department of Metallurgical and Material Engineering

This thesis is accepted by the examining committee with a unanimous vote in the Department of Metallurgical and Material Engineering as a Doctor of Philosophy thesis. 11/02/2019

Examining Committee Members (Institutions)	Signature
Chairman : Prof. Dr. Hakan ATEŞ (GU)	
Member : Prof. Dr. Ali GÜNGÖR (KBU)	
Member : Prof. Dr. Hasan GÖKKAYA (KBU)	
Member : Prof. Dr. Hayrettin AHLATÇI (KBU)	
Member : Assist. Prof. Dr. Javad RAHEBI (THKU)	

...../...../2019

The degree of Doctor of Philosophy by the thesis submitted is approved by the Administrative Board of the Graduate School Natural and Applied Sciences, Karabük University.

Prof. Dr. Filiz ERSÖZ
Head of Graduate School Natural and Applied Sciences

"I declare that all the information within this thesis has been gathered and presented in accordance with academic regulations and ethical principles and I have according to the requirements of these regulations and principles cited all those which do not originate in this work as well."

Ahmed El Barouni HADYIA

ABSTRACT

Ph.D. Thesis

A NOVEL INTELLIGENT FATIGUE SENSOR FOR MONITORING THE HEALTH STATE OF STRUCTURAL MEMBERS

Ahmed El Barouni HADYIA

Karabük University
Graduate School of Natural and Applied Sciences
The Department of Metallurgical and Material Engineering

Thesis Advisors:
Prof. Dr. Ali GÜNGÖR
February 2019, 126 pages

Fatigue failure is responsible of a remarkable portion of structural damages. Fatigue failure occurs in structures subjected to cyclic loads. However, according to a number of scientific models that forecast fatigue crack propagation, the actual crack spread is exceptionally difficult to appraise. Therefore, it is necessary to develop and implement new methods and model to predict fatigue damages before a catastrophic failure occurs.

The main goals of this study are to design, implement, evaluate the stresses around V-notch passive sensors with different depths. To examine the stress distribution on the fracture surface, the finite element method (FEM) was employed. The ANSYS program was used to cross check the calculated stress values. In the ANSYS simulation, a piezoelectric sensor with six beams with opposite V-notches made from

A36 steel was designed such that the beams were parallel to the applied tension load of the structure.

ANSYS computations were performed using cyclic loads, V-notch geometry (such as angle orientation and notch depth) and boundary conditions of the sensor. In addition, both element and nodul solutions were used in the ANSYS simulations. In the element solution, we used 8795 elements, while 18474 nodes were used in the nodul solution. In both solutions, the Solid 5 type element, containing 3D magnetic, electrical, thermal, piezo-electrical and structural simulations, was used. Solid 5 has eight nodes, each of which has six degrees of freedom. The degree of freedom uses displacement (UX, UY and UZ), TEMP, VOLT and MAG.

It was seen that the depth and angle of the notch affect fatigue life. It was observed that the maximum Von Mises stress occurs on the beam that has greater depth than the other beams. In other words, Von Mises stress increases with the notch depth of the beam. This implies that the failure depends on the mechanical properties of the material, applied loads, boundary conditions and V notch parameters such as depth and angle of the notch. Therefore, it can be said that model generated through fatigue-life analysis using ANSYS software for a given specimen can be used to predict the fatigue-life of notched specimens.

Keywords **:** Fatigue sensor, damage monitoring, V-notch sensor, failure analysis.
Science Code **:** 915.1.092

ÖZET

Doktora Tezi

YAPISAL BİLEŞENLERİN HASAR TESPİTİNİN İZLENMESİ İÇİN YENİ BİR AKILLI YORULMA SENSÖRÜ

Ahmed El Barouni HADYIA

Karabük Üniversitesi
Fen Bilimleri Enstitüsü
Metalurji ve Malzeme Mühendisliği Anabilim Dalı

Tez Danışmanı:
Prof. Dr. Ali GÜNGÖR
Şubat 2019, 126 sayfa

Yorulma hasarı, yapısal hasarların önemli bir kısmından sorumludur. Yorulma hasarı çevrimsel yüklere maruz kalan yapılarda meydana gelir. Bununla birlikte, yorulma çatlağı yayılımını öngören birçok bilimsel modele göre, gerçek çatlak yayılımının değerlendirilmesi son derece zordur. Bu nedenle, felaketle sonuçlanan bir hasar meydana gelmeden önce yorulma hasarlarını tespit etmek için yeni yöntemler ve modeller geliştirmek ve uygulamak gerekir.

Bu çalışmanın temel amaçları; farklı çentik derinliklerine sahip pasif sensörlerde V çentik etrafındaki gerilmeleri tasarlamak, uygulamak ve değerlendirmektir. Kırılma yüzeyindeki gerilme dağılımını incelemek için sonlu elemanlar yöntemi (FEM) kullanılmıştır. ANSYS programı hesaplanan stres değerlerini çapraz kontrol etmek için kullanılmıştır. ANSYS simülasyonunda, A36 çelikden yapılmış karşıt V

çentiklere sahip altı kirişli bir piezoelektrik sensör, kirişlerin yapının uygulanan gerilim yüküne paralel olacağı şekilde tasarlanmıştır.

ANSYS hesaplamaları, döngüsel yükler, V çentik geometrisi (açı yönü ve çentik derinliği gibi) ve sensörün sınır şartları kullanılarak yapıldı. Ayrıca, ANSYS simülasyonlarında hem element hem de nodul çözümleri kullanılmıştır. Element çözümünde 8.795 element kullanılırken, nodül çözümlerinde 18.474 nod kullanılmıştır. Her iki çözümde de 3D manyetik, elektrik, termal, piezo-elektriksel ve yapısal simülasyonlar içeren Solid 5 tipi eleman kullanılmıştır. Solid 5, her biri altı serbestlik derecesine sahip sekiz noda sahiptir. Serbestlik derecesi yer değiştirme (UX, UY ve UZ), TEMP, VOLT ve MAG kullanır.

Çentik derinliğinin ve açısının yorulma ömrünü etkilediği görülmüştür. Maksimum Von Mises stresinin diğer kirişlerden daha fazla derinliğe sahip kiriş üzerinde meydana geldiği görülmüştür. Bir başka deyişle, Von Mises stresi, kirişin çentik derinliği ile artar. Bu, hasarın malzemenin mekanik özelliklerine, uygulanan yüklere, sınır koşullarına ve çentiğin derinliği ve açısı gibi V çentik parametrelerine bağlı olduğunu gösterir. Bu nedenle, belirli bir örnek için ANSYS yazılımı kullanılarak yapılan yorulma ömrü analizi ile üretilen modelin çentikli numunelerin yorulma ömrünü tahmin etmek için kullanılabileceği söylenebilir.

Anahtar Sözcükler : Yorulma sensörü, hasar izleme, V-çentik sensörü, hasar analizi.
Bilim Kodu **:** 915.1.092

ACKNOWLEDGMENT

First of all, I would like to express deepest gratitude to my supervisor Prof. Dr. Ali GÜNGÖR for his grateful motivation, guidance, support, continuous advice and constructive suggestions toward the completion of this thesis.

I would like to acknowledge my committee for their contributions in time and advice to improve this work.

To my mother, I appreciate her for encouraging me to bring passion and love to whatever endeavor I undertake. She has been there since the beginning, supporting me throughout my degree programs, and even stayed with me to ensure the completion of this thesis, I am lucky to have such a wonderful family.

I would like to thank my family and my wife for their support, encouragement and patience throughout my studies.

If I overlooked anyone, please accept my apologies, since there are so many nice and kind people, who provided me with moral support throughout this endeavor.

CONTENTS

Page

Page

LIST OF FIGURES

Page

Page

Page

TABLE INDEX

Page

LIST OF SYMBOLS AND ABBREVIATIONS

AASHTO : American Association Of State Highway And Transportation Official.

EFS : Electrochemical Fatigue Sensor.

EM : Electromechanical.

FBG : Fiber Bragg Grating.

FEA : Finite Element Analysis.

FDS : Fatigue Damage Sensor.

FE : Finite Element.

HCF : High- Cycle Fatigue.

IDT : Interdigital Transducer.

K_F : Fatigue Stress Concentration Factor.

K_T : Stress Concentration Factor.

K_{IC} : The Fracture Toughness.

LCF : Low- Cycle Fatigue.

LEFM : Linear Elastic Fracture Mechanics.

MEMS : Micro-Electro-Mechanical Systems.

MWM : Meandering Winding Magnetometer.

Q : Notch Sensitivity Ratio.

PZT : Piezo Ceramic.

PWAS : Piezoelectric Wafer Active Sensor.

RFC : Rain Flow Counting.

S_F : True Fracture Stress.

SHM : Structural Health Monitoring.

S_U : Ultimate Strength.

S_Y : Yield Strength of Material.

PART 1

INTRODUCTION

1.1. HISTORY

Fatigue is a major reason behind the failure of significant fundamental components. It begins with microscopic defects in structural materials and these microscopic defects gradually turn into macro or larger cracks. Generally, this phenomenon occurs near high-stress zones such as notches and holes [1]. In addition, the assessment of fatigue is significant for component design. Generally, stress affects the design and makes it inappropriate.

However, the failure cycles of a structure are based on different stress levels, and this governs a structure's fatigue life throughout its stress history. Generally, the S-N method is applied to determine fatigue life; however, empirical rules/accumulative damage assessment laws are inadequate.

An S-N fatigue-life device is a means for determining accumulated fatigue damage. Mechanical distresses occur because of fatigue, which have been a subject of design endeavors for more than 150 years. Fatigue failure is an important concern for building plans. The mechanical monetary frustrations because of fatigue have been the subject of design endeavors. The occurrence of most of the failures in parts of mechanical systems went through the procedure of progressive aggregation of the destruction in material in order to bring about nucleation and break development. These cores are exhibited before the operation occurred on the assembling stage.

The expansion of the crack size until they are unsafe or of undesirable size are regarded as the reasons for failure. If a crack is not confined in time, its further growth may cause serious failure. Large numbers of failures and cutoff states are associated with

the wear and tear of surfaces linked with a working or encompassing environment. Phenomena such as consumption fatigue impulses, erosion cracking and fracture improvement through hydrogen embrittlement are associated with life support and system building structures [2].

The term fatigue is used to refer to the complete set of fracture and damage phenomena. In particular, fatigue means fracture and loss because of cyclical and frequently applied stresses. In general, fatigue consists of all the phenomena of delayed damage and fracturing under constant loads in addition to any environmental actions. Later, when we discuss fatigue with no additional concepts, we mean the situation of cyclic loading and operations.

In 1839, Ponselle presented the idea of fatigue as found in the literature. A systematic study of fatigue was then introduced later. This is associated with the name of one of the most important pioneers, 'Wohler,' who conducted the first systematic experimental study of this phenomenon from 1858 to 1860. In particular, the aforementioned pioneer Wohler presented the idea of the fatigue curve, referring the cycle number up to fatigue failure, to a specific volume of the stress process. To date, fatigue curves and the form fundamentals of engineering analysis are widely used.

1.2. FATIGUE SENSORS

In a broader sense, a sensor can be defined as a device that works during differentiated occasions or it can take into account any changes occurring in its surroundings, after which it takes any necessary action or gives a required signal. A sensor is a type of transducer, which may give different types of yields; however, it is widely used in optical as well as electrical signs. For example, a thermocouple produces the yields (of an identified voltage), which occurs due to the temperature of the earth. On the other hand, the mercury-in-glass thermometer corresponds to changes over the measured temperature into the expansion and contraction of a fluid that can be checked with an adjusted glass tube.

Sensors are used for common purposes, such as touch-touchy lift catches (material sensors) and lights. This can be reduced or lightened by touching the base rather than via multiple uses, with which a large number of people are not familiar. Nevertheless, with advances in small-scale machinery and simple-to-employ small-scale controller stages, sensor use has extended past the most common fields of temperature, stream or weight estimation, such as Marg sensors. Moreover, simple sensors such as potentiometers and constrain detecting resistors are still generally applied.

On the other hand, applications such as hardware, planes, automobiles, pharmaceuticals and robotics are integrated into our daily life.

According to Bennett et al, the effect of the sensor determines to what extent the sensor's field will change when it senses a specific activity or change in its surroundings. Similarly, some sensors can affect what they measure; for example, the thermometer of a room temperature can be set on a hot measure of fluid, and it cools the fluid while the fluid warms the thermometer. Sensors should be intended to affect slightly what is being measured. In other words, making the sensor small improves the process that may introduce further points of interest. Mechanical advancement allows increasing the use of sensors to be used on a minute scale because small-scale sensors use MEMS innovation. Largely, a small-scale sensor gains a higher speed [3].

With regard to piezoelectric sensors, the word *piezo* originated from the Greek word piezeinc, which means 'intention to press or crush.' Piezoelectricity refers to the era of power or of electric extremity in dielectric gems when they are subjected to mechanical pressure or a period of stress in certain gemstones because of a connected voltage. In 1880, the Curie siblings observed that quartz changed its measurements when it is exposed to an electrical field and creates an electrical charge when weight is applied to it. Since that time, scientists have discovered the piezoelectric properties in many combustible and plastic materials. Numerous piezoelectric materials additionally indicate electrical effects due to temperature changes and radiation. Furthermore, piezoelectric components are used to build transducers for many

applications. Piezoelectric materials create electrical charge in mechanical structures [4].

When the piezoelectric material is exposed to mechanical pressure, it offers either a potential contrast or it can show dimensional changes as it is subject to the external electrical field. These uncommon changes take place because of the movement of the dipoles. This results in the modification of the dipole minute inside the material. Nevertheless, this trademark can be wiped out if over-the-top mechanical pressure, electrical stress or high temperature exists and it is connected to the materials, which results in the dipole of the material to occur.

The electro-mechanical attributes of a piezoelectric material make it reasonable to be utilized as actuators or sensors. However, piezoelectric components have demonstrated expansion in top-to-crest voltage as split length increments.

Piezoelectric components are utilized to develop transducers for many applications. Piezoelectric materials create an electrical charge because of mechanical development, and conversely, deliver mechanical development in the light of electrical information [5].

Athens et al pointed out that piezoelectric material, when it is subject to the mechanical pressure, offers ascent to potential contrast or it can show dimensional changes if it has an external electrical field. This uncommon phenomenon occurs because of the movement of the dipoles, which results in the modification of the dipole minute inside the material. It can be disposed of, if in-temperate mechanical pressure, high temperature or electrical stress are linked with materials, which results in the de-poling materials [6].

1.3. OBJECTIVES

The significance of the current study is the need of researchers and professionals handling sensors. Sensors are installed in our bodies, automobiles, aeroplanes, cellular

telephones, radios, chemical plants, industrial facilities and numerous other applications. Without the use of sensors, automation would be impossible.

The current topic is that of fatigue sensors that work with the help of several parallel beams created to assess fatigue levels and cycles through a single sensor. It is attached with a structural component that goes through a continuous cyclical bending, such as an aircraft wing or bridge beam. However, beams have unique geometry and other features which are very helpful when predicting the fatigue cycle of beams within a sensor. Fatigue cycle prediction of any V-notch beam is clarified in this thesis. We have sought support of the ANSYS simulation software. On the other hand, the sensor is designed to take a V-shape notch and apply many parameters to estimate the fatigue failure by using the analysis software to predict sensor fatigue failure. This enables measures to be taken before any failure actually begins.

A sensor allows the replacement of parts before any failure starts. The main objectives are as follows:

1. Describe V-notch fatigue sensors.
2. Identify which parameters should be included in a fatigue sensor system.
3. Propose suitable fatigue sensor dimensions to detect fatigue life.
4. Use the mechanical properties of steel (S-36).
5. Evaluate the stress and fatigue life of V-notch fatigue sensors and measurement techniques.

1.4. MOTIVATION

The main motivation for this thesis is to protect any fundamental structure from fatigue failure damage and reduce future repair costs. Fatigue is often the cause of serious problems in important objects such as bridges and aircraft. Using new techniques for predictions under constant and variable stresses confirms that the considered fatigue sensor is useful for steel welded joints. In addition, it warns about the speed of deterioration.

1.5. MAIN CONTRIBUTIONS

This thesis makes contributions to V-notch fatigue sensor design, which helps to address practical problems, as discussed in Section 1.3 in the context of V-notch fatigue sensor application.

The points given below show how this thesis contributes to the overall research on sensors:

1. An analysis of V-notch Sensors for Structural Health Monitoring of Serious Modules
2. An Evaluation Study on Fatigue Life of V-shape of Structural Steel Fatigue Sensors.

PART 2

LITERATURE REVIEW

Fatigue has been under study for more than two centuries, so, it is an old area of concern. It takes place because of existence of metallic substances in structures. Recently, researchers and scientists have taken steps for the improvement of analytical numerical models to have a better idea about fatigue for critical structures.

Developing A fatigue damage detection sensor for monitoring structural damages through important mechanical/ structural component accumulation that performs with cyclic loads until before fatigue failures. That life and economic losses must be prevented; however, the practice of designing structures for fatigue prevention is difficult because the actual loading history of the structure is mostly unknown and cannot be precisely predicted. Consequently, there is a requirement for a device to monitor fatigue damage and provide a consistent estimation of remaining fatigue life of a specific structure altogether in order to provide a warning of impending fatigue failure. This device is called fatigue sensor.

The work on Structural Health Monitoring by Boller and Meyendorf is a holistic method to look at structural strength. It monitors loads, which are directly fed into a digital damage accumulation of any structure. It helps identifying damages as show in Figure 2.1 [7].

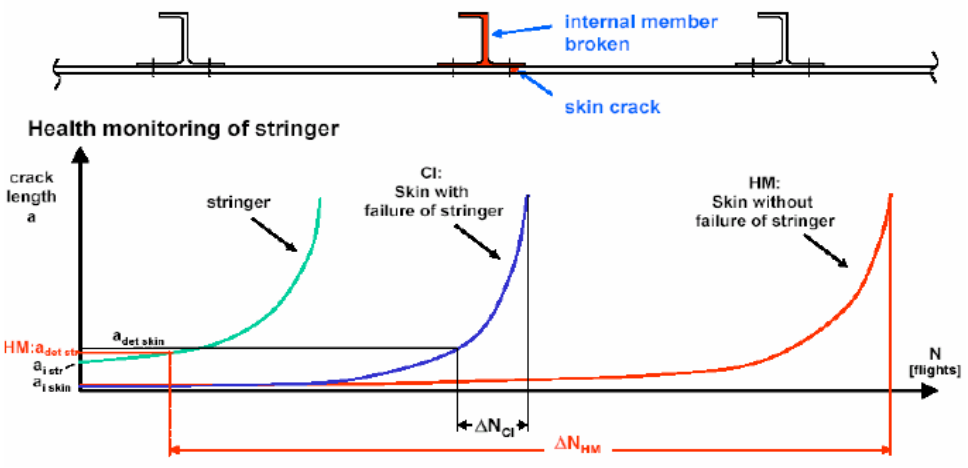

Figure 2.1. Comparison in crack propagation intervals for monitored and on monitored damage tolerant structures [7].

On the other hand, Duan, Wang and Quek discovered that piezoelectric substances possess significant sensing capabilities. From this study, it is understood that actuators, piezoelectric sensors, and interdigital transducers (IDTs) can discover cracks in beams, plates and pipes with a high level of accuracy. Furthermore, piezoelectric materials have the capability to alter traditional structural repair materials as show in Figure 2.2 [8].

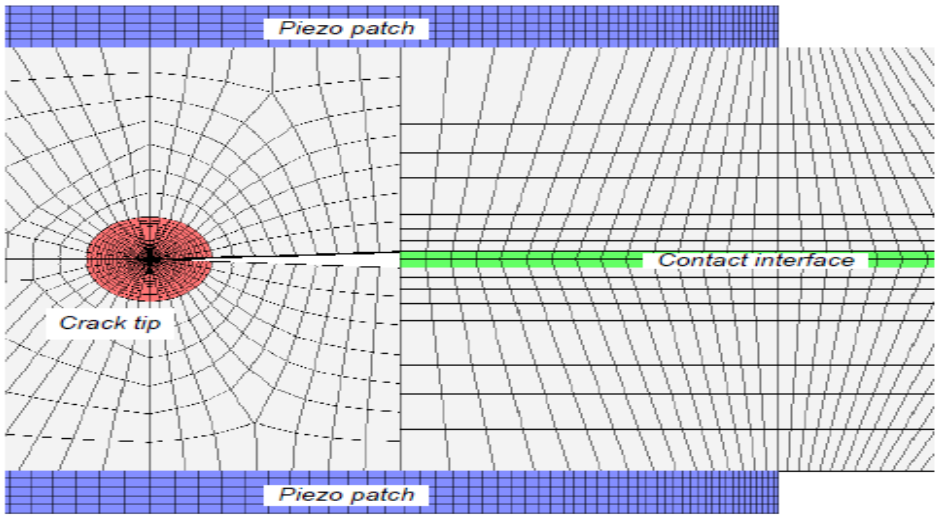

Figure 2.2. Finite element discretization for crack tip, piezoelectric patches and Contact interface [8].

Song et al. argue that their project includes novel and capable sensing approaches based on the piezoelectric active and passive sensing in order to decrease the dramatic uncertainty intrinsic of any inspection and maintenance plan [6].

In addition, Bader & Njim assess in their work that notched specimens' bending fatigue life (having multiple-angle V-notched geometry) was investigated by conducting experiments and by Finite Element Analysis as show in Figure 2.3 FEA Method [9].

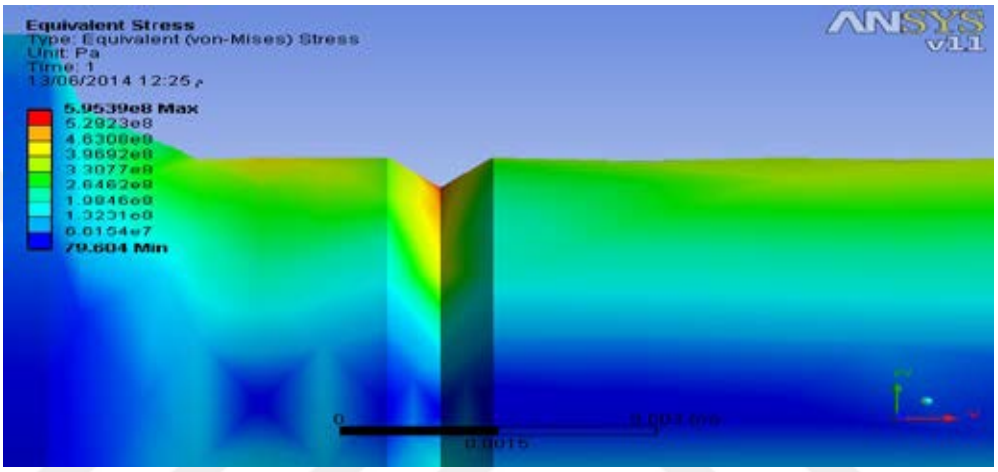

Figure 2.3. Model and normal stresses for smooth specimen and Von – Mises stress for notched bar [9].

Another study by Fadare, Okoronkwo & Olasehindde states that the FEA has been implemented to demonstrate the effect of the stress mean value ($R \neq -1$). It is drawn according to They are stress-correction theories presented by Goodman, Soderberg, and Gerber. An important benefit of our research is a fact that average stress effect correction relies on failure cycle number [10].

However, R, Baldwin, Forslid, Martin, Ottaviano & Robert-Nicoud Investigated the deep U-notch prototype developed in this research, which shows promising results towards a final design of in-situ fatigue sensors. Still, there are certain limitations pertaining to the current design that need to be addressed in the future. The notch design needs further improvements in order to find appropriate gap (cycle-wise) between the notches, which helps accomplishing better fatigue life coverage of the monitored structural elements. Furthermore, sensor arms can be added in the current

design increased for accommodating more notches possibly addressing lower stress ranges with larger number of loading cycles. Sensor mounting modification and a size-wise scaling down of the current prototype sensor design is also necessary to attach them closer to the structural details in bridges where high stress concentrations are possible as show in Figure 2.4 [11].

Figure 2.4. Close up of mounted fatigue sensor [11].

In addition, Hodge introduced and discussed a unique fatigue sensor developed by Metal Fatigue Solutions, that has been in commercial use throughout North America for over 5 years. First introduced in The Electrochemical Fatigue Sensor EFS system has proven itself valuable for timely detection of growing fatigue cracks typically well before unassisted sense spots them. Its functions are as follows:

1. Define crack growth (whether the crack is growing or not).
2. How rapid or slow is the growth.
3. Define the presence of micro-plasticity (in similar details elsewhere on the same bridge).
4. Assist in evaluation of effective retrofits (if the retrofit stops the crack growth).
5. Retrofit selection (which retrofit is the most effective in stopping the crack growth) [12].

Kim et al. Year specified and investigated a procedure that makes a piezo ceramic (PZT) piece to find out details of structural damages. Specifically, impedance-centric health-monitoring process, which utilizes piezo ceramic transducers as sensing equipment.

Nevertheless, damage identification process detects mechanical impedance variations because of the damage to evaluate the structural health of welded materials. Fiber Bragg Grating (FBG) sensors was applied for finding stress values concerning traditional welded structures [13].

A further study by Yu et al. was about the piezoelectric wafer active sensors (PWAS). They demonstrate potential for use as AE sensors because they have in-plane displacement sensitivity that takes place due to growing cracks. Still, many issues of these sensors should be dealt with for substituting the AE sensors made up of piezoelectric crystals. Extensive tests have been accomplished pertaining to crack increase and monitoring accelerated corrosion using AEs. Outcomes point towards significant correlation between occurrence of damage and the AE as show in Figure 2.5 [14].

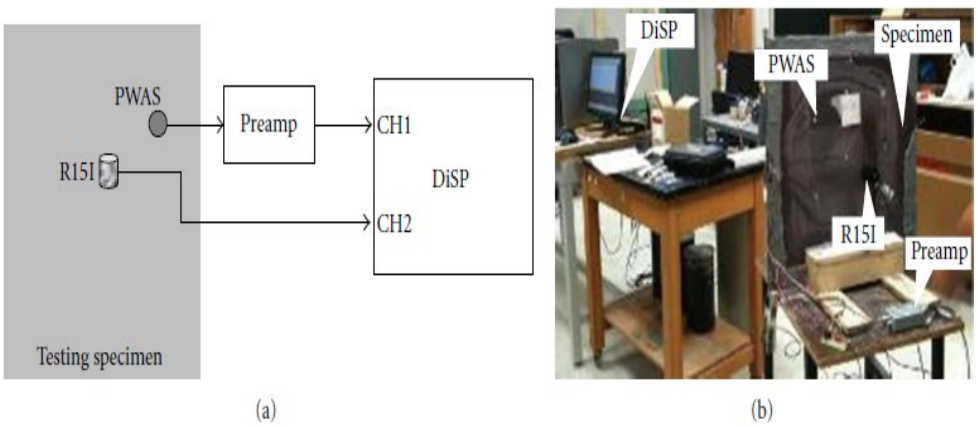

Figure 2.5. AE testing setup a) test setup schematic, b) laboratory test setup [14].

On the other hand, Wijesinghe, Zacharie, Mish, & Baldwin presented another study and improvement of in-situ fatigue sensors, which are utilized for finding out fatigue

damage in bridges made up of steel. The geometries of two sensors having five stress concentration factors (SCFs), which were tested for carrier steel beam specimens applying consistent amplitude tensile cyclical loading. An FE analysis was conducted to analyze sensor stress as well as output stress using a Mat lab code for calculating fatigue-life [15].

Carpinteri, Cornetti, Pugno, & Sapora Investigated the problem is related to finding the most serious notch-opening angle. According to generally agreed upon linear elastic fracture mechanics (LEFM) take into account K_I ¼ K_{IC}(Equation that shows dangerousness of an edge crack). Moreover, we also take into account the critical amplitude, which relates to notch-depth and material specifications using brittleness value as show in Figure 2.6 [16].

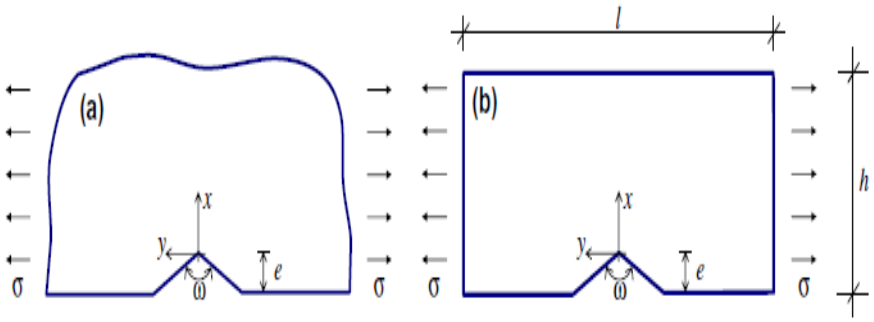

Figure 2.6. Semi-infinite a) and finite-size, b) V-notched plate under uniaxial Remote tension [16].

With regard to the damage of individual sensors, Glišić et al. demonstrate that it decreases damage characterization accuracy. However, it plays no significant role for weakening the sensing sheet's overall damage-detection capability. This proves that the direct-sensing concept applies to strain sensors and the sensing sheet [17].

However, the study of Varsakelis & Papalexandris concluded that these acoustic emission parameters need further studies in order to establish early warning signs against final fracture and to characterize the damage status at any point of the materials' life. In addition, this work confirmed that the rate of crack growth could be effectively monitored by the use of lock-in thermography in metallic materials undergoing cyclic

loading. It can be concluded that the lock-in thermography index can be regarded as a prediction of the crack propagation rate, which is measured by the compliance technique in AA7075 aluminum alloys [18].

In addition, Koston Investigated fatigue crack monitoring in metallic structures using Eddy current micro-sensor. Fatigue cracks can take place in the aircraft joints. For quantitative damage discoveries, Eddy current sensors are utilized because they are equipped with flexible printed circuits [19].

In terms of how surface deformation-relief in AL clad aluminum alloy takes place under varying loads. Confirm that it indicates the overall fatigue damage; however, latest fatigue sensors monitor joint health, aircraft structure and structures of bridges and ships as show in Figure 2.7 [20].

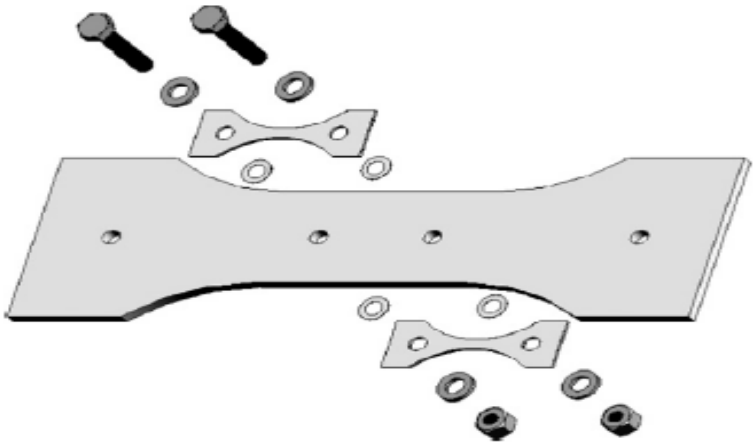

Figure 2.7. 3-D image of the sensor attachment to the specimen for fatigue test. [20].

Another study was carried out by LeClair & Jackson proposed use of carbon films for fatigue monitoring. It suggested that metals having diamond-like carbon films, also having optimum composition and microstructures are good options for use in fatigue-monitoring sensors [21].

On the other hand, described the phenomena of fatigue related to mechanical failure in terms of material specification, such as structure in their study by [22].

Balda proposed a new method of low-cycle fatigue data processing based on the evaluation of a relative damage and tested a series of low cycle fatigue. Materials of low cycle fatigue parameters were searched by means of the optimization procedure. This procedure applied for the minimization of a sum of squared differences of calculated and measured relative damages. Practical applications of the method have revealed that fatigue life calculated from the estimated low-cycle fatigue coefficients may differ from those obtained from the identified parameters [23].

Another study by Veers et al. demonstrates that finite element model and the static tests were very accurate. In all blade designs, both the finite element analysis and static test failed at very similar forces [24].

Ciang, Lee, & Bang studied the sensors that provide enhanced diagnostics and the capabilities of damage progression prediction as well as new capabilities for load monitoring of structures and dynamic components [25].

Khan& Zafar discussed recent progress regarding the application of the electromechanical (E/M) impedance approach to structural health monitoring, failure prevention and damage detection. A brief review of the principles of E/M impedance method was followed by applications to bolted and spot riveted structural joints, and to polymeric composite overlays to construction engineering structures as show in Figure 2.8 [26].

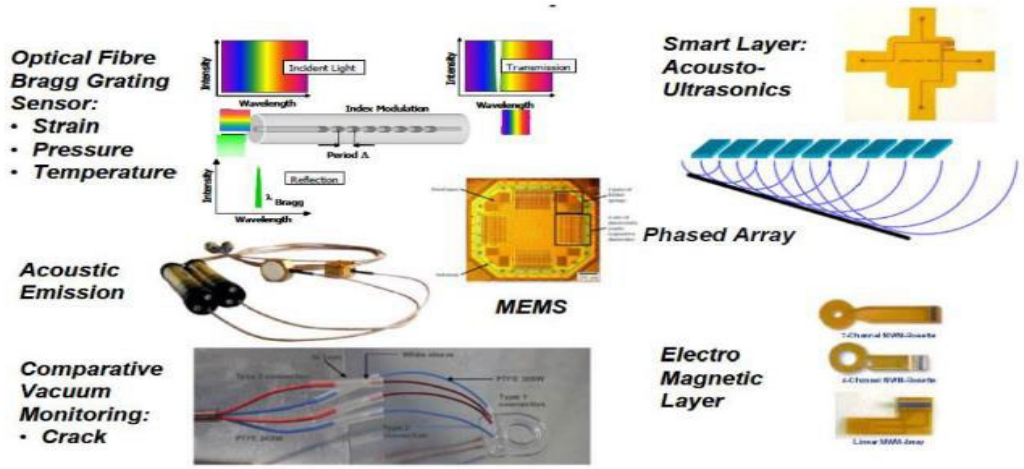

Figure 2.8. Sensors options for SHM [26].

Hardin & Beckermann studied the development of finite element (FE) analysis to accurately predict notched cross-sectional strain. This applies for predicting life components with complicated structures. It is possible to draw strain-life curve with the help of notched specimens' experimental outcomes while strain correction can be evaluated through FE analysis, which is listed as follows:

1. The fatigue life of the component decreases due to the presence of notch, which creates similar multi-axial state of stress as created by small cracks, flaws etc. present in the actual component.
2. Life prediction using notch specimens should be used to predict the life of a component.
3. Life of a component decreases with increase in stress concentration factor.
4. Life of a component at high temperature (823K) is less than what it is at room temperature.
5. Life estimation by simulation agrees reasonably with the experimental values, which can used for prediction as show in Figure 2.9 [27].

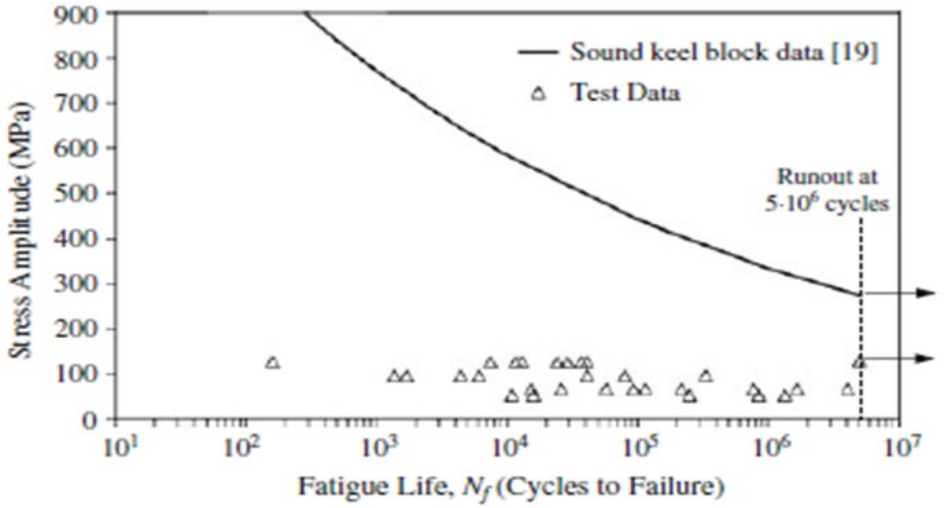

Figure 2.9. Fatigue life measurements of specimens with porosity Compared With sound data [27].

As far as steel bridges' fatigue performance is concerned, which Al-Emrani et al. have examined. Their work showed that most fatigue damages occur on bridges on highways and railways. In the majority of issues, some unexpected, unforeseen or overlooked load interacts with load-carrying segments of a bridge, which has poor detail and finally, cracks emerge in it. A few cases were reported, which gave evidence of complicated stress within the structure as show in Figure 2.10 [27, 28, and 29].

Figure 2.10. Examples of fatigue damage in riveted stringer-to-floor-beam connections [28,29].

Smith, Landis, & Gong evaluated notched components' fatigue life both for proportional as well as non-proportional multi-axial cyclical load. However, the

process requires elastically calculation as a fundamental input, which is feasible in case of engineering applications. This method accurately predicts fatigue life information for SAE-notched shaft specimens [30].

Regarding the fatigue analysis, Reifsnider investigated more than 50 different cases with different behavior to reach the optimal solution for failure analysis of metal fatigue [31].

Su & Ye which elaborated Lamb wave propagation measurements through PZT sensors conducted another study. Furthermore, it helps quantifying influence of bonding problems in Lamb wave signal processing algorithms [32].

Kuang, et al. which offers a high sensing performance for determining the extent to fatigue damage stability caused to a structural material, based on the amount and the rate of crack propagation, developed another sensor [33].

Kaplan & Ozkul they also find out place of a crack using EFS (electrochemical fatigue sensor) devices, which were originally meant to facilitate the U.S. Air Force for manufacturing aerospace applications. These sensors detect mainly cracks in airframes and engines. Right now, there are numerous financially accessible fatigue sensors in the market. Audits was conducted on electrochemical fatigue sensors to establish their effectiveness as show in Figure 2.11 [34, 35].

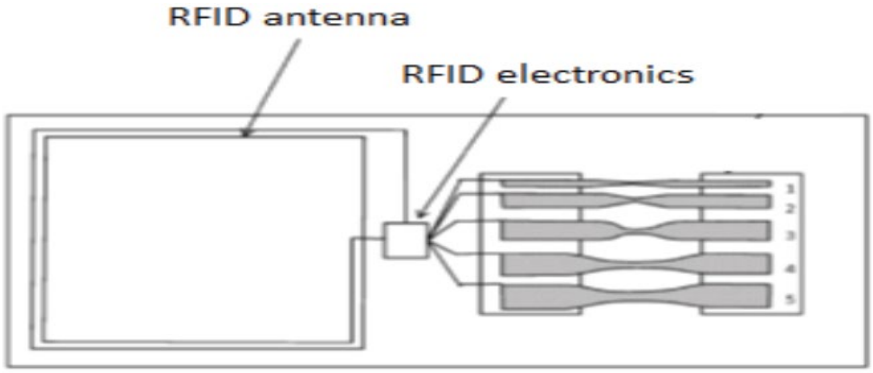

Figure 2.11. Battery free version of the sensor powered by RF power loop [34, 35].

Excellent technologies developed a device referred to as "Good Layer," that was made from piezoelectric sensors/actuators. They conjointly established an analytical system to sentinel multi-crack growth at riveted Lap joints. Vodicks, Lin & Chang mentioned the utilization of PVDF (polyvinylidene fluoride) electricity strain sensors in similar secured composite patches. Boeing, under USAF contract, has built up a damage securing unit called the injury dosimeter to recognize the frequency and temperature connected with the maximum strain movement to advance the damping proficiency by [36].

Another review by J. D. Baldwin, et al. discussed in-situ fatigue sensor development, design, execution, and assessment. An in-situ sensor was mounted on the structure, which was monitored for fatigue [37].

Merit Enckell investigated SHM as well as other sensing advancements through monitoring engineering structures including bridges. The SHM in the long haul with fiber optic sensor was analyzed along with the existing SHMSs with the end goal to create change [38].

Tarik Ozkul, Halit Kaplan, and Melik Dolen developed a type of fatigue sensor, which has many parallel beams to detect diverse fatigue levels within a solitary sensor that is intended to attach with a structure that is likely to experience cyclical bending the way an aircraft wing or a bridge beam does [39].

Majzoobi's paper depicts the idea of devoted fatigue-monitoring sensor alongside vital plan subtle elements, reproduction information, and test outcomes that would give approval. Henceforth, the current research promotes a sensor design that can keep away previous mentioned impediments. It has benefits including appropriate separation far from the structure. This type of fatigue sensors is subject to an indistinguishable surrounding condition from those accomplished by the structure [40]**.**

Majzoobi, G., & Daemi, N. researched the impact of notch geometry and sensitivity on fatigue life. They found that the notch sensitivity actually measures the extent to which a material is sensitive to geometric discontinuities or notches. Notch sensitivity accepts the impact of several parameters including notch geometries including U-shaped, V-shaped, which were observed during the study. A high-strength and low-strength steel alloys were used for investigation. It was found that the stress concentration can be achieved through numerical simulation as well as fatigue reduction factor in a bending/rotating fatigue device as show in Figure 2.12 [41].

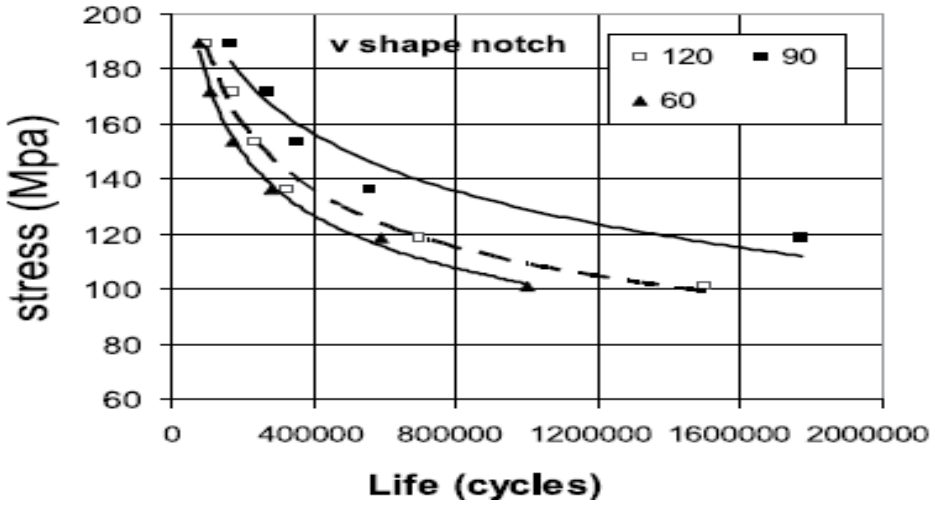

Figure 2.12. S-N curves for V-shape notched specimens made of HS steel [41].

A Certain kinds of break recognition gages were likewise created before, nonetheless forced in an exceeding method, these crack gauges should set essential stress concentration zone wherever the cracks exist. They have many thin strands. The sensor monitors the place where a crack proliferates in the mentioned strands and cuts those [42].

A fatigue damage indicator is equipped with a slit, which was introduced by Smith. Normally, fatigue life can be estimated through physically monitoring the length of crack length on a sensor's notch tip. In another example, crack length had the same stacking. There is a need to regularly monitor the poorly performing components. The antecedently mentioned sensing devices are ordered for passive sensors, whereas other

sensors are active having capability for piezoelectric development, engaging flux spillage, swirl current sensors, etc. [43].

Wu, Liou & Tse tested the application of different processes, which have been proposed so far to estimate fatigue damage and components' lives in random loading conditions. Palmgren-Miner & Morrow's interaction rule considers the effect of stress sequence, which was verified during the strain-controlled low fatigue cycle tests of aluminum alloy 7075-T651. Results have shown that Morrow's plastic work interaction damage rule is far better as compared to commonly utilized Palmgren-Miner's linear damage principle. Morrow's rule estimated the damage, but it was a conservative method. Test results show that the specimens' fatigue life is assessed using Gaussian method as show in Figure 2.13 [44].

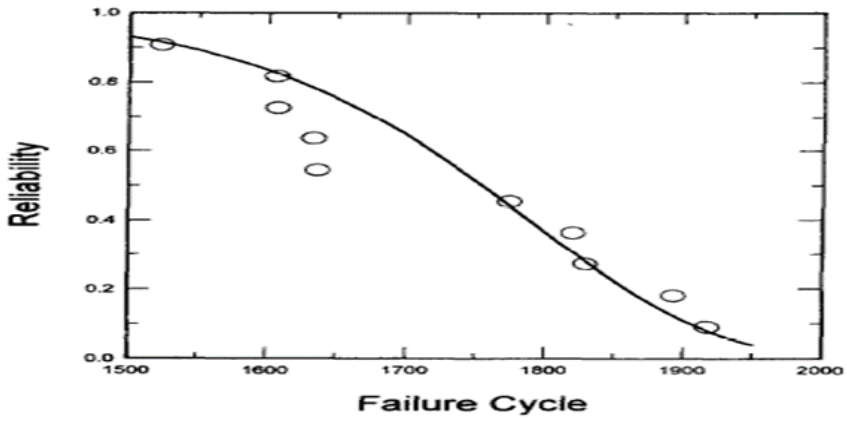

Figure 2.13. Fatigue reliability function under random loading C [44].

Mesmacque, Garcia et al. proposed their damage indicator model as a reaction to famous Miner's damage accumulation rule because the rule excludes loading history. When this approach was implemented to loading, damage indicator model gave higher results than Miner is for increasing loading and lower for reducing loading. For damage indicator model, damages are reported from a stress level to another while, the damage stress corresponds to residual life, and that leads to ultimate stress on last cycle prior to failure. This model only needs S-N curve. A stress field is equivalent to Von Misses stress or highest shear stress. Consequently, the presented model applies to multi-axial loading. For estimating importance of the said model to predict life of a

structure, some results were obtained. The experimental literature shows that the mentioned model considers loading history, which precisely predicts fatigue life in separate loading conditions as show in Figure 2.14 [45].

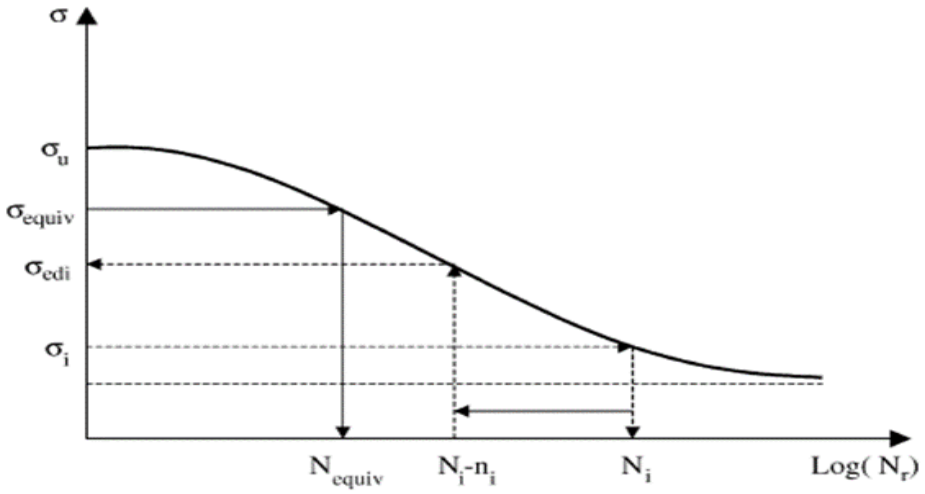

Figure 2.14. Definition of the used parameters [45].

Pyttel et al. provided an overview discussing the current researches on failures and fatigue mechanisms having greater cycles ($Nf > 10^7$). They have listed testing facilities in their study. Materials are classified with the help of traditional S–N curves, which has impact over other processes including residual stress, notches, and environment. Many failures are possible to occur due to very high cycle fatigue (VHCF) which is a cause of sub-surface failures. The homogeneity of microstructures as well as statistics play a significant role. Double S–N curves help describing fatigue and different other failures. Some studied materials using different metals such as steels having different strengths including tempered and quenched steel and face-centered substances such as aluminum and copper alloys. They have also given recommendations regarding the components' fatigue design [46].

Papazian et al. published an article: "Sensors for monitoring early-stage fatigue cracking" that highlights eddy current usage, ultrasonic sensing and electro-chemical fatigue sensor (EFS). The disappointment of the primary half crushes a thin conductor-Sensing circle, which uncovers the essential half frustration. It is completely different

from others because it is projected to acknowledge the break once the split happens. The break on the structural surface annihilates a delicate circle, and it helps a sensor detect a crack as show in Figure 2.15 [47].

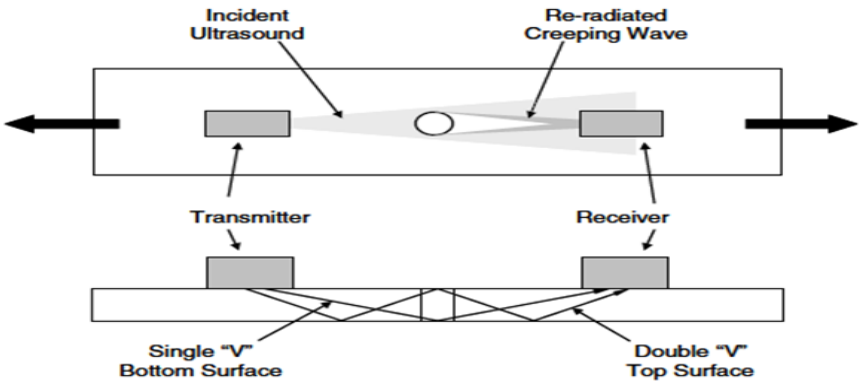

Figure 2. 15. Schematic views of the ultrasonic sensor system showing selected Signal paths [47].

Lei et al. like the prior patent, outlined the design for distinguishing breaks after the split. When a crack becomes longer, swirl current sensors assess that circumstance and report the information. Using a sensor without physical wires is a subject of interest because its related strategies are exceptionally notable. Lei et al. have clarified how to develop a wireless sensor network that works as show in Figure in 2.16 [48].

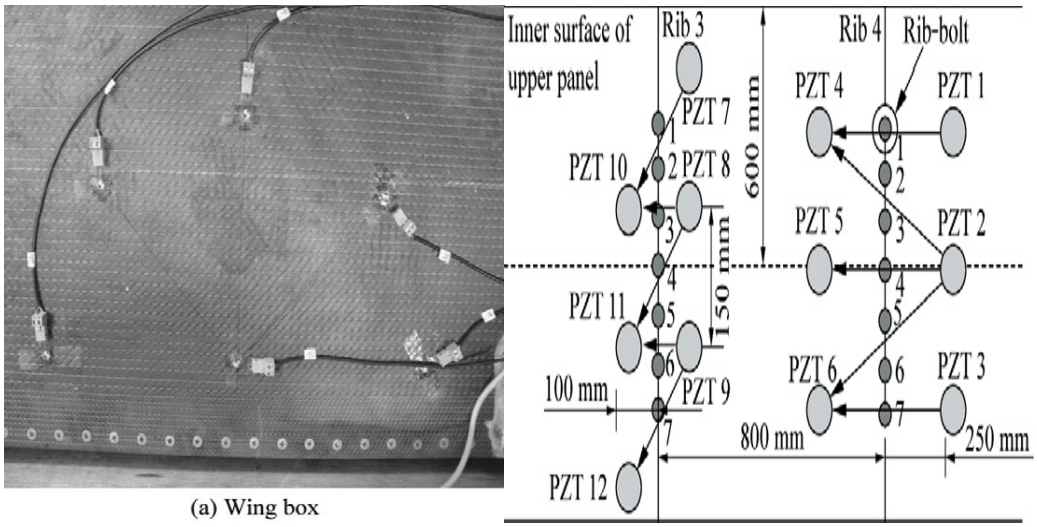

Figure 2.16. Wing box and Response Signal [48].

PART 3

THEORETICAL BACKGROUND

3.1. FATIGUE PHENOMENA IN MATERIALS

3.1.1. Fatigue History

Both Morin and Suresh agree on that concept of fatigue was presented by Albert in 1830, in Oberharz mines. In , initial fatigue-test outcomes were published with the help of testing machine that tested failed conveyor chains. Because of more expenses on those materials, Albert used wire rope, which is significant as compared to initial tests. Metals and their usage improvements for bridges and railway lines because they are likely to rupture because of fatigue more than any other structure.

The fatigue's cycling includes the micro-structural damages and failures under changing weights. It seldom happens that structural materials have composition and microstructures with advanced resistance against fatigue. In general, metal alloys are strong, ductile, and tough; however, continuous engineering usage deteriorates their structural strength because of cyclical loads. Experts have found that approximately 80 percent service failures take place because of mechanical fatigue. This can happen because of cyclical plasticity, friction, environmental damage/corrosion, or high temperature. Consequently, over the past twenty-five years, voluminous literature has been gathered that deals with the mechanics and mechanisms of mechanical fatigue failure [49].

Many failure modes of different mechanicals apply in most engineering fields. Fatigue failures mostly take place because of mechanical failures.

On the other hand, the applicable fatigue behavior and fatigue design principles have been formulated for about 150 years since the time of Wohler's early work. These principles have been improved, used as well as tested by engineers and scientists in the majority of fields in different countries. Computers have capacity to create a decisive effect on the quality as well as proficiency of latest fatigue design processes. It is essential to link/integrate computer-aided synthesis with field-testing with consistent monitoring and maintenance. This includes nondestructive inspections [50]. The fatigue of metals, which now so rightly fills the minds with dread regarding mechanisms or structures, on which, human safety depends, but it was a late discovery. However, in spite of what the popular press might lead one, it is by no means a contemporary one. About a century and a half ago, a German engineer, about whom, we know little, noted that wrought used in mine hoists, after a period of satisfactory service, breaks showing fracture, like that of china, under a load well below their capacity. In France, somewhere about the same time, the breaking of wrought iron tires of the wheels of stagecoaches was observed, and later two engineers Marcia and Maroux investigated it.

Those two engineers noted the brittle fractures, characteristic as they say that iron has bad quality. Nevertheless, they were satisfied that the iron had no bad ab initio - it had become bad or brittle in service - the terms were synonymous at that time. They also noted that their use had not produced general and local losses in the ductility of the metal, with which, the tires were made.

Finally, in England, less than a century ago McConnell, in papers given before the very young Institution of Mechanical Engineers reported that railway axles failed under normal loads after long periods of satisfactory service. Like his German and French forerunners, he observed that though the actual fracture was like that of brittle material, the metal away from the fracture-possessed ductility as comparable to its original one [51].

The initial understanding concerning fatigue failure of metals began in 19th Century during the technological revolution in Europe, when industrial instruments like

engines and boilers failed below their cyclical loads. William Albert Francis Charles Augustus Emmanuel first wrote about fatigue, which was correlated with cyclic load and metal strength.

As per inspection of failure, device having motor axles was treated with controlled loads. He gave the idea of "rotating bendable fatigue test" to find advanced stress-rpm (S-N) design for evaluating endurance and fatigue life. In sight of those assumptions, specialists began to recognize fatigue inspection in article improvement and will predict item life beyond anyone's imagination, which recently happened [52].

3.1.2. Fatigue of Material

According to Naser and Toledano fatigue takes place because of multiple exposure of a material to stress cycles, which vary from time to time. Therefore, it takes time. In other words, this process begins with formation of slip, which increases and acquires critical size/shape, which is significant enough to fracture a structure but slip formation increases when there is concentration of stress because of the defects within or outer holes in plates. This load sometimes acquires a cyclic trend, which further opens and closes micro-sized cracks. When load cycles increase or become intense, cracks become longer and wider as a consequence. A time comes when crack become critical and the structure is fractured [53].

3.1.3. The Type of Fatigue Load

The load cycle sometimes, have consistent adequacy and/or adaptable sufficiency. Devices moving in circles typically work below the pre-chosen stable load cycles such as aircrafts and ships, which bear varying load cycles because of speedy wind or marine waves.

Some loads change during performance, which can cause fatigue failure/s. These loads may differ substantially from one application to another. Their stress-type can be axial, flexible, or twistable. Generally, there are three varying stress modes. First is shown

through sinusoidal time dependence as shown in Figure (3.1a) below. It has average zero stress level, its highest tensile stress (σ_{max}) and least compressive stress (σ_{min}) have similar magnitude, so it is stress-reversed case. Figure (3.1b) shows repeated stress that shows stress starting from zero to the highest level. Figure (3.1b) shows a repeated stress that varies between zero to a maximum and the average stress equals the alternating component. In Figure (3.1c), fluctuating stress has been illustrated showing nonzero component values [54].

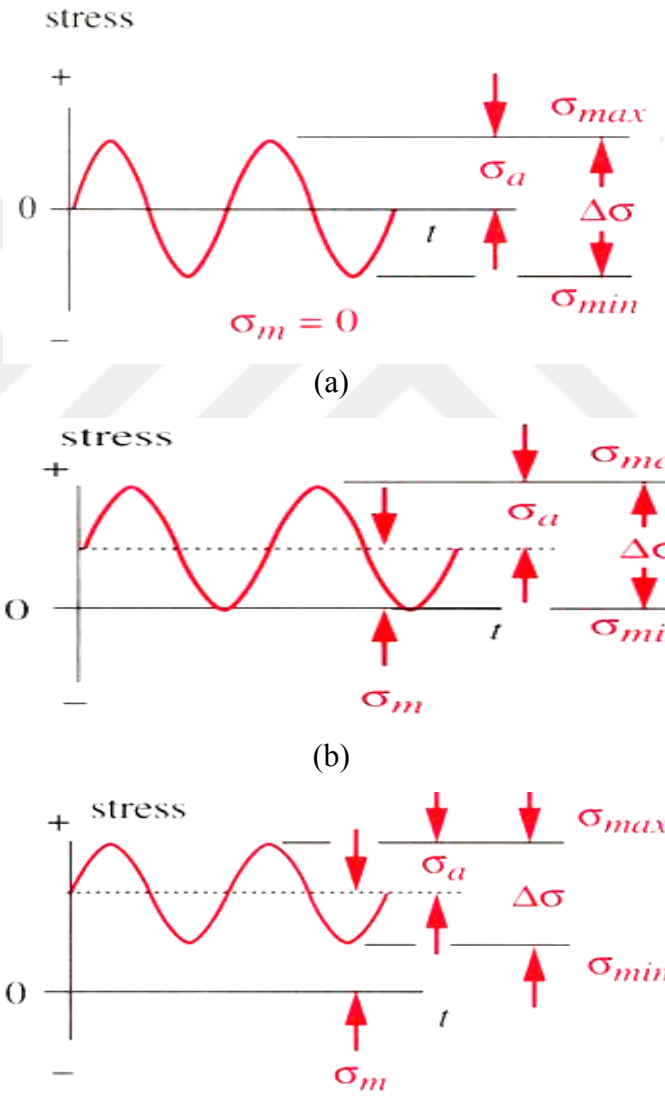

Figure 3.1. a) Fully reversed stress, b) repeated stress, c) fluctuating stress [55].

The waveform has three parameters, which are mean, alternating components, and their highest and least values, or even the ratio of these values.

The stress Range $\Delta\sigma$ is defined as:

$$\Delta\sigma = \sigma_{max} - \sigma_{min} \tag{3.1a}$$

The alternating component σ_a is found form

$$\Delta\sigma = \frac{\sigma_{max} - \sigma_{min}}{2} \tag{3.1b}$$

In addition, the mean component σ_m is

$$\sigma_m = \frac{\sigma_{max} + \sigma_{min}}{2} \tag{3.1c}$$

Two ratios can be found

$$R = \frac{\sigma_{min}}{\sigma_{max}} \qquad A = \frac{\sigma_a}{\sigma_m} \tag{3.1d}$$

(R refers to the stress ratio while A refers to the amplitude ratio.

To generate useful data to aid fatigue design through stress-life method, stress-life fatigue test is generally conducted using many samples showing different completely reversed stress amplitude values. This happens through fatigue lives of arranged specimen. This obtained fatigue test data is generally represented through plotting on semi-log or log-log axis.

Moreover, Figure (3.1a) indicates bending fatigue values pertaining to steel-plotted on semi-log coordinates. The figure shows a curve, called as the S-N/Wohler curve [56].

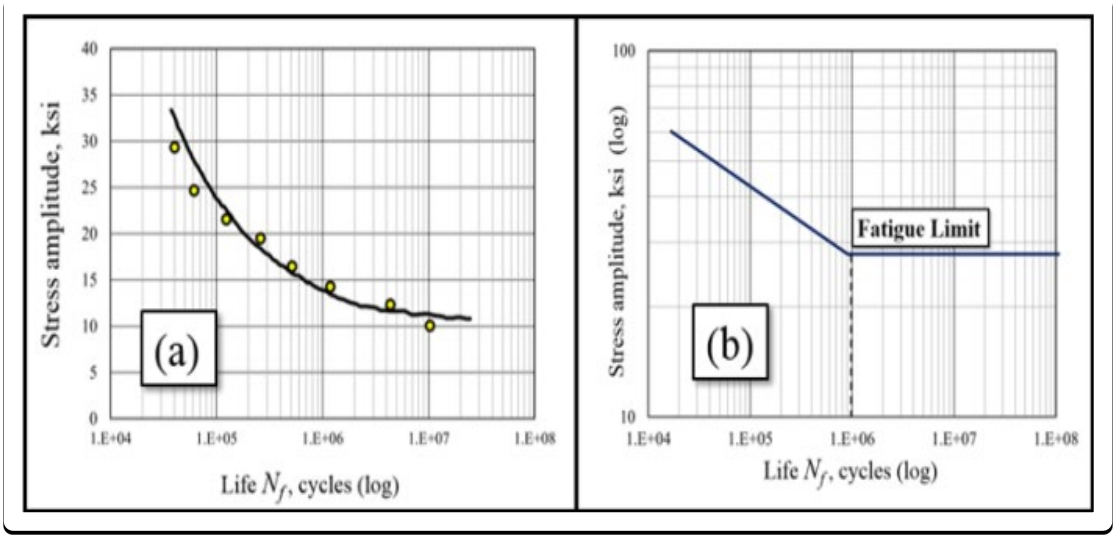

(a) (b)

Figure 3.2. A plot of the S-N curve. a) Semi-Log plot, b) Log-Log plot [56].

The data is plotted on a log-log scale, illustrated in Figure (3.12b) which makes the curve linear. This line/curve is negatively sloped called as finite life region while the horizontal line shows infinite life region. There is a point on an S-N curve that turns a curve to a horizontal line called as the "knee" of S-N curve. In addition, it embodies fatigue/ endurance limits, which is connected with the cracking nucleation, which can be arrested through initially a grain boundary/major micro-structural barrier, when creating log-log plots for practical stress-vs-fatigue life out of S-N fatigue.

According to Lee and Lee et al. when producing log-log plots of practical stress versus fatigue life through S-N fatigue test, y-coordinate shows stress amplitude/range while x- coordinate shows the number of reversals to failure. In this case, fatigue-life points towards required life for nucleating and growing small cracks with visible lengths. The following equation shows traditional S-N curve in terms of log-log coordinates through the following equation [57].

$$\sigma_{a=}\sigma_f(2N_f)^b \tag{3.2}$$

Where ‘b’ represents fatigue-strength exponent (the slope of the curve) and σ_f, means fatigue strength coefficient. The log-log S-N played a role for developing this

expression, and it is a popular equation for fatigue studies. The above equation is also called a Morrow's relation [57].

3.1.4. The Kind of Fatigue

There are many types of fatigue, which can be illustrated as follows:

3.1.4.1. Load Based

It is experienced whenever stress levels are low with elastic deformation; the fatigue is regarded as high-cycle fatigue. It needs higher number of cycles to cause a fracture. This is more useful for its stress regime, but stress is more than the endurance, so it causes plastic deformation with low cyclical fatigue. The cycles are few as compared to what can cause a fracture. Here, the stress is not very dangerous, and strain of the material is appropriate. Low cyclical fatigue is also called as strain-based fatigue. Load direction is another factor that affects fatigue. Multi-axial weights cause varying features of fatigue as compared to single -axial loads. Pure mechanical fatigue is generally rate-independent.

3.1.4.2. Environment Based

Nieslony argues that operational temperatures and vaporous and corrosive atmospheres influence fatigue features. Under high temperatures, fatigue is rate-dependent [58].

3.1.5. Factors Influencing on Fatigue Life

There are some factors affecting the life of the fatigue, these factors are as follows:

3.1.5.1. Manufacturing Process

Fatigue properties refer to higher shaping, extrusion and rolling processes and show up within the transversal direction. Some detailed procedures like shot peening, cold rolling, and different solidifying/heat treatment procedures prompt compressive excess anxieties, and decline the percentages of fracture, which begins and improves fatigue properties. Tensile residual stresses increase crack emergence.

Different collecting forms include forming, drawing, expulsion, rolling, machining, punching and so on. That delivers unclean surfaces and reduces fatigue life. An uncomfortable surface has more fracture start destinations because of roughness and severities. Cleaned and ground surfaces have super high fatigue life because of least severities.

3.1.5.2. Component Geometry

In general, holes/notches/joints, which refer to the stress source, increase/encourage emergence of cracks; however, fatigue lifetime of a notch part is not the maximum amount as that of secondary un-scored one once exposed to like loads.

3.1.5.3. Type of Environment

Watery and destructive atmospheres advance crack start and increase fracture development rate. On the other hand, crack tip dampening begins because of the buildup of ecological items at the crack tip, which may plunge fracture event rate to some degree.

Nonetheless, the general impact of such situations promotes crack growth rate. Below specific temperature, fatigue resistance in many metals reduces with the expansion in crack growth ratio because of the influence of the creeping crack.

3.1.5.4. Loading Condition

Multi-axial loads diminish fatigue life in correlation with uniaxial loads because of pure torsional loading. Mean stress impacts fatigue life. Positive tensile average stresses reduce it as well while positive average anxiety might expand it. However, the effect of little stress is important with little strain or great cycle fatigue system [59].

3.1.6. Notches and their Effects

Notch influence has been an important problem in the fatigue information for more than 125 years, since Wohler showed that adding material to a railway axle might make it weaker in terms of fatigue endurance. He stated that the radius at the shoulder between smaller and a larger diameter has prime importance to the fatigue life of axles and that fatigue cracks will start at the transition from a smaller to a larger section.

Nevertheless, notches cannot be run-away in several constructions and machinery. Notches are risky, so they should be frequently decreased for reducing damages through an appropriate treatment.

To recognize the impact of notches and to deal with them, we should consider performance of flat specimens and the following five factors:

1. Stress and strain concentrations.
2. Stress gradient.
3. The effects of mean and residual stresses.
4. Local yielding.
5. Nucleation and crack growth.

In some cases, one of the five parameters by itself may explain the difference in behavior between a smooth part and a notched part that has an equal cross section at the root of the notch. Even when several parameters are involved, it is often possible to use “variable constants” or “notch factors” that correlate the test results. We intend

to avoid the use of adjustable factors and must therefore consider the effects of all five parameters. At the end, this will be less difficult than the adjustment of a single notch factor.

Notches focus on stress as well as strain factors. It can be measured by the elastic stress concentration factor K_t. "a" is ratio of the maximum stress, and strain is E at the nominal stress notch S or strain e.

$$K_t = \frac{\sigma}{S} = \frac{\varepsilon}{e} \qquad \text{As} \quad \text{long} \quad \text{as} \quad \frac{\sigma}{\varepsilon} = constant = E \tag{3.3}$$

Where σ and ε represent local stress and strain while S and e represent nominal stress and strain, respectively. Let us consider a sheet with a central circular hole. K_t, which depends on the ratio of hole diameter to sheet width. Figure (3.3) below showsK_t, plotted versus the ratio of hole diameter to sheet width. Two curves are shown. Higher one shows nominal stress, which is well defined, and the load is separated by sum area (w*t). However, the lower curve shows nominal stress, which is well defined because the overall load was divided by the area. The area remaining after the hole has been cut out. The net area was taken for identifying nominal stress because stress concentration influences unless otherwise stated.

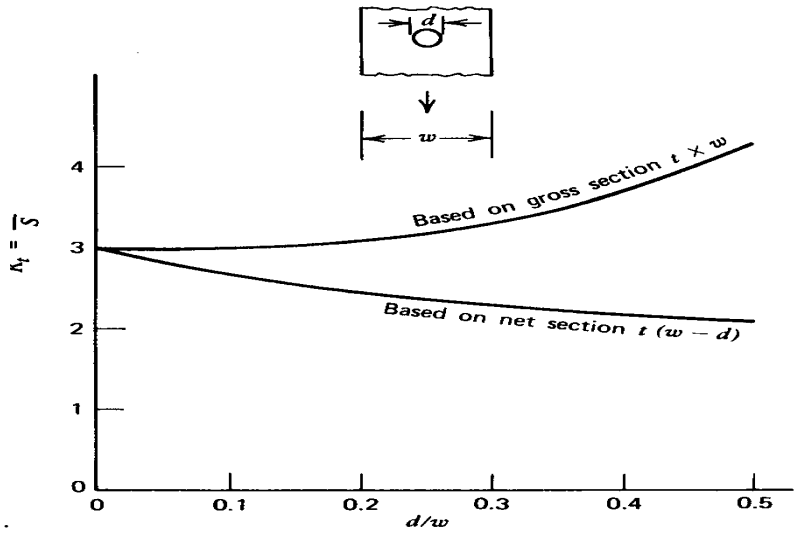

Figure 3.3. Elastic stress concentration factor for a central circular hole in a sheet [60].

When load is divided by total space, within the higher curve, load is divided by total or gross area. That is to say that the hole is remaining when the opening has been cut out. The net space is used to outline the nominal stress once utilizing stress concentration factors unless otherwise expressed. Stress intensity issues begin with nominal stress and have a tendency for gross space usage when crack does not exist. Figure (3.3) shows the stresses close to a hole in the middle of a large sheet. This downside was investigated and resolved as early as 1898 by brandy [60].

The next equations are about the axial stress $\sigma_y$and the transverse stress σ_x on a transverse line through the center of the hole for plane. Stress are taken from Grover, [61].

$$\frac{\sigma_y}{S} = 1 + 0.5(\frac{r}{x})^2 + 1.5(\frac{r}{x})^4 \tag{3.4}$$

$$\frac{\sigma_x}{S} = 1.5(\frac{r}{x})^2 - 1.5(\frac{r}{x})^4 \tag{3.5}$$

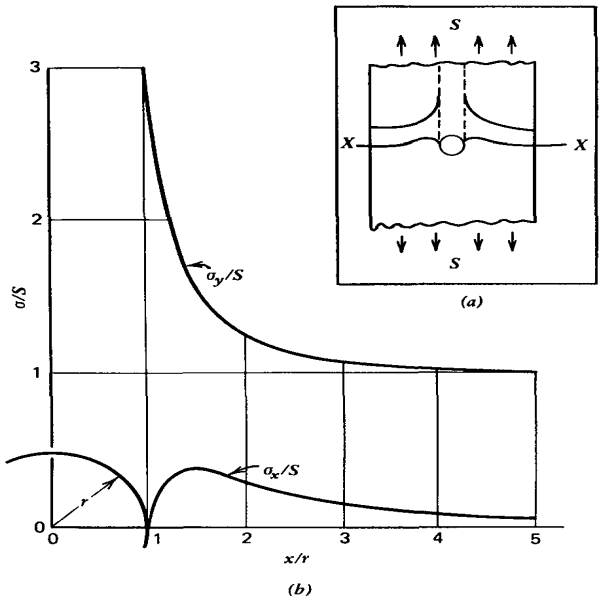

Figure 3.4. Stress distribution along the section X-X near a hole in a wide sheet [62].

Where,

S = nominal stress.

σ_y= axial stress.

σ_x= transverse stress.

x = distance from center of hole.

r = hole radius.

Values are put versus in Figure (3.7), It can be noticed that σ_y / S decreases quickly because the hole's edge has greater distance before. Kt, which is 3 at 0.2% distance. The σ_y / S value is just two. Nonetheless, at $(2r)$ distance, the value is just 1.07.

In other words, the stress at hole's edge is three times nominal stress. However, the distance from hole's edge is equal to the diameter; it is only around 7% higher than the nominal stress. In addition, the state of stress at the notch is uniaxial and away from the notch, and it is biaxial for this plane stress condition.

The slope of the σ_y versus x curve at the hole's edge is another rapid decrease measurement of stress reduction as we move away from the edge of the hole. The rapid stress decline when the distance increases from the notch and biaxial or triaxle stress existence takes place at a little distance from the notch, which generally happen in case of stress concentration. They explained why we could not expect to predict the behavior of notched parts with great accuracy by applying stress concentration factors to the fatigue strength values obtained from smooth parts.

According to Creager, the numerical values of stress gradients or simple design formulas for stress distribution near notches are not often readily available in the literature. In case of deeper and thinner notches having ends like semi-circle, a formula just like the one, which is applicable in linear elastic fracture mechanics (LEFM) shows stress distribution [62]. It is as follows:

$$\sigma_y = \sigma_{max}(\frac{0.5r}{0.5r+d})^{\frac{1}{2}} \quad (3.6)$$

Where (d) refers to the distance between the edge and the notch having radius (r). The evaluated stress concentration is not unique because it relies on the loading mode and stress type that is used to estimate Stress Concentration FactorK_t. Regarding circular hole in an extensive sheet, we have the following stress concentration factors:

In Tension	3
In Biaxial Tension	2
In Shear	4 based on maximum tension.
	2 based on maximum shear.

The elastic stress concentration issues test is mostly concerned with elasticity, which is numerically as well as experimentally measurable. The common principal and most multipurpose numerical methodology are the finite part technique [50].

3.1.7. Factors Causing Fatigue Failure

As far as the factors causing fatigue failure are concerned, there are basic factors and additional factors, which can be clarified as follows:

3.1.7.1. Basic Factors

Dieter and Bacon (1986) point out that some basic factors result in fatigue failures, which include:

1. High tensile stress.
2. Significant stress fluctuation.
3. Repetitive stress or more cycles of applied stress in comparison with the endurance limit.

3.1.7.2. Additional Factors

1. Stress concentration.
2. Corrosive atmosphere.
3. High temperatures.
4. Overloading.
5. Vulnerable structural details.
6. Combined and Residual stress.

3.1.8. The Mechanism of Fatigue

Nucleation and causing of breaks create significant fatigue components. The start of fatigue-induced cracks on a plain surface under encompassing situations can account for 90% connected cycles whereas break creating can demand just staying 10% cycles. Circulation of cyclical changes damages while assuming it as unique. The procedure under repeated loading separates into three phases.

3.1.8.1. Initiation of Cracking Stage

This is the total of sequences cycles, which is necessary to begin cracking. It typically dislocates piles and create issues including roughness of surfaces, voids, and scratches. Consequently, during this age, fatigue can affect the surface material. The stress concentration factor k_t is another factor to be thought of during the crack initiation prediction.

On the other hand, crack nucleation and growth square measure sometimes believed to initial crack propagation. During the generation, slip features substantially affect crack tip malleability, and they have grain sized orientations and stress levels. This takes place as a result of the size of crack size such as metal microstructure [63].

3.1.8.2. Crack Propagation Stage

This is the quantity of cycles, which is necessary to develop a steady crack and transform it into a significant and threatening size that is largely measured through finding stress levels. Since most regular material contains marks, the crack development of fatigue is the most expected part of it. Crack development resistance, when the break infiltrates into the material, relies on the material as a figure property. It is no longer a surface phenomenon. The stress concentration factor is an essential factor for fatigue growth prediction.

Crack development means extended crack dissemination ordinary for basic tensile stress plane and highest shear stretch. During this step, extended crack attributes slightly affect the microstructure properties as compared to Stage I split [2]. This is due to the crack front and plastic crack tip in Stage II, which is typically and significantly bigger than the material microstructure.

3.1.8.3. Rapid Fracture

Extremely fast and critical crack growth happens once the crack length achieves an important value. Since quick crack happens almost instantly, there is no fast fracture term in fatigue life expression. The toughness of fracture K_{IC} of metal is a main factor for rapid fracture prediction or design against fracture. In other words, the steps of fatigue mechanism start like this:

1. For the duration of a substantial total number of cycles, the harm is created on the microscopic level and developed up to a naturally visible split.
2. The perceptible crack develops for every cycle until it achieves a necessary extent.
3. The broken part fractures since it can no longer manage the pinnacle load [64].

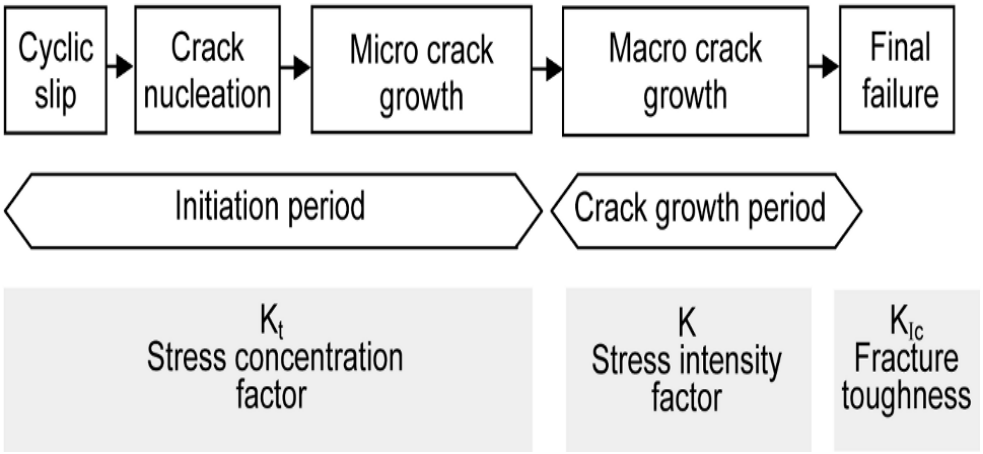

Figure 3.5. Dissimilar phases of the fatigue life and relevant factors [63].

3.1.9. Variables of Fatigue

When there is no constant external load, material state varies with time. Different variables like stress or strain can describe the state of the material. Fatigue is generally controlled through controlling variables. A typical load cycle peak to peak, as it gets back to its position and cycles have different amplitude. Elastic substances sometimes have cyclical load, which creates periodic stress reaction, and in those cases, load cycle is easy to define. The Figure (3.6) Illustrates that the stress is a variable that controls fatigue.

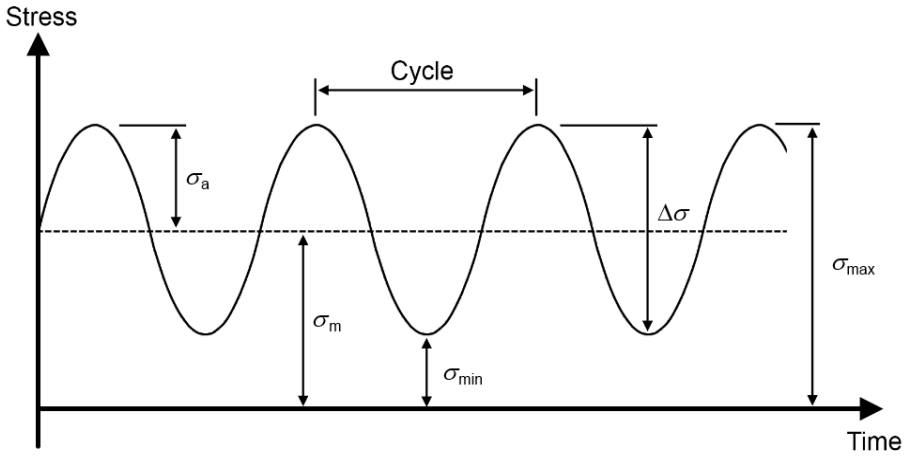

Figure 3.6. Commonly use variables for predicting fatigue [65].

3.1.10. Low and High-Cycle Fatigue

Fatigue analysis is not conducted just for stress response, but it gained substantial focus because large numbers of analyses were performed when stress-based models of the area unit were presented and deemed as helpful. Nevertheless, load cycles were differentiated based on creating low-cycle fatigue (LCF) or high-cycle fatigue (HCF). On the other hand, the difference between them is not so distinct because observations are made based on every 10,000 cycles. HCF stresses area unit that is low, and the stress-strain combination is somewhat elastic. Once operating with HCF, stress varies while for LCF, strain varies or profligate energy area unit as shown in Figure 3.7.

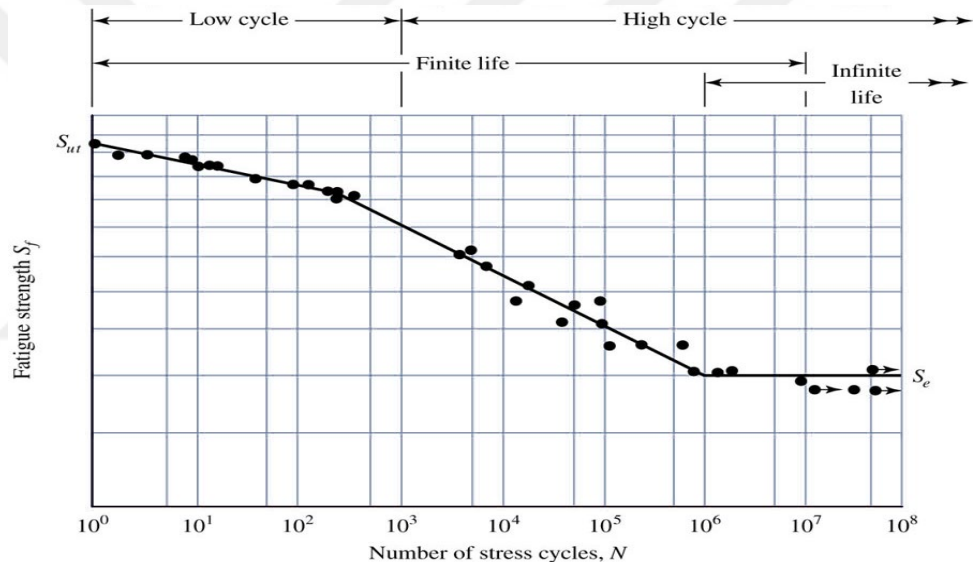

Figure 3.7. Low- and High-Cycle fatigue [66].

3.1.11. Fatigue Life Prediction

The fatigue life prediction approaches can be separated into two main groups according to the usage of particular method. The first group is made up of prototypes established on the prediction of crack nucleation, using a mixture of damage evolution rule and conditions established on stress/strain in the components. In addition, the key point of this approach is the lack of dependence on loading and specimen geometry because the fatigue life is determined only by a stress/strain criterion [67].

3.1.12. Crack Propagation Modes

In general, three loading modes exist involving varying crack surface displacements, which are illustrated in (Figure 3.8.), they are as under:

Mode I: Opening or tensile mode (crack faces stretch apart)
Mode II: Sliding or in-plane shear (crack surfaces slide over each other).
Mode III: Tearing or anti-plane shear (crack surfaces move parallel to each other).
However, our discussion focuses on Mode I as it is a predominantly loading mode, and later same treatments is extendible to Modes II and III.

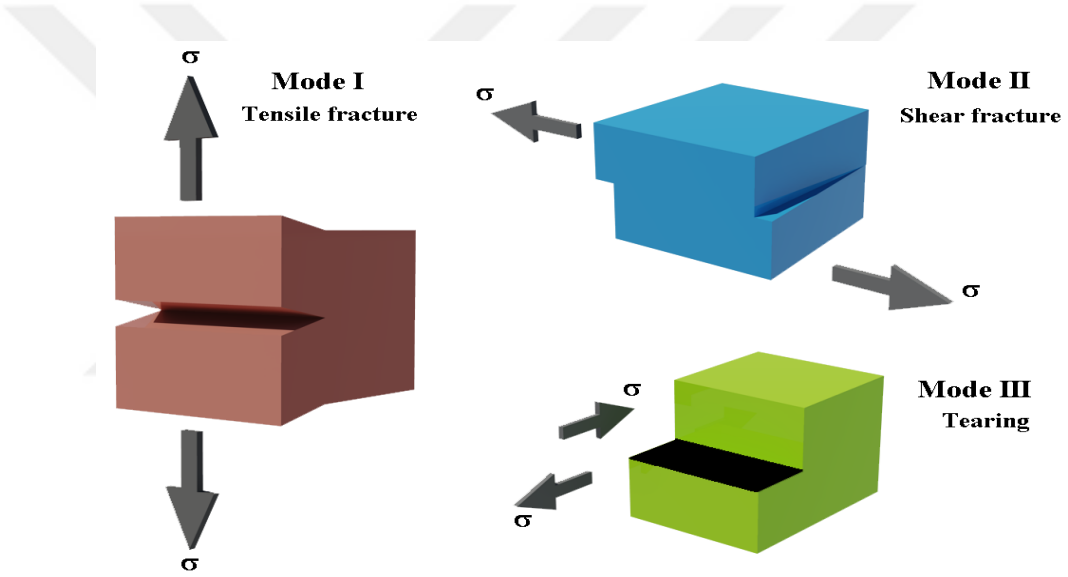

Figure 3.8. Three types crack propagation modes.

3.1.13. Effect of Stress Concentration on Fatigue

Falen and Whitley believe that the fatigue procedure starts with microscopic and macroscopic gaps inside the structure. These gaps cause a growth in local stress force within a stress field, donated to as stress concentration.

On the other hand, the intensity of the stress concentration is found out using stress concentration factor (SCF) denoted by the symbol K_t. The SCF in its most straightforward frame is characterized as the ratio of the highest natural stress and

reference stress. The most widely recognized stress concentration factor describes a hole located in the center of an infinite plate, loaded in tension, as seen in Figure 3.8. It is illustrated as the stress distribution due to the hole shown. For this situation, as goes to zero, K_t = 3 [68].

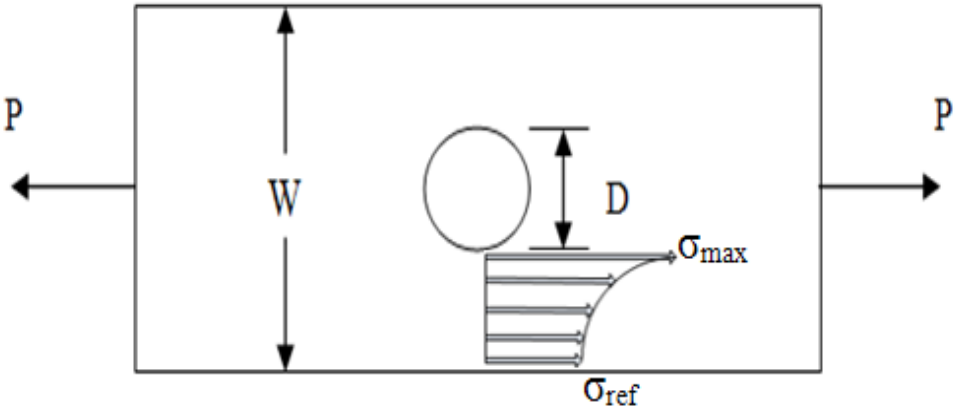

Figure 3.9. Infinite plate with centralized hole loaded in tension [68].

There is a broad range of sources that give K_t diagrams to parts containing different geometries, loading conditions, and features. SCFs are not all inclusive; therefore, engineers must give references for these charts to guarantee that the SCF precisely represents their specific analysis of metallic structures. The favored handbook for SCF values is Peterson's Stress Concentration Factors [69].

Stress concentration factors are an important aspect of any fatigue analysis. Cracks in the main nucleate in a specific range where stress is at its maximum along these lines as well as on the way to nucleate at a stress concentration. Because of this, proper stress concentration factors must be used to compute the maximum stresses. The structure precisely anticipates the fatigue life.

However, for analyzing fatigue, net stress concentration K_{tn} should be calculated to determine the maximum structural stress. Net stress concentration factor accounts for the net cross-sectional area at the position of interest, whereas the gross stress concentration factor, K_t accounts for the overall cross-sectional area at the site of

interest. Consider a flat plate with a centrally located hole loaded with tension with thickness h as shown in Figure 3.9.

In addition, the peak stress occurs at the critical points, C. Using the reference stress factor for both K_{tn} andK_{tg}, the difference between the two elements can be determined, as shown in equations 3.7, 3.8, and 3.9 and 3.10 through Figure 3.10.

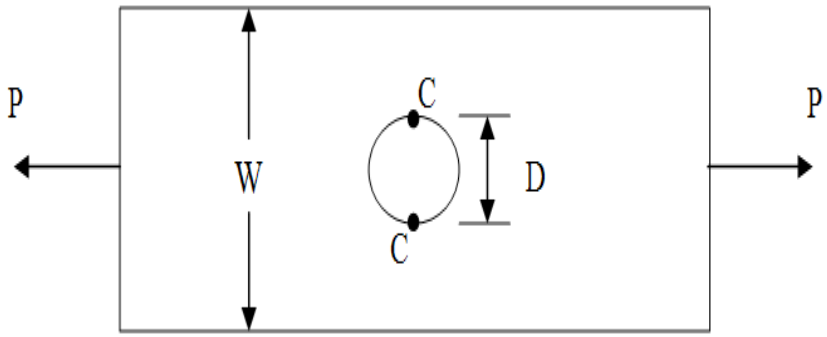

Figure 3.10. Plate with centralized hole loaded in tension [68].

$$K_{tn} = \frac{\sigma_{max}}{\sigma_{ref,net}} = \frac{\sigma_{max}(W-D)h}{P} \tag{3.7}$$

$$\mathrm{K_{tg}} = \frac{\sigma_{\mathrm{max}}}{\sigma_{\mathrm{ref,gross}}} = \frac{\sigma_{\mathrm{max}}\mathrm{Wh}}{\mathrm{P}} \tag{3.8}$$

$$\mathrm{K_{tn}} = \frac{\mathrm{K_{tg}(W-D)}}{\mathrm{W}} \tag{3.9}$$

The past conditions prove that the calculation of net stress concentration factor represents irregularity in the center point of the plate. However, the gross stress concentration factor affects the thickness of the plate [70].

Materials have unstable degrees of a property called notch sensitivity. Notch sensitivity material encounters the full theoretical stress concentration. Ductile metals can disperse the strain at a notch (or a crack tip) even more uniformly, accordingly reducing the crack and lessening the impact of stress concentration. Furthermore, the

factor of notch sensitivity (q) is an empirically determined constant that relies on the notch radius and material strength.

This property is measured by the notch sensitivity ratio (q), which is the proportion of definitive rigid qualities of a smooth malleable surface of a scored elastic specimen. The notch sensitivity of a metal may be an estimate; however, sensitive metal is likely to have notches or geometric discontinuities.

Consequently, the properly modified stress concentration factor is outlined by the following equation:

$$K_f = 1 + q(K_t - 1) \tag{3.10}$$

Here K_t represents stress concentration factor for a given geometrical shape, and q shows the material's notch sensitivity ratio. For a notch sensitivity ratio of one, the full stress concentration factor is considered as utilized. If the notch sensitivity ratio is zero, the stress concentration factor will be one. on the other hand, we do not have the information for the score, which affectingly proportional to the material we are utilizing, accept for when it is zero and while considering full theoretical stress concentration factor.

One approach is securing against initial fatigue failure, which minimizes the impact of stress concentration. This can be achieved by supplanting sharp corners in the high-push zone with adjusted filets ideally with a filet span as vast as conceivable. Whatever other unavoidable scores ought to limit or adjust in order to minimize the stress concentration. Any burrs on machine or stamped parts could likewise work as stress risers. Therefore, such parts would be mechanically built the fatigue life. Such strides may add minor expenses to the creation of the parts but that would often be far less costly than a rash of field failures due to careless design [69].

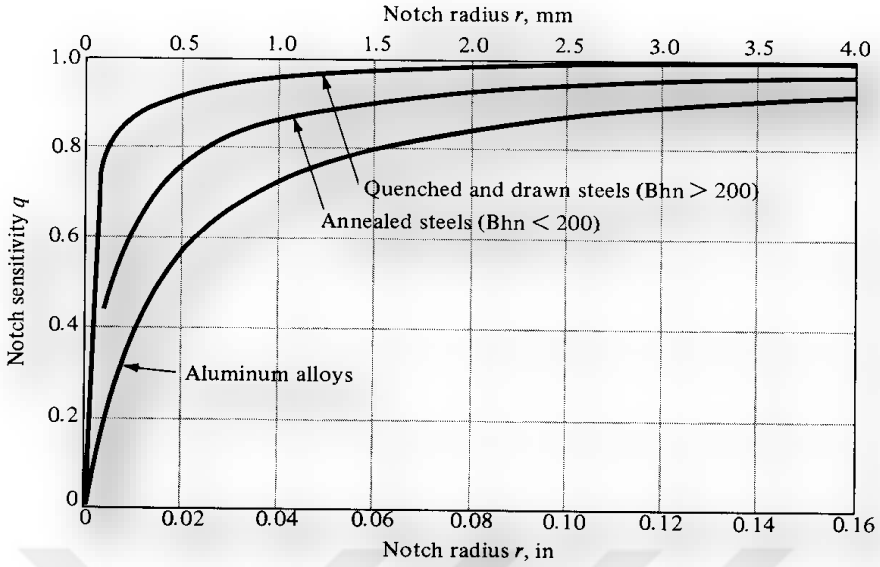

Figure 3.11. Notch sensitivity factors [71].

While evaluating the influence of notches on the fatigue resistance of a part, we use the factor of fatigue stress concentration K_f instead of the stress concentration issue k_t. The issue of fatigue stress concentration is usually smaller than the stress concentration factor. Furthermore, fatigue life is linked with the following:

1. The fatigue life of the component decreases due to the presence of notch, which creates similar multi-axial state of stress as created by small cracks, flaws etc., which is presented in the actual component.
2. Life prediction using notch specimens should be used to predict the life of a component.
3. Life of a component decreases with increase in stress concentration factor.
4. Life of a component at high temperature (823K) is less than that at room temperature.
5. Life estimation by simulation agrees reasonably with the experimental values, which can used to predict the life of the component if material properties are known.

3.1.14. Failure Criteria Methods

These ways describe varied curves, which link endurance limit with irregular stress axis for yielding either strength, S_y ultimately strengthS_u, or fracture stress S_f on stress axis. The relations established through Stress-Life module are as follows:

Goodman (England, 1899): $$\frac{\sigma_a}{\sigma_e} + \frac{\sigma_m}{\sigma_{uts}} = 1 \quad (3.11)$$

Gerber (Germany, 1874): $$\frac{\sigma_a}{\sigma_e} + (\frac{\sigma_m}{\sigma_{uts}})^2 = 1 \quad (3.12)$$

Soderberg (USA, 1930): $$\frac{\sigma_a}{\sigma_e} + \frac{\sigma_m}{\sigma_y} = 1 \quad (3.13)$$

Morrow (USA, 1960s): $$\frac{\sigma_a}{\sigma_e} + \frac{\sigma_m}{\sigma_f} = 1 \quad (3.14)$$

Graphic evaluation of those equations has been presented in Figure (3.12) Gerber and Goodman, Year) present two greatest generally acceptable ways. Literature shows test information reduces between the curves presented by Goodman and Gerber, which give simplicity as well as somewhat traditional values. Different factors are relevant to mean stress equations used for the standards of tensile mean stress [72].

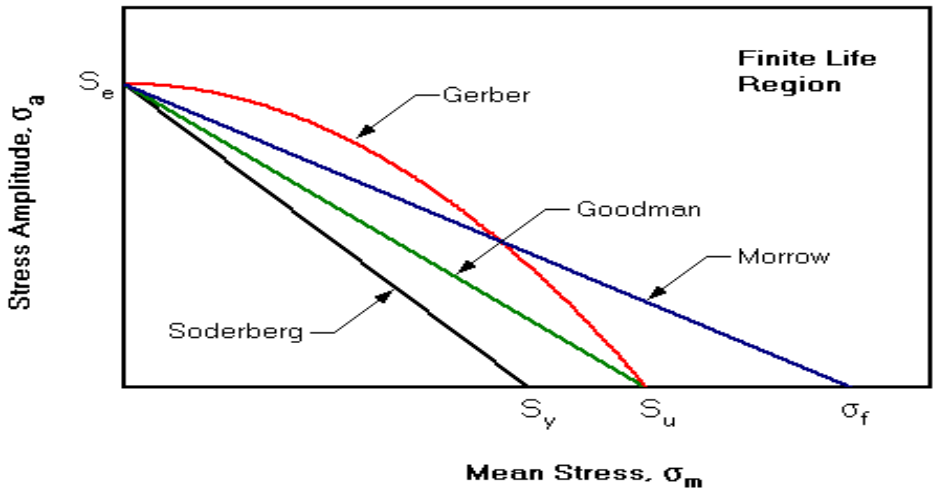

Figure 3.12. Comparison of mean stress equation [72].

Wherever mean stress has little relavancetive to the alternating stress (R<1), very less distinction exists between ways. Soderberg technique is traditionally used for applications with no expectation of fatigue failure but tough steels, Goodman curves and Solar Day model measure it. For ductile steels (S_f>S_U), solar day model forecasts less sensitivity. This is because R approaches one, and the models that show giant variations. There is absence of experimental information obtainable in this state.

3.1.15. Von Mises Stress Method

In (1904) Huber first introduced the concept of Von Mises stress, but it became popular in (1913) when Richard Von Mises presented his version. Both versions proposed a mathematical equation, but "Von Mises stress" is indeed an appropriate physical interpretation.

Yield stress happens when a material converts its behavior from elastic to plastic. Here we often say that if stress is more than the yield strength, the material yields. Nevertheless, it should be noted that stress tenses and it is not possible to represent it using a specific value. If a material is pulled in the x-x direction, the material will start yielding when the x-x stress component is more as compared to the yield stress.

On the other hand, stress tensors are generic and are not uniaxial. If the stress component is non-zero, the material will begin to yield.

3.1.16. Maximum Principal Stress Theory

As selected by this model, failures occur as the maximum stress reaches closer to the total strength. For the surface stress, we have given an equation below (3.9).

$$\sigma_1 = \frac{1}{2}(\sigma_x - \sigma_y) + \frac{1}{2}\sqrt{(\sigma_x - \sigma_y)^2 + 4{\tau_{xy}}^2} \tag{3.15}$$

3.1.17. Distortion Energy Theory

It suggests that overall strain isolates in two parts. The first component is the volumetrically (hydrostatic) strain life. The second component is the form. The theory suggest that the yield occurs once the distortion exceeds the yield purpose in an easy tensile test, which leads to failure criteria represented by the equation below:

$$(\sigma_1 - \sigma_2)^2 + (\sigma_1 - \sigma_2)^2 + (\sigma_1 - \sigma_2)^2 = 2\sigma_y \quad (3.16)$$

Von Mises hypothesis is more famous because of its approach of giving failure criteria the energy perspective. A significant portion of the ductile materials can be expected using Von Mises.

Principal stress theory, then again, has exceptionally constrained applications. It can be used for brittle materials like cast iron. When a mechanical engineer predicts failure, it is possible for the Von Mises to be significantly used more than principal stress criteria. However, designers use Von Mises stress to find out whether their design is capable of bearing a specific load [69].

3.1.18. Uses of Von Mises Stress

Generally, this method is considered as Von Mises safe haven for design engineers because it helps an engineer to predict when that a design will fail, if he/she finds highest Von Mises stress value more than the material strength. It works well for majority of cases specifically for-ductile materials.

Von Mises a simple tension test is regarded as an easy way to find out material failure. When a material is pulled from both sides, it reaches a yield point, where it is considered as failed. This basic tension test is unidirectional.

3.1.18.1. Expression for Von Mises Stress

The two quantities given above have a relation when we use the distortion theory of energy failure. In that case, the failure condition is as follows:

$$\left[\frac{(\sigma_1-\sigma_2)^2+(\sigma_2-\sigma_3)^2+(\sigma_3-\sigma_1)^2}{2}\right]^{1/2} \geq \sigma_y \tag{3.17}$$

Left side of this equation shows Von Mises stress.

$$\left[\frac{(\sigma_1-\sigma_2)^2+(\sigma_2-\sigma_3)^2+(\sigma_3-\sigma_1)^2}{2}\right]^{1/2} = \sigma_v \tag{3.18}$$

Consequently, an engineer checks whether Von Mises stress is actually exceeding the yield strength. Here, the failure condition will be

$$\sigma_v \geq \sigma_y \tag{3.19}$$

Von Mises on the other hand, in many fields, Von Mises yield criterion is applicable, which is formulated through Von Mises stress. In this case, a specimen should start yielding at the point where the Von Mises stress reaches closer to the yield strength. Von Mises Since Von Mises is not fully relevant to first stress invariant, it applies to plastic deformation and ductile material analyses.

James Clerk Maxwell (1865) explained general conditions in his letter to Lord Kelvin but Richard Edler Von Mises worked on it until he presented it in (1913). Tytus Maksymilian Hube (1904) described this phenomenon in a polish paper, which shows that it depends on total strain energy and not on second deviatory stress.

3.1.19. Predicting Fatigue Failures

Engineers design structures from end towards beginning, as they understand that the used materials might fail or might develop certain defects during loading and unloading cycles.

For materials vulnerable to fatigue failure, like paper clips, which easily bends and so, predicting failure is easier because it is a ductile and not a brittle material. Nevertheless, many brittle substances such as advanced ceramics are used because of their low-densities and high-temperature tolerance. Experts emphasized the need for new processes to identify or predict cyclic fatigue failures of different substances. Failure models should be improved because predictions fail on a microscopic level. Ductile materials easily fail because of their atomic rearrangement/readjustment properties in their crystals called as dislocations. A paper clip fails because of many dislocation defects that later makes atomic rearrangement difficult, which ultimately brittles the metal and creates cracks. In case if we try a testing rig for determining fatigue response of a paper clip, we will be able to determine the alloy's future behavior with more accuracy.

Intrinsically brittle materials have a tendency to fail, for example, a dish drops down and turns into pieces. This happens because in brittle materials, atoms have less mobility. Despite the fact that they withstand compression better than ductile substances, they have a tendency to crack and break rather than bend/deform. Nevertheless, cracks emerge out of a single heterogeneous site, which is difficult to assess, which is evident from the fact that if some dishes are dropped, not all of them will break. When a design includes brittle substances, hundreds of samples are tested to determine their failure possibilities [73].

3.1.20. Prevention of Fatigue Failure

Enhancement in design is the most effective methodology of improving fatigue performance. The following guidelines help preventing fatigue failures because they eliminate/reduce stress through streamlining a part or the whole design.

1. Avoid sharp surface because they are more likely to tear apart because of punching, stamping, shearing, or other activities. It is also imperative to stop surface discontinuity development while processing because that has a similar effect.
2. Try Reducing/eliminating residual tensile stress/as during the manufacturing process.
3. Develop the fabrication and fastening procedural details.

3.1.21. Design against Fatigue

There are four major ways, which can change life validation for mechanical components. That shows growing degrees of refinement, these ways are as follows:

1. Design to keep stress under line of fatigue limit (limitless period of time idea).
2. Fail-protected, swish degradation and fault-tolerant styles: Instruct the shopper to come after components once they return up short, style specified there is no single purpose of failure. Therefore, once any section or the whole fails, it does not prompt destructive failure of the total system.
3. Safe-life design: One must style (conservatively) for a hard and fast life. Once that the user is educated to exchange the spare a brand new one (a supposed half-life, finite period of time conception, or "safe-life" style practice); planned degeneration and disposable product square measure variants that style for a hard and fast life once the user is educated to exchange the complete device.
4. Damage tolerant plan: A producer should utilize the research and ask workers to observe the cracked part periodically and replace it once the crack crises basic length. This approach needs a definite expectation of the speed of crack growth

between inspections. However, the designer sets some aircraft repair checkup visit to measure whether the components need replacement even when the crack remains within the “slow growth " stage. This can be often alluded to as damage accepting "retirement-for-cause [74, 75].

3.1.22. Factors Influencing S-N Behavior

The situational fatigue condition for S-N behavior is generally fully reversed R= -1 bending or axial loading using small, un-notched specimens. They showed how mean stresses affect the fatigue condition. In addition, many other factors affect the reference fatigue condition. Nevertheless, some of these are complex.

3.1.22.1. Microstructure

Some metals have big grains with low yielding strength and a lower fatigue limit; however, thick-grained metals have better fatigue properties at more temperature. Crack growth barriers exist in precipitates, impurities, phase transformations and grain boundaries, etc.

3.1.22.2. Manufacturing Process

The features of fatigue include forging, extrusion and rolling, which are less towards the transverse direction. Processes like as shot peening and cold rolling involves it. In addition to hardening or heating, compressive residual stress inducing processes might create crack or enhance the substances' fatigue properties. Moreover, tensile residual stresses increase chances of crack initiation. Manufacturing processes such as forming, forging, extrusion, drawing, and rolling create roughness and rough surfaces have more crack initiation sites. Polished/ground surfaces have better fatigue life because of low asperities.

3.1.22.3. Component Geometry

Discontinuities such as holes, notches and joints increase the overall stress and increase initiation chances; therefore, a notched component's fatigue life is lower as compared to an un-notched under Similar Loads.

3.1.22.4. Type of Environment

Aqueous/corrosive atmospheres stimulate cracks and rate of crack growth, but crack tip blunting/closure can dip crack growth to a certain extent. Most of the metals lose their fatigue resistance under high temperatures, which promotes crack growth.

3.1.22.5. Loading Condition

The multi-axial loads decrease the fatigue resistance as compared to uniaxial loads while the case of pure torsional load is an exception. Nonetheless, mean stress influences fatigue life, positive \mean stress diminishes it while negative mean stress increases it. The mean stress effect becomes highly significant under low strain or high cyclical fatigue regimens.

3.1.22.6. Surface Finish

Since most weakness disappointments begin on surfaces, a surface significantly influences fatigue conduct. Its impact on fatigue life is negative in cases of surface roughness and microstructure formation.

Most designing parts, in any case, are not very cleaned, and crushing or machining, anyway of the possibility that done carefully, will make corruption in fatigue quality relative that appeared in Figure 3.13.

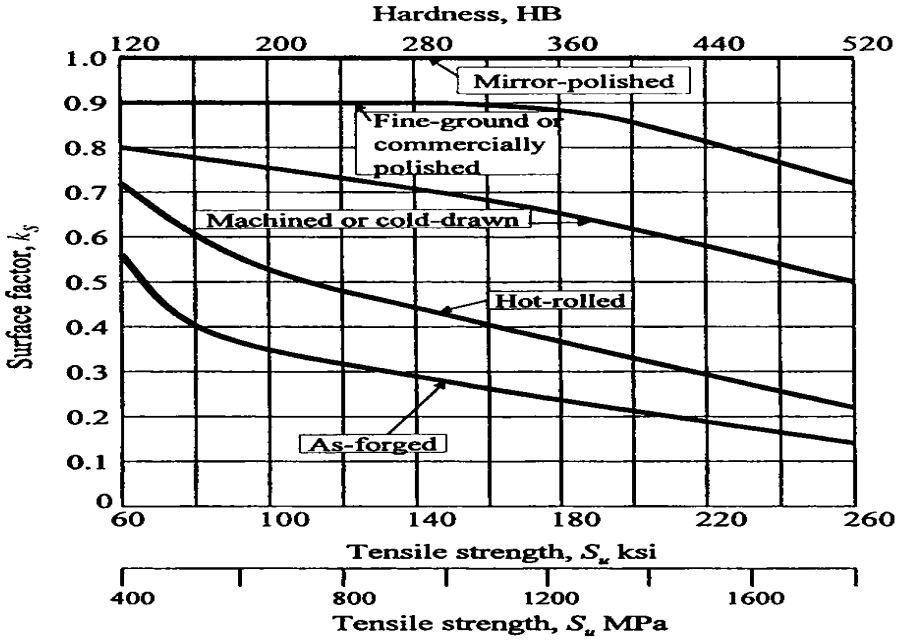

Figure 3.13. Surface finish effects on fatigue limit of steel [76].

Fatigue limit manipulation: Surface element diminishments for pasting ranges from 0.9 to 0.7 and for machining from 0.8 to 0.5 which is expandable. These are critical diminishments. One clear conclusion here is to stay away from the hot-rolled and-fashioned surfaces [77] & [78].

3.2. SENSOR

A sensor can be defined as an information sensing and collecting device. Moreover, it gives an output signal according to the measured parameter. For long time, its data was classified regarding the type of energy domains but Micro-Electro-Mechanical Systems (MEMS) devices commonly overlap many fields and do not fit just in single category. Their energy fields are as follows:

1. Mechanical - force, velocity, acceleration, pressure, position.
2. Thermal - temperature, heat flow, entropy.
3. Chemical - concentration, composition, reaction.
4. Radiant - electromagnetic intensity, wavelength, polarization reflectance, refraction, transmittance.

5. Magnetic - permeability, field intensity, flux density, magnetic moment.
6. Electrical - voltage, current, charge, resistance, capacitance [79].

In addition, the sensitivity of the sensor specifies what proportion the sensor has output changes once the input quantity is measured for changes. However, if the mercury in a measuring device moves 1 cm once the temperature changes by 1 °C, the sensitivity is 1 cm/°C (it is that the slope with a linear characteristic). Some sensors may affect what they measure.

Miller and Ibrahim pointed out that sensors must be designed to have little impact on what is measured. That has to say, making the device smaller typically improves this and should introduce alternative supports. This generally takes place near extreme stress concentration areas [2].

However, cycle count to failure relies on changing applied stress levels. Consequently, a structure's fatigue life is identified by individual stress duration earlier. In general, the S-N method as well as some empirical laws/cumulative damage rules help finding out service fatigue life. Non-destructive tests or microscopic observation cannot determine the accumulative fatigue damage.

Furthermore, real service loading of a structure cannot be considered when the actual loading significantly varies. The currently applied inspection procedures are complicated, time taking, labor-intensive and costly [57].

With regard to the condition of enormous and complicated assemblies, some components may have to be assembled/ reassembled for inspection those results in equipment downtime. Consequently, practical requirement to introduce effective sophisticated structural health monitoring technique (SHM) exists that can assure reliable fatigue life prediction.

3.2.1. Types of Sensors

Sensors are recognized in the natural surroundings with the help of number they measure. However, the types of sensors with few models are as follows:

1. Acoustic and sound sensors.
2. Chemical sensors.
3. Environmental sensors.
4. Optical sensors.
5. Thermal temperature sensors.

Sensors are categorized depending on power/energy source they use for sensing. For instance, active sensors are those, which need electricity. On the other hand, passive sensors do not need power source [80].

3.2.2. Standards to Choose a Sensor

Some features should be defined to know the exact need for a sensor. They are as under:

1. Precision.
2. Environment.
3. Limit/range.
4. Calibration.
5. Resolution.
6. Financial feasibility.
7. Frequency of services [81].

3.2.3. Characteristics of Sensors

A good device should have high sensitivity. In other words, sensitivity designates what quantity the output of the device modifies with unit change in input (quantity to be

measured). To illustrate the voltage of temperature device modifications by (1mV) for each (1°C) change in temperature than the sensitivity of the detector is claimed to be (1mV/°C). In addition, other characteristics need to be available, which are:

1. Linearity: the output should vary linearly with the input.
2. High Resolution: Resolution is the smallest modification within the input that the device will discover.
3. Less Noise and Disturbance.
4. Less power consumption.

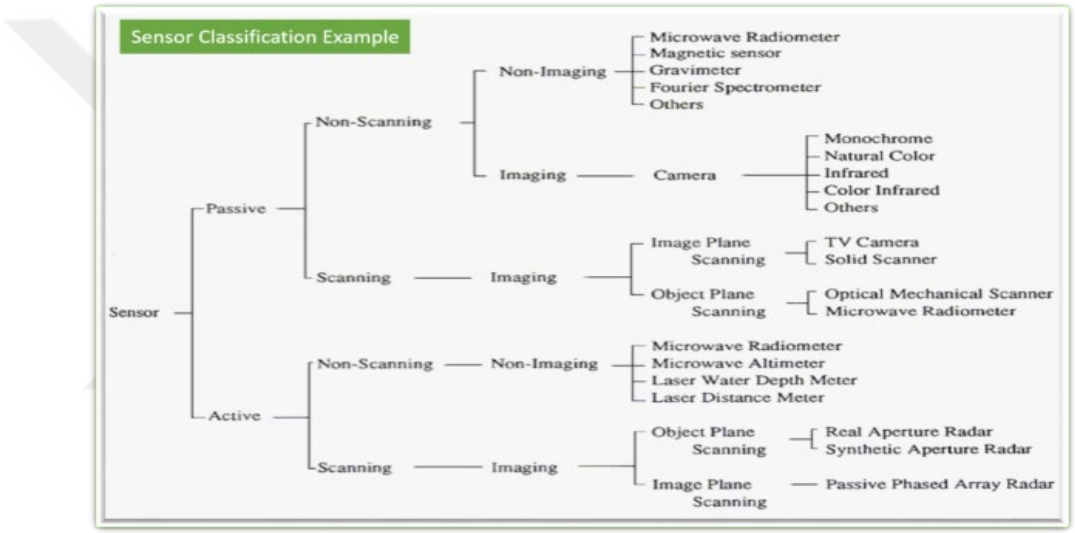

Figure 3.14. Classification of sensors.

The sensing element is managed/programmed in such way is that the strips can feel the stress. It should closely fit to a particular strain distribution within a notch/dynamic space. A sensor should be located out of a notch; however, it would still find the fatigue damage with the help of tip of the notch.

Sensing elements curve up to support that is being monitored. The strips fail in an exceedingly serial method from the best to all-time low. The stripe failure is right according to the real fatigue injury in the structure. The fatigue-sensing element observes a particular fatigue damage. Furthermore, this could be good for each diagnosis and prognosis regarding the residual life span. Structural elements that can

be operated in dynamic load surroundings serve important applications; need continuous observation as the applicable maintenance procedures do.

Fatigue damage is recognized as bridge safety threat. Cracks typically occur at stresses below the expected levels of style stress. In contrast to yielding or corrosion, fatigue cracks are rarely visible enough to be detected by visual examination, and so, it is simply unmarked. In the meanwhile, a sizeable life portion of a structure spends on crack nucleation, it is vital to develop methods to detect fatigue crack nucleation. Unfortunately, most of the methods that are advanced to distinguish fatigue cracks, which do not accommodate crack nucleation, and they are not sensitive enough to detect it.

The Structural Health Monitoring (SHM) it is an active technique for identifying fatigue damage. The important design criteria is that the fatigue endurance limit of fatigue sensor should be less as compared to fatigue endurance limits of any dangerous structural component. The sensor of fatigue damage detection aims to observe structural damage within important mechanical/structural components. The sensor coordinates electronics transfer unit to report fatigue damage history in many critical fatigue sensitive locations. Two main parts, mechanical and electronic compose the mechatronic type of fatigue sensor. The mechanical part uses some specially designed beams with notch or geometry as a safety factor to sense the fatigue life of critical structural components. The electronic part, on the other hand, collects the information and transmits information regarding fatigue history.

The system often put in fatigue-sensitive surfaces. In addition, they are often established inside fatigue-sensitive mechanical and structural elements. This happens in correspondence with rotating heavier-than-air craft shafts, gears, etc. by utilization of Micro-Electro-Mechanical Systems (MEMS) technologies; they developed a fatigue-sensing element for welded steel structures.

A variety of methods were solicited for facilitating in the timely actions needed to be taken to avoid any shocking consequences as Shows in Figure 3.14.

3.2.4. Fatigue Monitoring Devices

There are many devices that can help in fatigue monitoring, these devices are:

1. Fatigue fuses.
2. Piezo-electric based sensors.
3. Electro-chemical sensors.
4. Eddy current based sensors.
5. Ultrasonic based sensors.
6. Magnetic flux leakage sensors.

The above devices can be illustrated as follows:

3.2.4.1. Fatigue Fuses

Fatigue fuses can also be considered as crack gage type devices. The fatigue fuses, in general, are made up of a sheet of metal just like that of the structure under study. The fatigue fuse contains a thin ribbon or strand of wires, which are adhered to the structure generally near the site of the crack initiation. Some of the fatigue fuse gages are recently used in industries [82].

Henkel, confirms that a fuse consists of a small coupon made-up using aluminum or other material that is known to form well-defined striations. It is designed to contain a pre-crack that assists in providing a location for the striation formation. Figure 3.15. Illustrates a Schematic diagram offside and top views of a fatigue fuse (A). This is attached to the structure whose fatigue is to be monitored with (D) as the bonding faces. The face (C) is not in contact with the structure. The coupon is pre-cracked (B) at the center and the operation of this device is based on this pre-crack, which advances the fracture surface in incremental distances proportional to the applied cyclic stress. The loading, which is experienced by the structure, is transferred to the coupon through the adhesive bonding [83].

With increasing cyclic loads on the structure, the crack increases and well-defined striations are produced. The device is removed from the structure and split apart. Moreover, the pre-rack location is chosen to observe the striations that were developed.

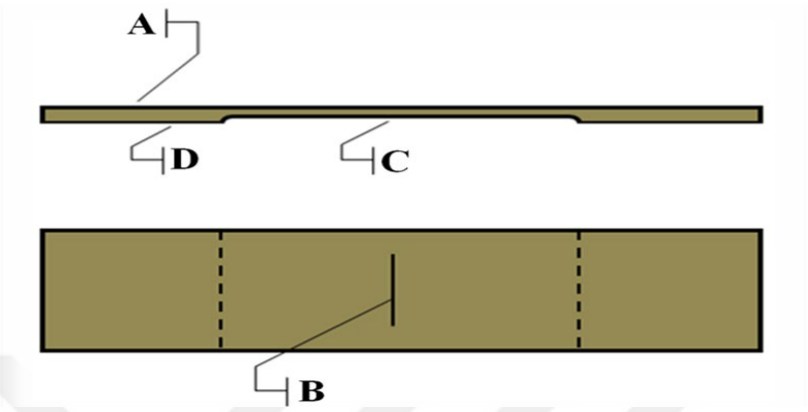

Figure 3.15. The side view and plan view of the remote and powerless miniature fatigue monitoring device [83].

Because of the cyclic loading. Whenever a stress cycle is experienced in the structure, a striation is formed in the fatigue monitor device.

In order to evaluate the striations for the peaks and valleys, the coupon surface is contrast-enhanced by adding carbon to the surface. Its surfaces are scanned using a laser source to illuminate the spacing between the dark stripes and a detector, which produces a voltage pulse train over different time intervals and captures the reflected energy. However, the voltage pulses are related to the striation spacing, which in turn, is linked with the stress intensity ranges.

The device measures the stress, intensity ranges because of the loading experienced by the sensor coupon, which are then linked with the fatigue life. There are, however, some drawbacks of the sensor.

3.2.4.1.1. Fatigue Indicator with Slots

According to Nelson and Crites, the fatigue-indicating device is an invention that consists of an electrically conductive foil coupon having crack-initiating slots of

different sizes oriented at different angles. The coupon is securely placed at the selected portion to the structure by means of an adhesive. The stresses and strains experienced by the structural member during the operation are transmitted to the coupon (C) via an adhesive layer. The adhesive comprises of an epoxy, polyester or Cyanoacrylate. In response to the loading, the coupon starts to crack at the crack initiating sites in the coupon. The Figure (3.16) Illustrates Schematic diagram of fatigue-sensing gage with slots done by those researchers. Figure (3.17) shows the top view and side view of the fatigue-monitoring sensor with slots. The crack initiating zones (A) are typical slots or notches oriented at different angles.

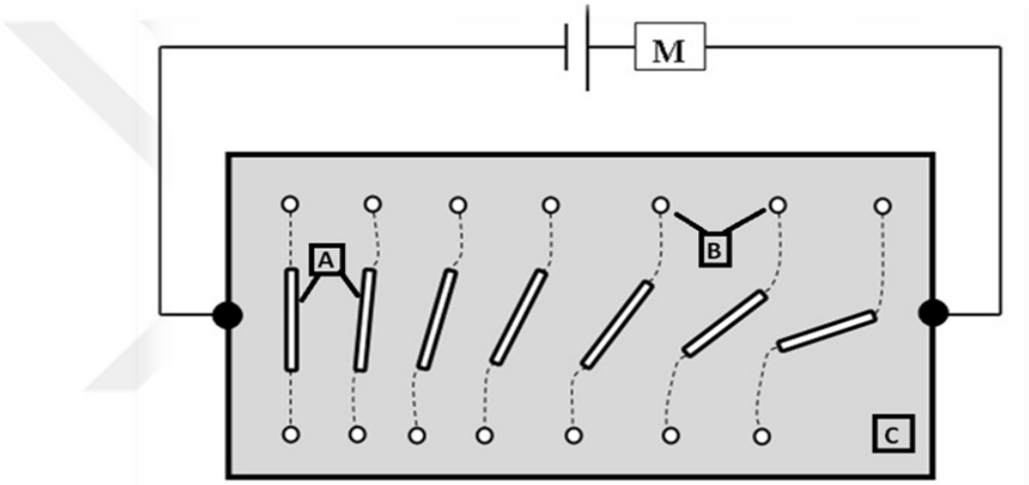

Figure 3.16. The fatigue indicator with slots [84].

They are responsive to different ranges of the accumulated fatigue depending on the relative geometry with respect to the other. The holes (B) on either ends of the coupon act as crack terminators.

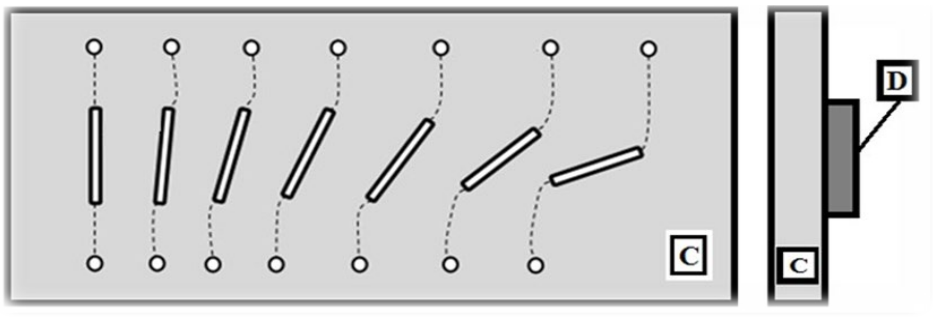

Figure 3.17. The top and side view of fatigue sensor with slots [84].

The provision of crack terminators is to avoid the rupture between the pre-determined locations that may result in the separation of one portion of the coupon from another. In order to avoid any risk of initiation of cracks at regions where they are intended only to terminate, the adhesive (D) is not applied over the complete area of the coupon but it is confined only to the central regions where crack initiating slots (A) are present. Accordingly, the strains on structural components are not transmitted to regions containing the crack terminating holes. The crack initiating slots zones are made responsive to different amounts of fatigue damage by varying their size, shape etc. Thereby, the coupon can progressively sample the strains in the selected region (region where the coupon is linked with the structure) of the structural component, to which, it is attached [84].

On the other hand, the coupon is electrically conductive for the purpose that a voltage source and a millimeter (m) or other current responsive device can be connected to the coupon to measure any small changes in the electrical resistance. This happens as the coupon ruptures in the crack initiating zones and relates it to the generated stress. Hence, these assistances help analyzing the collected fatigue by means of S-N curves.

3.2.4.1.2. Longitudinal Rib Load Counter with Notches

Fussinger points out that fussing projected the fatigue-sensing element that could be a longitudinal rib load counter with notches. The device consists of a longitudinal rib (E) attached or integrated to the surface of the structure (H) whose fatigue behavior is to be monitored. The device (rib) has a number of transverse notches (F) of different heights. Each of the notches has a rounded finish adjacent to the surface of the structure and a pointed finish extending far from the structure as shown in Figure 3.18 below.

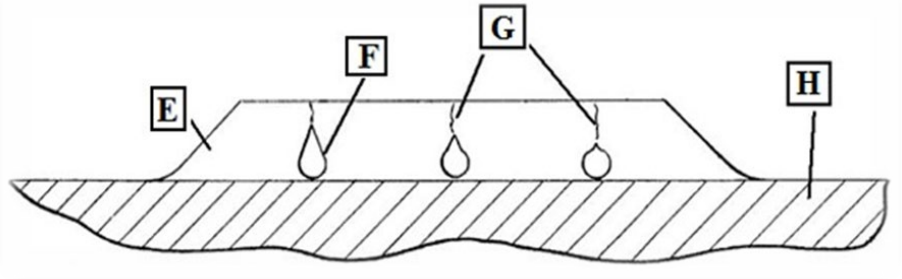

Figure 3.18. The longitudinal rib load counter with notches attached to the structure [85].

The opposite aspect of the notch towards the bottom of the notch is intended in an exceedingly manner as no cracks will occur throughout the whole lifetime of the structure. This is due to the provision of large rounding radii of the notches at their basis and the root of the notch being situated directly at the base of the ribbon. As a result, the cross-section at the root of the notch increases considerably and the increase of tension by the linking of the test piece remains at low and uncritical. The fatigue life of the structure can be estimated based on the visual inspection of the rib during the operation [85].

3.4.2.1 3. Fatigue Monitoring Coupon with Notches

This sensor consists of one or more flat and elongated forms fabricated with the same material as that of the structural component that is still to be monitored for fatigue.

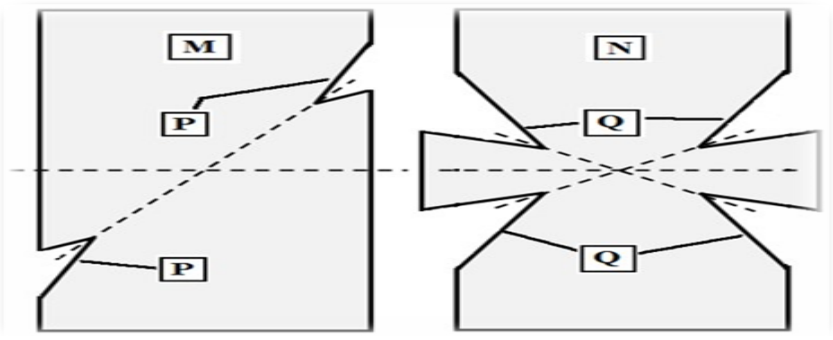

Figure 3.19. The fatigue-monitoring coupon with mild stress raisers [86].

Behavior. Each of the coupons has different stress concentration zones that differ from the intensity of the notch pattern on the coupons from very mild stress concentration to very severe stress concentration. Due to this, the stress developed in the forms varies from one another even for the same loading conditions. This results in the coupons to have a different fatigue life and so they all fail at different times before the structure failure, which gives warning regarding a structure's failure chances as showing in Figure 3.19 &3.20 [86].

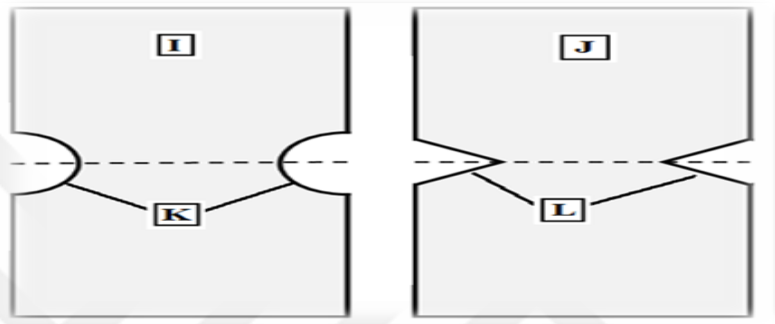

Figure 3.20. The fatigue-monitoring coupon with severe stress raisers [86].

Nevertheless, the austerity of the stress developed at the notches is controlled by the geometry of the notches in different sharp notches as illustrated in Figure 3.20. In addition, if there are many coupons within a fuse, every one of them has distinct stress concentrations, which has potential to predict a structure's residual lifetime. Due to this, the gage encounters only a spatial average of the strain that is experienced by the underlying structure. The pasting area of the fuse is shown by the shaded region in Figure 3.21.

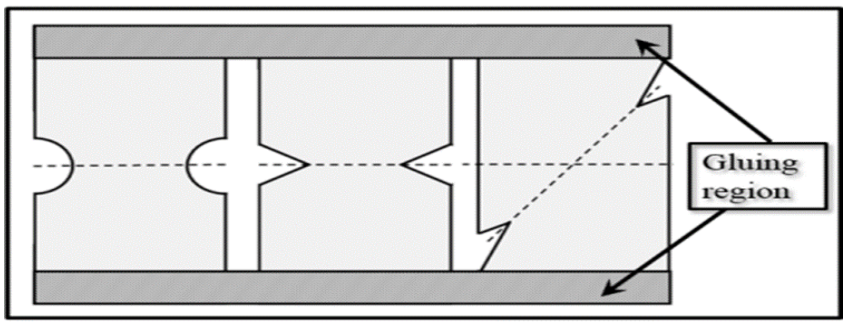

Figure 3.21. The fuse containing coupons with notches [86].

3.2.4.1.4. Fatigue Damage Indicator with Slit

The fatigue-sensing device discussed in this section consists of thin rectangular metallic base (U) having uniform thickness and a very thin slit (T), which is cut on a side and Teflon parting strip (V) as well, which is connected with the bottom of the slit as illustrated in Figure 3.22. The gage is attached to the structure with an adhesive (S). As the structure (R) is subject to fatigue loading during its regular operation, fatigue cracks might initiate on the inner slit end because of the continued loading in the structure, the length of the crack increases.

The device is installed on to the structure in a way that the longer ends should be perpendicular to principal stress in the structure. The sensor is linked with the structure through adhesive covering that covers the entire surface of the base except for the rectangular area covered by the Teflon strip that acts as a parting material, which is attached to the surface under base of the sensor parallel to the direction of the slit.

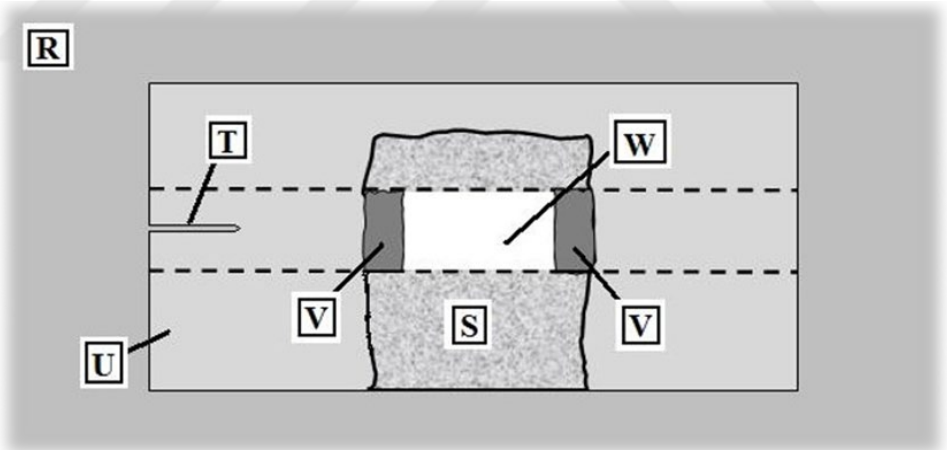

Figure 3.22. A Schematic diagram of the fatigue damage indicator with a slit [43].

The purpose of this parting layer is to supply a section of uniform dimension focused on the slit wherever the indicator is not connected to the structure and to produce a section wherever in the crack can propagate freely from one finish to the opposite within the longitudinal direction below displacement-controlled condition.

When load applies on a structure, the stress concentration forms near the tip of the slit and hence a fatigue crack is initiated at that location, which will start to propagate to the other end of the device as the loading is repeated. A fatigue damage indicator is first attached onto the structure in a way as to enable the sensor to be exposed to the principal loads in the structure. In the next stage, an identical gage is located in a similar manner on an identical piece of structure for laboratory testing, which is then exposed to repeated loading, which might be different from the actual loading pattern [43].

3.2.4.1.5. Fatigue Sensor with Variable Slots

Creager proposed the fatigue sensor. This fatigue fuse has cut out portion (Y) that defines the fuse elements (X) and variable unbounded areas are formed about the fuse elements that might result in the fatigue failure at different times long before the failure of the structure onto which it is mounted. The structure and therefore the sensing element are subjects to similar loading throughout the particular operation. The shapes of the fuse elements vary by the depths in the slots ($X1, X2, and\ X3$) and when combined with variable unbounded lengths that are configured to fail at different timings in a sequence. Figure 3.23 Shows a schematic blueprint of the front and side view of the sensor [87].

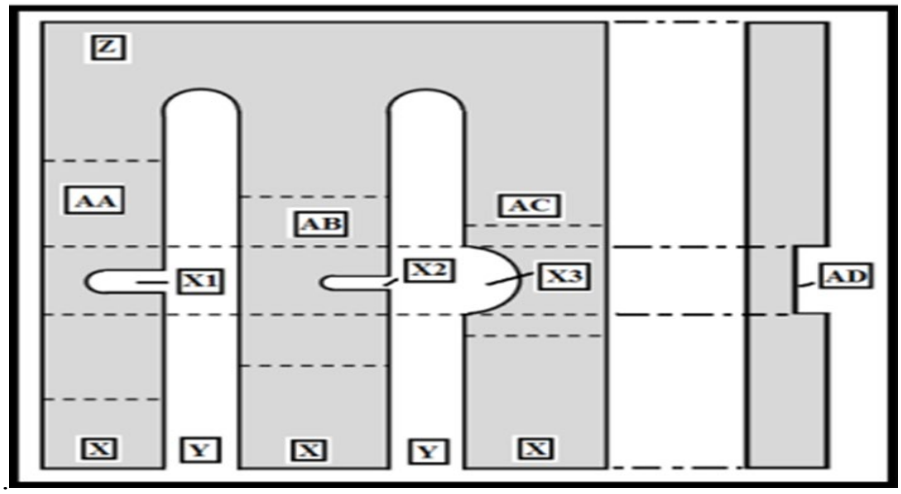

Figure 3.23. The front and the side view of the fatigue sensor with variable slots [87].

The sensitivity of the fuse can be increased by focusing both stress and strain in the notch area. This is achieved by the variation of length of the boundless region (AD) of every fuse and thinning of the fuse leg (AA, AB, AC) on the central portion of the boundless region. In addition to this, the sensitivity can be improved by simultaneously thickening the fuse leg, which is external to the central portion of the unbounded region or by attaching a stiffer material to the fuse leg in the external region to the unbounded region. However, the fatigue life at which each of the fuse legs fails is controlled by the unbounded areas that vary in length. The unbounded areas can also be formed symmetrically and asymmetrically about the cut out portions. The fuse elements (X) are expected to fail at different intervals in a particular sequence because of the fatigue loading. The electrical processes can remotely monitor the fatigue accumulation in the fuse legs.

3.4.2.1.6. Fatigue Sensor with Slots and Ligament

The fatigue sensor discussed in this section is a metallic coupon designed to have breakable ligaments with two layouts. In the first layout Figure 3.24a the ligaments have variable lengths whereas the sensor can be used for measuring fatigue strength or fatigue damage in metallic or polymeric substances. Nevertheless, in the second layout Figure 3.24b show that the ligaments are of equal lengths but made of different materials with different elastic modulus wherein the sensor can be used for measuring fatigue strength and damage in some composite substances.

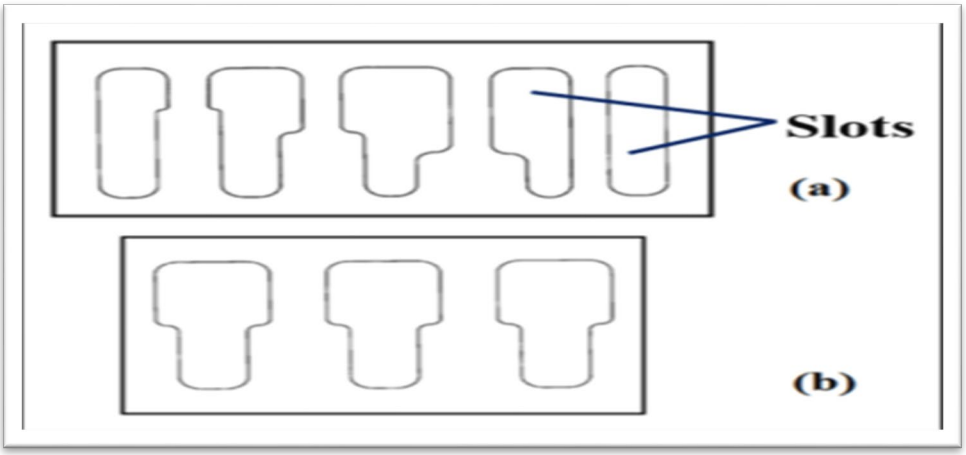

Figure 3.24. Fatigue sensor with ligaments and slots [88].

The sensor coupon shown in Figure 3.24a above, has ligaments with varying lengths and varying surface areas. The sensor coupon is attached on to the structure to be tested and when the structure is subjected to fatigue loading, the loads experienced by the structure, are transferred onto the sensor coupon. As a result, the entire ligament fails within the order ranging from the weaker ligament to the stronger ligament; therefore, by observing the failing ligaments, fatigue damage is estimated by the S-N curves of the coupon material [88].

The aforementioned fatigue sensors are passive, which provide the fatigue life by determining the extent to damage observed by the sensor.

3.2.4.2. Piezo-Electric Based Fatigue Sensors

Stroh and Chopra point out that the piezoelectric fatigue sensors are based on the principle that they develop a potential in proportion to an applied mechanical stress. It can exhibit dimensional changes, which are subject to the external electrical field. This particular feature takes place because of the motion of the dipoles, which results in the change of the dipole moment inside the material [89].

The electro-mechanical features of the piezoelectric material make it appropriate to be used as actuators or sensors. In many cases, one piezoelectric material is used as the source to create ultrasonic signal and another piezoelectric material can be used as a source to receive the signal. In this case, any modification within the signal because of the defect indicates the presence of a crack, which would cut back the amplitude of the received signal.

Nevertheless, in one of these applications, a piezoelectric element is used in combination with an impedance analyzer to find out the crack on the structure's surface. The method illustrated that electro-mechanical impedance of the piezoelectric element, which is located close to the crack, could be influenced by the existence of the crack. Moreover, a self-diagnosis procedure, to determine the status of the bond between the piezoelectric material and the structure, can be presented with the use of

the electro-mechanical impedance. Whilst there is profuse amount of work stated in the open literature [90].

As far as the use of piezoelectric material for damage detection and structural integrity assessment is concerned, the piezoelectric material is not exposed to operating environment.

A constitutional electricity device/mechanism network: The piezoelectric gage projected by the work who employed detector signals generated from piezoelectric actuators in its locality. Besides that, area unit designed into the structures, during which, the crack growth must be detected. The crack gage has of three parts, first for diagnostic signal generation, second for processing signals and the third for diagnosing damage [90].

In contrast, piezoelectric actuators produce analytic waves, which move throughout the structure to investigate damages. These variations in received signals as the structure undergoes the fatigue loading during its actual operation, which reveals structural issues. Figure 3.25 Illustrates Schematic diagram of arrangement of piezoelectric sensors and actuator arrangement in a structure.

The measurements are performed using an integral piezoelectric actuator network and structurally installed sensors embody the primary structural condition of the structure. The elastic waves propagate within the area, where material properties change takes place.

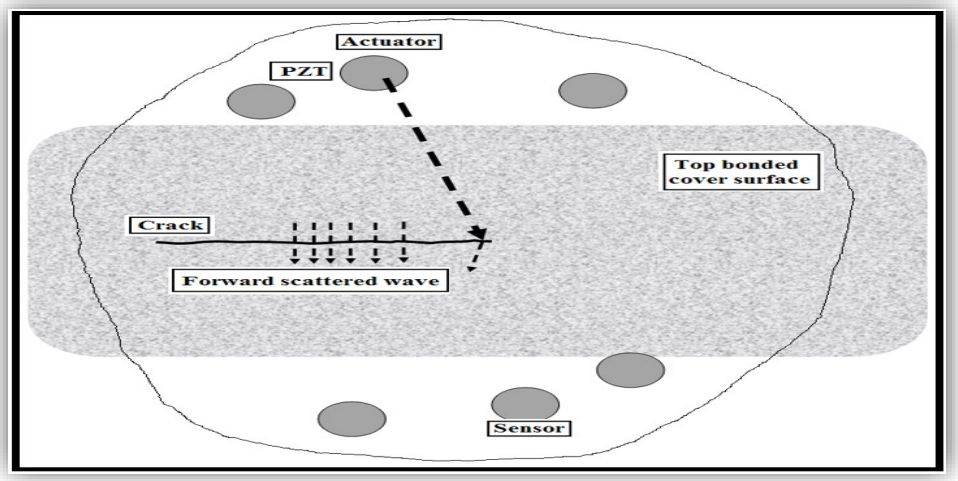

Figure 3.25. The built-in Piezo-Electric sensor/actuator network [90].

On the other hand, the signals transmitted from the sensor are changed and forwarded for scattering waves. Furthermore, scattered energy offers accurate crack propagating data through the sensor and actuator. These scattered waves exist within time domain, which is possible to obtain through subtracting baseline-recorded information. This can happen using the primary crack size to assess the later damage. The scattered waves can be used as a means of the crack detection. It transfers data for amplitude modifications as well as for phase change to understand lengthening of crack. The sensor measurements at certain intervals of time are subtracted from the baseline as well as the damage index is evaluated. This procedure needs repetition to assure continued monitoring of the structural health.

In terms of Structural Impedance Sensors, Park et al. suggest a method to detect and locate structural damage by using two different damage detection techniques. The schemes employed for the damage detection utilizes the electro-mechanical coupling property of piezo-electric materials and tracking the changes in the data of frequency response function. It is based on mechanical impedance, which measures structural resistance to motion if a force is applied. Mechanical impedance at any given point is the ratio of force applied to the resulting velocity on that point. It thus shows that force having velocities, which act within the same mechanical system. Electromechanical resistance may also be expressed due to the inverse of mechanical admittance. Since electro-mechanical coupling is a property of the piezo-electric substances, the

modification within the mechanical electric resistance of the structure can end. In addition, within the electrical electric resistance of the piezoelectric detector, the detector is connected with the structure. Thus, the occurrence of the structural damage can be qualitatively detected by monitoring the change in the electrical piezo-electric sensor impedance as illustrated in Figure 3.26 [91].

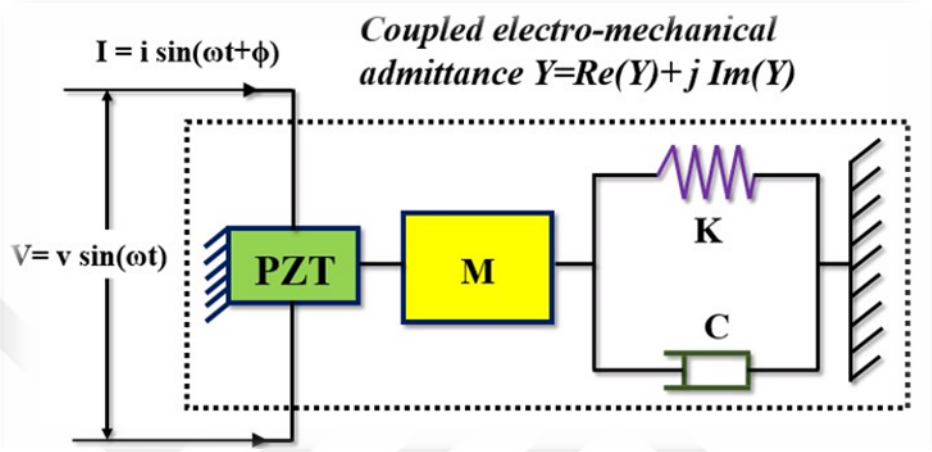

Figure 3.26. A schematic diagram of the PZT-driven dynamic structural sensor [91].

The PZT is surface bonded in such a way that it undergoes axial vibration when being subjected to an externally applied voltage. One end of the PZT is fixed and the other end is linked with main structure.

Piezoelectric paint sensor: Zhang discussed the piezo-electric paint sensor for detection of surface fatigue cracks. The working principle of the piezoelectric paint sensor is based on the electromechanical coupling properties of the sensor. The detector once directly deposited on to the structure receives mechanical strain, which is transferred from the structure under loading. Thus, resulting mechanical strain in the sensor results in voltage signals is generated from it. This sensor is made of polymer-based piezo-electric paints, which sustains on the structure.

The piezoelectric paint contains tiny piezoelectric atoms mixed with a polymer matrix. The blend of the polymer matrix and the ferroelectric ceramics (a type of piezoelectric material) form piezoelectric composites. They result in the combination of the electro-

active features, formability and mechanical flexibility. These sensors are established on direct piezoelectric result i.e., when stress/strain applies to a piezo-electric paint perpendicular to the polarization as shown in Figure 3.27 [92].

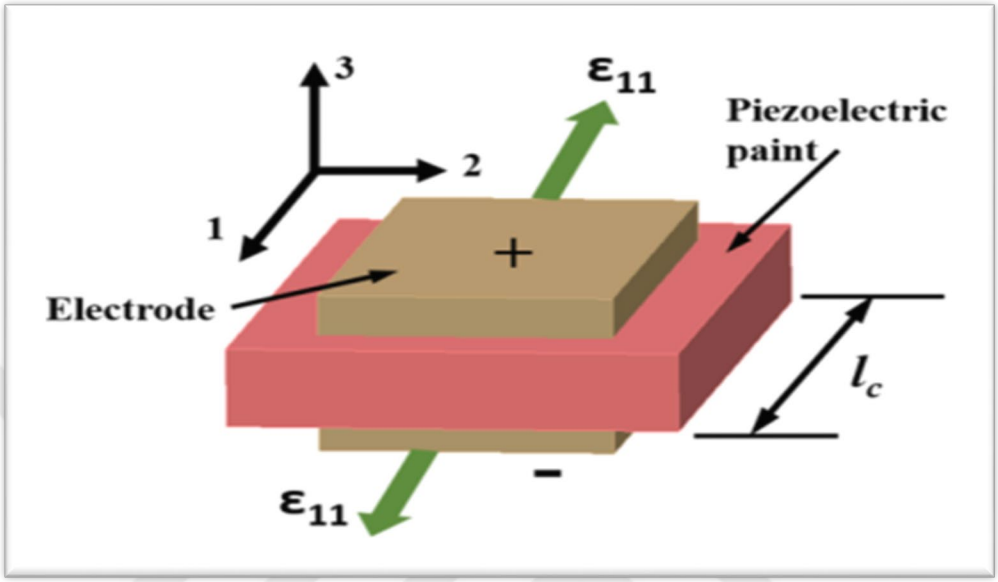

Figure 3.27. Schematic diagram of the Piezo-Electric paint sensor [92].

The crack detection scheme using this technique is done by employing a piezo-electric paint sensor having many electrodes for measuring a signal. The two electrodes area unit are related to very different input channels to a tool that reads the signal (such as oscilloscope). Once the structure with the sensing the connected element is subjected to excitation, just in case of a crack generated within the structure close to the device (i.e., the crack has got to go through the electrode), and calculated signals out of those two electrodes is totally different. This indicates that the crack takes place within the sensor-monitored part. The signals from the two electrodes would be identical if there is no crack generated near the sensor as illustrated by Figure 3.28 [92].

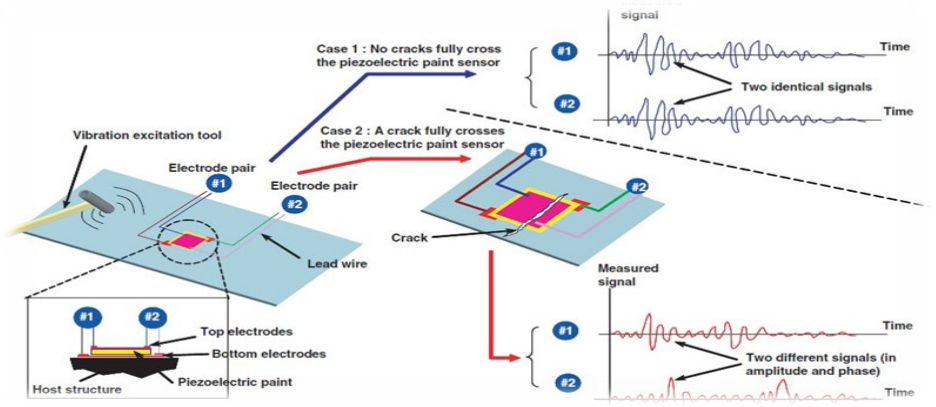

Figure 3.28. Schematic diagram of crack detection techniques of using Piezo-Electric paint sensors [92].

The two electrodes are connected to very different input sources and a tool that reads the signal (such as oscilloscope). In case of a crack generated in the structure near the sensor, the measured signals from the two electrodes are different. This would designate the rate of the crack in the sensor area. Then, the signals from the two electrodes would be identical if no crack is generated near the sensor.

3.2.4.3. Electro-Chemical Fatigue Sensor (EFS)

Kaplan argues that the electrochemical fatigue sensor during the applying process, associate EFS detector is applied to every position of interest and cracks are detected within the squares that are close to or within the immediate locality of the detector. The sensor makes a passive film of the target area. DC current is produced in an electro-chemical cell, and during the structure tests for stress, the current goes through the cell that helps responding to the applied mechanical stress. Therefore, AC current is super imposed on DC current. Depending on structural materials, loading, and fatigue damage, the transient current at intervals provides data regarding crack activity as exhibited in Figure 3.29.

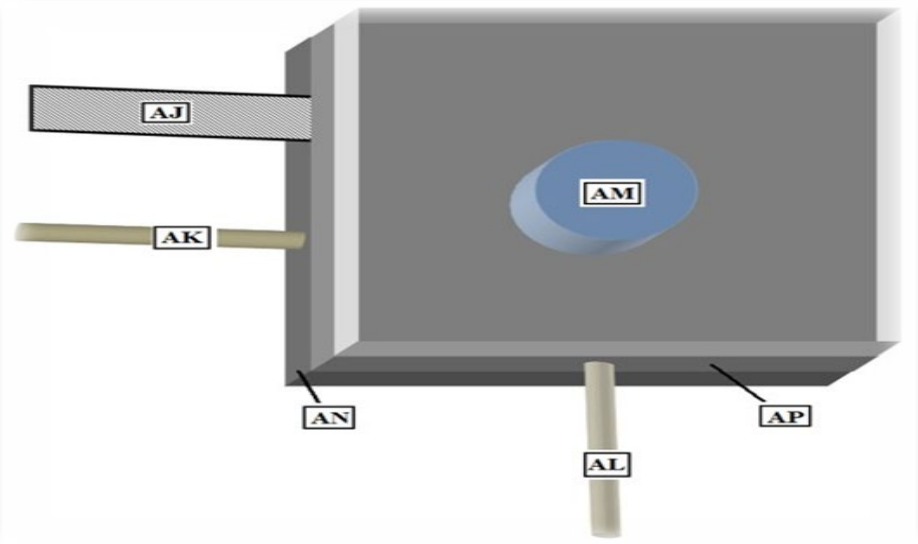

Figure 3.29. A schematic diagram of the electrochemical fatigue sensor [93].

The main components of the EFS system are the EFS sensor, electrolyte and potentials. Each of the EFS sensors has an adhesive layer on one side, which is attached to the structure under study. The open area (AM) in the midsensor is used to hold the electrolyte, which is filled with a filler tube (AL), and the air leaks from the bleeder tube (AK). The sensor electrode (AJ) has steel mesh which lies between upper (AP) and lower (AN) sections of a sensor. Moreover, it is completely covered, when the electrolyte fills the sensor. The electrolyte is a water-based solution that is amiable to most of the metals. The electrolyte is chemically inert as well as environmentally safe. The potentiostat is a power supply that provides the voltage differences between working and reference electrodes, through an electrolyte.

The conditions of electrochemical process while testing induce a stable and passive oxide film on a material's surface. The fatigue approach results in micro-plasticity and strain localization during cyclic loading.

Kaplan and Ozkul confirm that the dissolution and re-passivation procedures result in transient currents, which take place because of cyclical changes in a double layer on the metal interface and the electrolyte. However, these currents commonly have similar frequency as compared to mechanical stress and a complicated phase

relationship. Furthermore, the surface oxide film causes another component to have transient current that is twice as much as the elastic current frequency. This can be attributed to the plasticity influences that take place while compressive and loading cycle's tensile portions. Because fatigue damage occurs, crack-induced plasticity presents higher harmonic components to the transient current.

3.2.4.4. Eddy Current Sensors

Zilberstein et al. proposed the MWM (Meandering Winding Magnetometer) Eddy current arrays, which permit fatigue damage monitoring at various critical locations in a structure. MWM sensors are regarded as inductive sensors, which uses primary winding besides a number of parallel secondary windings, which are sensing elements. Some typical MWM sensor arrays are shown in Figure 3.30. [94].

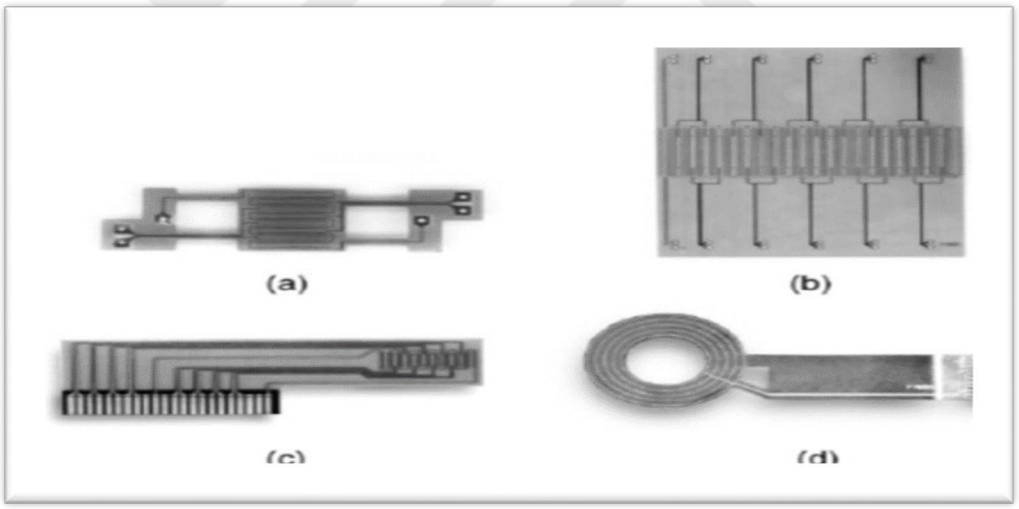

Figure 3.30. Typical MWM sensor and MWM sensor arrays. a) MWM sensor, b) Scanning five-element array, c) Eight-element array, d) Four-element MWM- Rosette for fatigue-crack detection [94].

On the other hand, a software package is working to convert the detector's electric resistance magnitude and partial response to material features like physical phenomenon. In an MWM array, a drive winding excitation is done through the current data prescribed frequency (from 1 kHz - 1 MHz). This current will provide a spatially distributed magnetic field, which in turn induces eddy current for conducting test

substances. Secondary windings sense magnetic field variation that takes place because of local defects, which alter the eddy current flow [94].

3.2.4.5. Ultrasonic Based Sensors

Baoet, have developed the ultrasonic based structural health monitoring sensors for real time monitoring of cracks in components made of ductile materials. The component under study is monitored using an angle beam through transmission technique using two transducers strategically placed on either sides of the critical location where the cracks are expected to initiate like holes. However, Figure 3.31 shows a schematic diagram of such sensors mounted on a specimen with the hole that is a stress-raiser/crack initiation point. As the applied stress is increased, the received signal shifts with respect to time due to the effects of changes in the geometry and change in ultrasonic velocity arising from the acoustic-elastic effect. When cracks exist, the signal also declines the amplitude because the crack opening occurs when it has stress. When such stress is predominantly intense to open a crack, the received ultrasonic energy to no stress energy ratio reliably indicates the crack. In addition, the growth of such cracks can be continuously monitored by tracking this energy ratio during the fatigue loading [95].

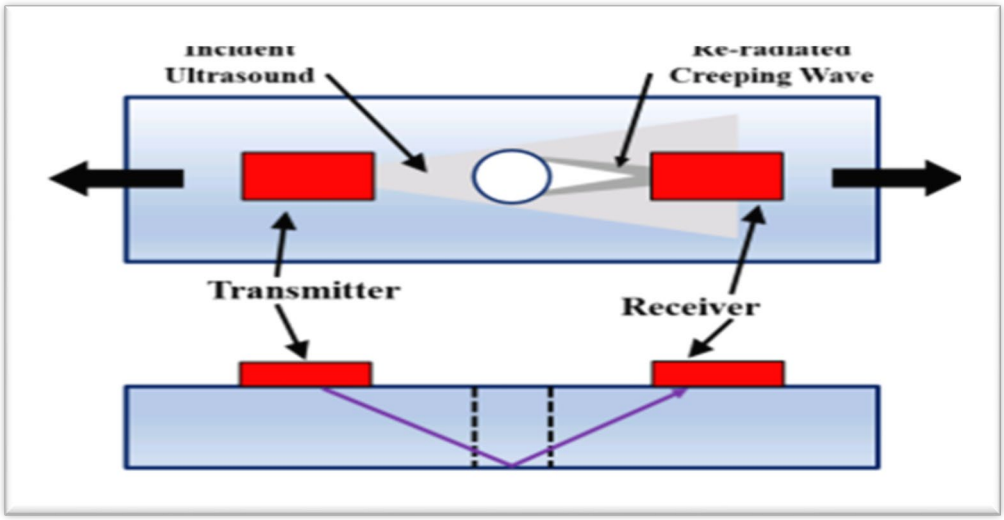

Figure 3.31. A schematic diagram of transducers' setup on a plate with center hole [95].

3.2.4.6. Magnetic Flux Leakage Sensors

Kuroda et al. developed magnetic sensors in order to detect plastic deformation and fatigue damage. The magnetic detector device is created using a semi-conductor (Ga). As the elements and the tools use x-ray diffraction, it estimates the residual stress distribution in parts below fatigue loading. Statistical processing of the data is obtained from the leakage of magnetic flux sensors, and residual stress factor is measured using X-ray diffraction approach, which is used to calculate the plastic deformation and the fatigue damage axis as indicated in the Figure 3.32. Below.

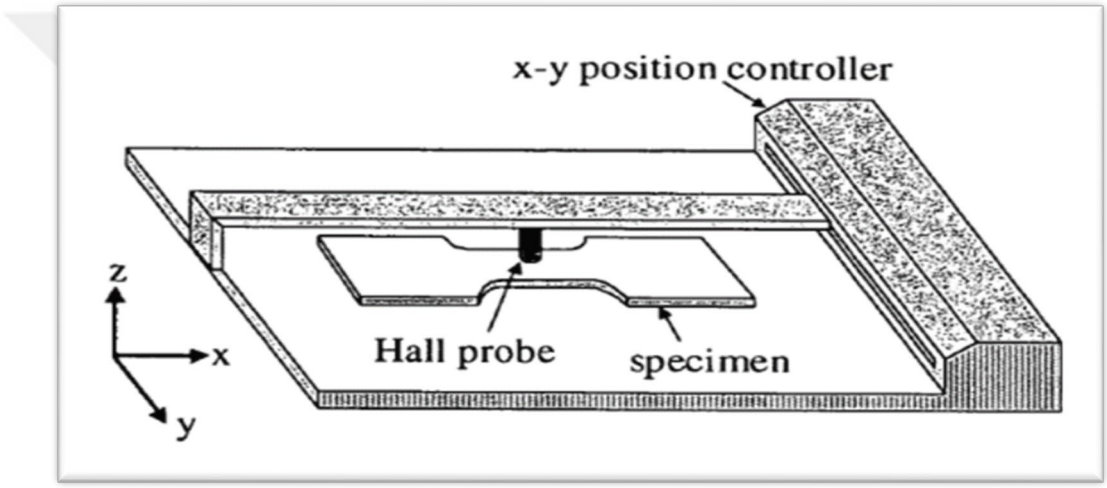

Figure 3.32. Schematic diagram of apparatus for leakage magnetic flux measurement [96].

Nevertheless, Table (3.1) below shows an outline of all the sensors. For example, the remote and powerless miniature fatigue-monitoring device, which has a demand and it, forms a cubical crystalline structure. This is due to the metal having crystalline structures. It is obvious that the method of sensing and analyzing the fatigue behavior of the support mistreatment of this sort of fatigue fused style of device, which involves variety of steps in crucial fatigue life. The fatigue-monitoring device having longitudinal rib load counter containing notches is integrated with the structure through the very means, by which, a detector plane lies perpendicular to a structure. During this case, there should be a provision to supply enough space on the surface of the structure [96].

Table 3.1. A summary of the fatigue sensors developed in the past [85].

No.	Sensor Name	Principle of operation	Comments (Cons)
1	Remote and powerless miniature fatigue monitoring device	Fatigue fuses (Passive Sensors) Comments (Cons) (1-4)	1. Some cases, the testing elements is subject to pre-cracking. 2. The testing elements have to be subjected to artificial weakening. 3. They can measure the fatigue damage or stress in a particular direction. 4. Complex fabrications have to be employed. 5. Not all the sensors per form in-situ fatigue sensing. 6. They would not account/mimic for the ambient conditions
2	Fatigue indicator with slots		
3	Longitudinal rib load counter with notches		
4	Fatigue monitoring coupon with notches		
5	Fatigue damage indicator with a slit		
6	Fatigue sensor with variable slots		
7	Fatigue sensor with slots and ligaments		
8	A built-in piezoelectric sensor/actuator network	Active Sensors	
9	Piezoelectric strain sensor array		
10	Structural Impedance sensors		
11	Piezoelectric paint sensor		
12	Electro-chemical Fatigue Sensor		
13	Eddy current sensors		
14	Ultrasonic based sensors		
15	Magnetic Flux Leakage sensors		

Moreover, fatigue life can be determined through comparison of crack-length on notch-tip of a sensor. This can stop monitoring process of fatigue behavior on consistent basis. Fatigue sensors have two special designed parts categorized as mechanical and electronic parts called as mechatronic-integrated system.

However, the mechanical part has some specially designed multiple parallel beams with different cycles of fatigue life. These beams target completely different fatigue levels and fail before time. This is due to the detector that goes through a similar fatigue cycle. Level of fatigue on a specific beam exceeds a designed fatigue cycle range. The individual beams fail to associate the physics detector, which discovers and wirelessly transmits the failure information.

In addition, the proposed smart fatigue sensor is unique in this context and senses the fatigue before the fracture actually occurs. It provides warning in some stages through the fracture stage methods so that the required corrective measures can be taken.
Cracks can start appearing in engineering structures through V-notches. Their notch tips can be categorized by tip radius, opening angle and V-notch depth. Nevertheless, the V-notches affect opening angle that increases intensity of stress as well as on T-stress of the crack that has been investigated in detail. In addition, V-notches in engineering structures increase the failure risks. Safe operations require in-depth stress understanding specifically its intensity around the notch tip. V-notch is typically a stress intensifier, and it has an immediate relation with notch angle and notch tip radius. This type of stress individuality results in fracture or at least crack propagation. Consequently, it is dynamic to review that stress is an individual and fracture characteristic on V-notches tip. The present development means to introduce lightweight as well as effective sensor that permits structural health of an aircraft or a bridge. The features of an ideal structural health monitoring system are as follows:

1. Micro-sensor should be permanently installable.
2. The performance should have two options including on request and continuous options.
3. Wireless operation.

4. Immediate sensor data interpretation.
5. Critical high-stress detection.
6. Capacity to monitor material damage.
7. Capacity to predict the actual damage.
8. Damage forecast options in short and long-run Ideal structural health monitoring system.
9. Capacity to overcome technical challenges.
10. Ideally, a sensor should have the following characteristics:

    a. Small/lightweight.
    b. Autonomously powered.
    c. Economical, effective, rectifiable, fixable and easy-to-install Easy to place in a structure without creating damages.

On the other hand, in the dominion of steel bridges, fatigue of the metal structural elements is one of the most pernicious failure modes in its early stages, which are invisible and not easily detected by non-destructive means. If we broadly divide the range of the fatigue process, beginning with an undamaged original structure, and progressing to a fracture condition into crack nucleation, crack propagation, and final fracture processes, the crack nucleation portion of the life is by far the most difficult to monitor. The fatigue sensor prototype developed in this project is intended to monitor a structure's life.

PART 4

METHODOLOGY

4.1. MATERIAL

ASTM A36 is a variety of strong and highly formable low-carbon steel. In addition, this steel is comparatively easier to process, and it has a safe welding property. A36 is also a generally used structural steel that has high resistance against corrosion.

A36 Carbon Steel was selected as a standard material for experimental analysis of sensors because of its widespread use in structural applications. It is relatively low cost and its ease of machining and welding makes it a popular choice as a building material. However, it requires regular maintenance and inspection since it is subject to corrosion and must be protected from the elements with paint.

Table 4.2 lists the material properties of the sensor and the figures in Part 5 show how they were defined in ANSYS. The thickness of the gusset plates in all models of the sensors are 0.001 mm [103].

Table 4.1. Properties of carbon steel A36 [103].

Property	Value
E	200 GPa
G	75 GPa
ν	0.26
ρ	7,800 kg/m^3
YS	36,000 psi (250 MPa)
UTS	(400-550 MPa)

Successful integration of the sensor in the bridge posed a challenge. The weld parts had rough surfaces, and this also posed a challenge. The conventional operations required the least roughness for accurate discovery of any cracks below.

The reasons for choosing this subject include the variety of sources of deterioration, the variety of locations of bridge defects, and the fact that there is currently no single method that can detect and address the potential sources globally.

The ANSYS program was used to analyze and cross check the calculated stress values. Stress analysis through ANSYS also showed that the maximum value of stress occurs in the vicinity of changes in the cross section of beams where a relief groove is present. Notched fatigue specimens with different notch depths were modeled and FE simulated results were generated for fatigue loading at different stress amplitudes using ANSYS version 14.5.

The mechanical properties and stress life data were obtained from ANSYS. Element meshes were generated and boundary conditions corresponding to the maximum loading conditions were given. Stress analysis through ANSYS also showed that the maximum value of stress occurs in the vicinity of a change in cross section of the beam where there is V-notch with different geometry.

4.2. METHOD USED FOR SIMULATION

ANSYS offers an inclusive software system applied to physics. Moreover, it provides access to nearly any field of engineering simulation that a procedure requires. Administrations around the world rely on ANSYS to provide the most effective cost to benefit ratio for investment in engineering simulation software systems.

Simulation-driven improvement raises engineering simulations to a different level with its unique depth and breadth and unmatched engineered measurability, comprehensive multi-phase foundation and adaptation design. The advantages of these ANSYS features are that they add value to the engineering design process by

delivering efficiency, reducing physical constraints, driving innovation, and enabling simulated tests that might not be otherwise possible.

4.2.1. ANSYS Mechanical

This is a tool that deals with finite analysis as a part of total structural analysis for all kinds of studies. It provides restricted model behavior and describes material models as well as equation solving processes to overcome mechanical design problems. ANSYS additionally allows the thermal analyses of properties, such as electricity, acoustics, as well as thermos-structural and thermo-electric analyses.

On the other hand, ANSYS may be a general-purpose package as it simulates connections between every discipline of physics, including properties of fluids, transfers through structures and vibrations, heat transfer, and magnetic forces of attraction. Therefore, ANSYS permits the simulation of tests and checking in virtual settings. In addition, it can make decisions regarding a useful life and make predictions of potential problems by means of 3D technologies. ANSYS also helps in making any necessary choices.

ANSYS works while being integrated/assisted/coordinated with engineering systems including CAD and FEA. ANSYS imports work, which is performed using CAD and allows the addition of dimensions of pure mathematics for pre-processing. The same preprocessor is required for computation. When shaping loadings and performing concluding analyses, results are presented in numerical and graphic forms. ANSYS conducts progressive engineering analyses almost instantaneously keeping in view every necessary aspect and factor. However, the ANSYS workbench is actually a platform that integrates simulation as well as para-metric CAD technologies through cutting edge performance. ANSYS workbench works with the help of ANSYS convergent thinker algorithms.

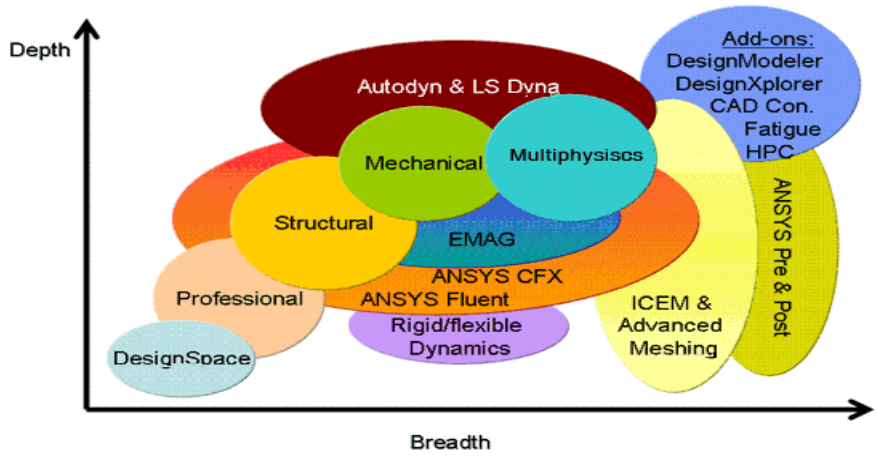

Figure 4.1. Schematic diagram of the ANSYS process.

ANSYS Workbench is popular for its high PC compatibility; therefore, it acts better in comparison to an interface. Professionals with Assns. certification are eligible to work on ANSYS Workbench. ANSYS may be a general finite part code, usually used if a deformable half is not undergoing large rigid-body motions. Nevertheless, it results in a high spatial resolution for stress or strain square measure, which is desired. A typical field of application is finding proof of the strength of elements. In addition, LS-DYNA is a finite-element code with specific stress on specific problem solvers. In other words, it is numerically efficient for the simulation of large short-time scenarios. A typical application is crash simulation. Nowadays, all these software packages present a variety of functionalities such that there is a huge overlap between them; e.g., ANSYS can also be used for multi-body simulations because it has an explicit solver. Nevertheless, each piece of software is typically very efficient in terms of modeling and numerical effort on its original domain.

4.2.2. Meshing Step

Meshing is a common term denoting the reduction of the pre-processing stage of the Finite Element Analysis (FEA) which uses the Finite Element Method (FEM).

Similar to Modal Analysis and Stress Analysis, Fatigue Analysis (FEA) is a method that mechanical engineers use to complete their analyses of a particular design. Since they are the people who perform the analysis, they also do the meshing (since meshing is a part of the analysis). The mesh or model may be an illustration of the laws of physics behind the model or mesh. The element works but the mesh may not be set up properly. The boundary situation can be closed, the contact definitions can be wrong, and even the mesh size can be too large or too small. In fact, most of the solutions here have the reasoning behind the wrong mesh size. Larger meshes with square measures are easier to resolve; however, their yield is less complex and needs focus. It is advisable to use very large meshes wherever we have a tendency to expect comparatively low activity when using finer meshes. Many activities need to be found within the half or in a region of focus. Only associate engineers would grasp the second part of this, and thus, only associate engineers would be able to optimize the model properly.

However, it is also important to note that since Finite Element Method (FEA) software, such as ANSYS, is an engineering tool, it will be highly likely that meshing will become increasingly automated (it is already quite automated). Eventually, the phase of pre-processing known as “meshing” will very likely disappear entirely from the software. When this occurs, engineers will be the users ensuring that the software meshes everything correctly and produce accurate results [99].

ANSYS is regarded as the package of all-purpose finite modeling numerically to overcome most mechanical issues. This also embodies statistical, dynamic and structural analyses, heat transfers and fluid issues.

4.2.3. Finite Element Steps

There are three finite element steps. These steps are presented as follows:

4.2.3.1. Pre-Processing

It is essential to define an issue to decide on the pre-processing steps, which are:

1. Define the variables, lines, areas and volumes;
2. Define the types of elements and their geometrical properties, and
3. Mesh lines being required with information such as area and volume; in other words, this helps in deciding whether the model will be 1D, 2D, or 3D.

4.2.3.2. Solution

The solution is related to the distribution of masses, to issues, and to findings. The identification of different constraints is essential, and these constraints can be mathematically expressed through equations.

4.2.3.3. Post Process

For any processing and observation of the leads to this stage, it is necessary to look at:

1. Nodal displacement lists;
2. Forces/moments of elements;
3. Deflection plots; and
4. Stress contour charts and temperature maps.

4.3. ANSYS Steps

1. The Physical Model.
2. Boundary Conditions.

3. Physical Features.

A researcher should solve the problem and present results. In numerical strategies, the most distant is an additional step known as mesh generation. This step distributes the complex model to small components that become solvable in an otherwise too complex condition. The following points illustrate the processes in terminology a little more attuned to the software.

4.3.1. Building the Geometry

Create a two- or three-dimensional illustration of the item to be modeled and tested using the work plan coordinates system in ANSYS.

4.3.2. Defining Material Properties

When the half part occurs, a researcher should describe a library of the required materials that comprise the object (or project) being modeled. This consists of mechanical and thermal features.

4.3.3. Generating a Mesh

At this time, ANSYS understands the makeup of the half. Currently the modeled system can be dampened into finite items.

Jweeg (2008) points out that having built the model geometry of a V-notch fatigue sensor, the structural sensor components can be signified by using appropriate substances/elements. ANSYS has an element library which has over 100 different element formulations or types, as illustrated in Table 5.3.

Table 4.2. Structural components.

Material	Element	Representation	D.O.F	No. of nodes
Isotropic	3-D. Solid 5	V-notches	6	8

4.3.4. Applying Load

Once the system is totally constructed, the final task is to pressure the system with constraints, such as with boundary situations or physical loadings.

4.3.5. Solution

This is often merely a step because the ANSYS has to decide under what state (steady state, transient, etc.), the problem can be solved.

4.3.6. Presenting the Results

After finding the solution, there are many means to introduce ANSYS results. In other words, a researcher can select from many choices, such as tables, graphs, and contour plots, as shown in Figure 4.2.

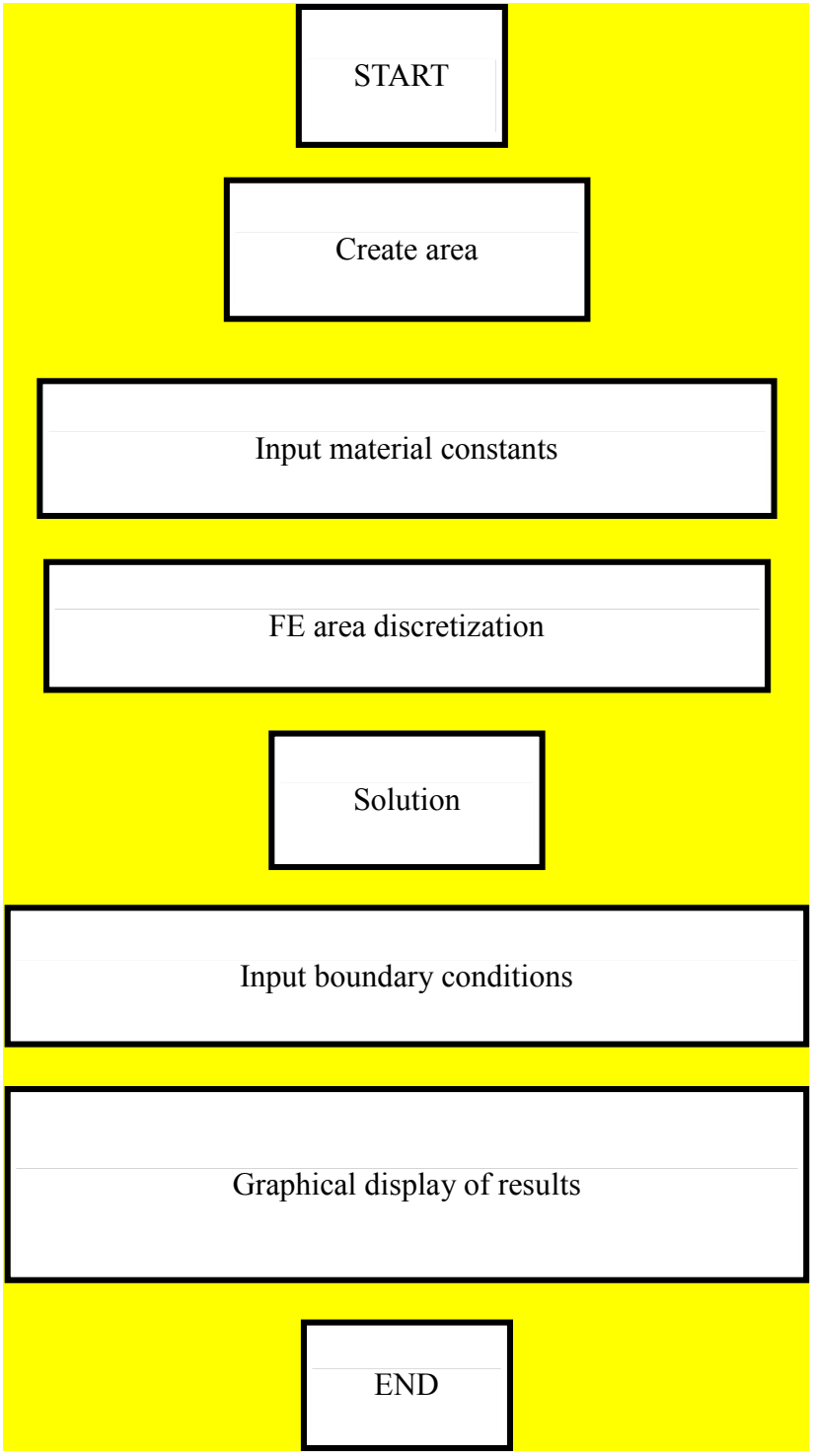

Figure 4.2. Flow chart of the structural analyses by ANSYS.

4.4. DESIGN OF THE SENSOR

4.4.1. Introduction

The fatigue sensors described were broadly classified as active and passive devices. In particular, fatigue fuses fall into the passive sensor category whereas the piezoelectric based sensors and the electrochemical fatigue sensors fall into the passive device category. Nevertheless, bearing the disadvantages of the existing sensors in mind, a novel fatigue-monitoring device has been conceived. Some of the important features of this sensor are its simplicity in design, ease of installation and the fact that the sensor does not need to be located in a critical location. The sensor can be placed near stress concentration zones such as holes, notches, and so on.

In addition, novel fatigue monitoring sensors (FMS) can detect and monitor any fatigue damage as well as evaluate structural life and cyclical loads. The idea is constructed on the stress life features of an engineering material. However, sensors include alternating slots/strips which have different stress magnification aspects regarding nominal strain. Sensors are designed to make strips experience some strain, not unlike genuine stress distribution. As far as a sensor's location is concerned, it is located externally with the structure. A sensor links to a surface of a structural component, and observations are made when the strips sequentially fail from greatest stress magnification to the minimum. Strip failures indicate some important failure of the structure. A fatigue detector detects fatigue harm to a structure and indicates the remaining structural life. The current research mostly includes design/simulation of a fatigue sensor pertaining to several geometrical properties. Numerical as well as diagnostic modeling help to create effective designs.

Gokanakonda points out that a finite element analysis can be performed using ANSYS software. A fatigue sensor comprises a significant part. Prototype fatigue sensors were invented with the help of Wire EDM (Electro Discharge Machining) technology and micro fabrication. These processes are relatively advantageous, which has been discussed. Nevertheless, a sensor has appropriate data collection capability and it

works in different situations. In the final part of this thesis, we present an analysis of the gathered experimental data.

Zhang, Tubby and Mason argue that different fatigue damage monitoring devices have been improved for better services, and the fatigue process on weld joints creates specific needs for fatigue sensors to function. Fine cracks, as if flaws in the weld parts would mostly reduce crack initiation, can be a significant part of the fatigue life of non-welded components. Furthermore, the residual tensile stresses considerably increase the damaging influences of loading cycles.

In addition, micro-electromechanical system (MEMS) processes and parts square measure changes in instrument design, processing and applications. Analysis may be a comparatively new area in comparison with ICs. MEMS style, fabrication, packaging, and dependability are still in the forming stages and need continuous improvement. In this context, MEMS failure analysis is a new field in comparison to MEMS fabrications and style. MEMS has been used for many years for failure analysis. However, the tools/procedures help to diagnose the causes of failures. The MEMS failure detection mechanism is distinctive because of the instrument. In ICs, appreciable effort has been made for accurate handling and testing to evaluate device performance. A main distinction between MEMS and ICs is the environment. In several cases, IC square measure was tested under varied conditions starting from varying temperatures and humidity. MEMS has similar handling and testing techniques; however, the device is needed to determine what is suitable in a given condition [102].

In addition, changing the test environment can effectively change instrumental sensitivity as well as functionality. The additional quality of mechanical movement needs additional precautions to be taken while handling or testing. MEMS provides a benefit of using ICFA style equipment and procedures pertaining to MEMS analysis. Nevertheless, as the instruments and applications increase, MEMS failure analysis has to be varied and multi-faceted in order to accurately determine the genuine reason for failure.

4.4.2. Design Concept

A fatigue-monitoring sensor has alternate slots and strips which have varying strain magnifying factors to check nominal strain. This device is installed to make the strips correspond to particular strain distributions. Sensing elements are often located outside a notch; however, identical fatigue damage will be experienced because of the notch tip. A detector is connected to a supporting surface in order to monitor fatigue behavior. The strips are also termed as ligaments, and they fail whenever they experience high to low strain magnification. Every ligament failure takes place in response to fatigue damage. This data helps to forecast residual module life. A fatigue sensor along with its arrangement are illustrated in Figure 4.3.

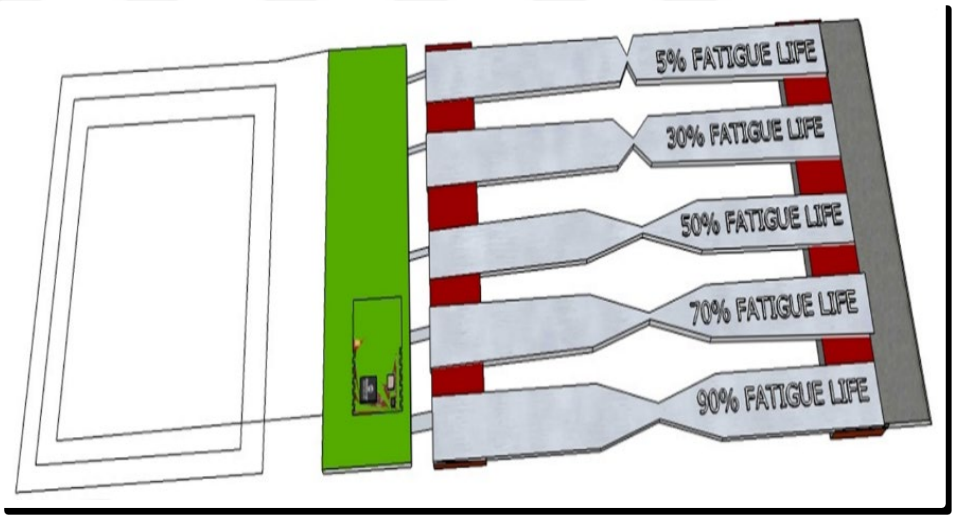

Figure 4.3. A general view of the sensor.

In order to examine the stress distribution on a fractured surface, the finite element method (FEM) is employed. The ANSYS program was used to analyze and cross check the calculated stress values. Stress analysis through ANSYS also showed that the maximum stress value occurs in the vicinity of the change in the cross section of the beam where a relief groove is present. In the ANSYS simulation, a piezoelectric sensor with six beams with opposite V-notches made from Steel 36 was designed parallel to the applied tension load of the structure. Figure 4.3 shows the percentage of fatigue life with respect to the geometry of the V-notch sensor.

ANSYS computations were performed using cyclic loads which depended on V-notch geometry (such as angle orientation), notch depth, boundary conditions and the applied tension load of the sensor. Both element and nodal solutions were used in the ANSYS simulations. In the element solution, we used 8795 elements and 18474 nodes were used in the nodal solution. In both solutions, the Solid 5 type element, containing 3D magnetic, electrical, thermal, piezo-electrical and structural simulations, was used. Solid 5 has eight nodes each with six degrees of freedom. The degree of freedom uses displacement (UX, UY and UZ), TEMP, VOLT and MAG.

4.4.3. Sensor Dimensions

Engineering sensor skin can distinguish small cracks over an expansive region. The central objective of developing sensing systems was to explore the stresses in V-notch sensors. Fatigue is a common failure in any structural component where cyclic loading appears, especially in a bridge due to fatigue failure. In addition, applying these techniques to solve this problem of fatigue structure for the predication of fatigue failure helps to provide indications for maintenance before any disastrous failures. This sensor senses fatigue associated deprivation well prior to any disastrous failure occurring thereby giving sufficient time for that component to be replaced.

The aim of this work is to describe the design of, the improvement of V-notch sensors, as well as examining the V-notch. Moreover, this paper evaluates the stresses in the sensor with a boundary on the right side and applied tension loads on the left side of the sensor. In addition, as shown in Figure 4.3, the sensor is installed on the left side on this structure. In this model, the five situations with different fatigue lives are used. The lowest percentage for resistance is 5% and the highest is 90%. In other words, in the 90% fatigue life, more resistance for damage is noticed, but in the 5% fatigue life, less resistance for the other beams is noticed. This means that failure starts at 5%. This value depends on the geometry of the sensor and the shape of the V-notch. The increase in this value is related to the application of welding shapes. Normally this value depends on different dimensions.

In this work, a new structure of this sensor is applied. For the proposed method, the six beams are used, as illustrated in Figure 4.4.

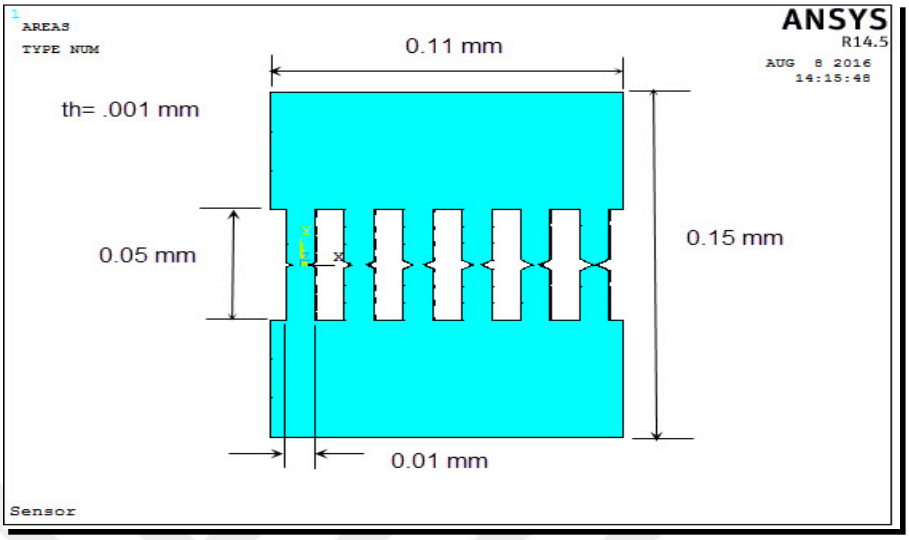

Figure 4.4. The V-notch dimensions.

This figure shows the width, height and thickness of the sensor. The dimensions that are used for this sensor are shown in Table 4.1 below.

The sensor was designed to suit welded joint details with a fatigue strength close to the design curve. Nevertheless, one class on either side can be assessed with reasonable accuracy. The fatigue performance of the sensor therefore matches many common fatigue-limiting joints in welded structures.

Table 4.3. Sensor dimensions.

Width	Height	Thickness
0.11 mm	0.15 mm	0.001 mm

We used a steel material for the sensor assembly with a fixed edge condition on one side and a tension load on the other.

The procedure of this work includes:

1. Building the geometry;
2. Defining Material Properties;
3. Generating a mesh.
4. Applying loads.
5. Obtaining solutions; and
6. Presenting the results.

To examine the stress distribution at the fracture surface, the Finite Element Method (FEM) was employed. The ANSYS program was used for analysis to crosscheck the calculated values of stress, especially the Von Mises stress for fatigue failure. These procedures are suitable for estimating Von Mises stress.

The Von Mises yield criterion predicts that yielding will occur whenever the distortion energy in a unit volume equals the distortion energy in the same volume when uniaxial stress is equal to the yield strength.

4.5. SENSOR SIMULATION STEPS WITH ANSYS

There are a number of steps that help in sensor simulations which are illustrated as follows:

4.5.1. Building the Geometry

We construct a two- or three-dimensional representation of the object to be modeled, as illustrated:

1. Length = 5E−2.
2. Width = 2E−2.
3. TH = 1E−3.
4. Theta = 60.

5. Radius = W/2.
6. L shift = 2E−2.
7. X shift = 0.5E−3.

In order to build the sensor, V-notch geometry using the dimensional data, mentioned above, is required. V-notch geometry refers to the scalar parameters, and with this information, the model will be ready.

4.5.2. Defining Material Properties

In the pre-processor step, material types as electrical conduction (scalar brick 5) with options such as the Solid 5 element and the 2-D Coupled-Field Solid are described below:

Solid 5 contains 3D magnetic, electrical, thermal, piezo-electrical and structural properties that cause limited coupling. It has eight nodes each with six degrees of freedom. Scalar potential formulations are accessible for modeling. For piezoelectric and structural analyses, Solid 5 shows major deflection and stress stiffening capabilities. Nevertheless, for the degree of freedom, a researcher should use (UX, UY, UZ, TEMP, VOLT, and MAG). Moreover, for material properties, we select an SI unit, and for the model of the material, we define Model 3 while using the density of material applied to the sensor (density = 7850 kg/m^3). Currently with the aforementioned information, in order to describe a library of the required materials that is composed of items being modeled, we include mechanical and thermal properties.

4.5.3. Generating a Mesh

The procedure for generating a mesh of nodes and components comprises three main steps:

1. Set the element attributes.
2. Mesh the controls.
3. Generate the mesh and select ‘refine meshing’ from the meshing toolbox (sweep) and begin to mesh the part we wish to mesh. At this time, ANSYS recognizes the composition of the half. Now the shape of the modeled system must be reduced to finite items.

4.5.4. Applying Load

For the solution step, we define the load as being structural and displaced on the tops and bottoms of both areas. In addition, we apply U, Rot on the area as (U) represents the displacement value on the top and bottom, which is +0.001, −0.001, respectively, and we apply a voltage to the top and bottom (+5, −5 volts, respectively), as shown in Figure 4.4.

After the structure is completely designed, the latest task is to load the system with restraints, such as physical loadings or boundary conditions.

4.5.5. Solution

In the solution step, we define the load again and start to solve with the steps of using the current load after which the solution will be found. During this moment, a transfer to general post processes occurs to read the results following different methods as either a nodal or element solution. This is actually a step because ANSYS has to observe under what state (steady state, transient, etc.) the problem needs to be solved in different steps in the general post processes step to read the results following different methods as either a nodal or element solution.

PART 5

FINDINGS AND DISCUSSION

5.1. FINITE ELEMENT SOLUTION

According to the fundamentals of using sensors for sensing the fatigue failure in steel bridges, it is important to consider the following stages:

Using the ANSYS software package for analysis of fatigue failure in the A36 steel structure for bridge systems with V-shaped notched fatigue sensors simulates different welding structures as can be seen in Figures 5.1, 5.2 and 5.3 with minimum and maximum stress concentrations. The software describes the behavior of the displacement of every beam. Sensors with different dimensions, angles and depths for every structure of the sensors show where the critical zones for high stress concentrations lie and which ones will fail or are damaged because of its behavior.

Later on, one must investigate different directions of analysis for the same sensor to make comparisons between the values of both results. This can be done through starting with the x-coordinate and then the y-coordinate. We can save our real component and protect it from damage. It is easy to maintain from time to time before damage starts due to fatigue failure.

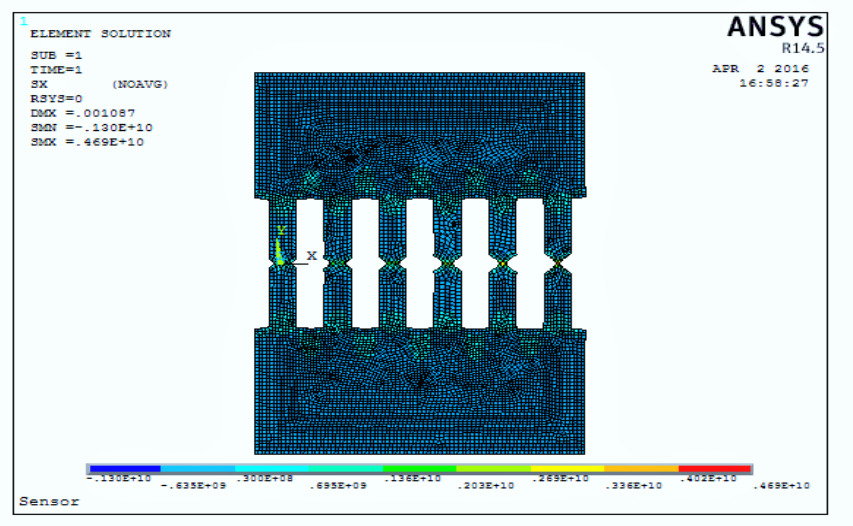

Figure 5.1. Element solution of V-notch fatigue sensor stress in the x-direction.

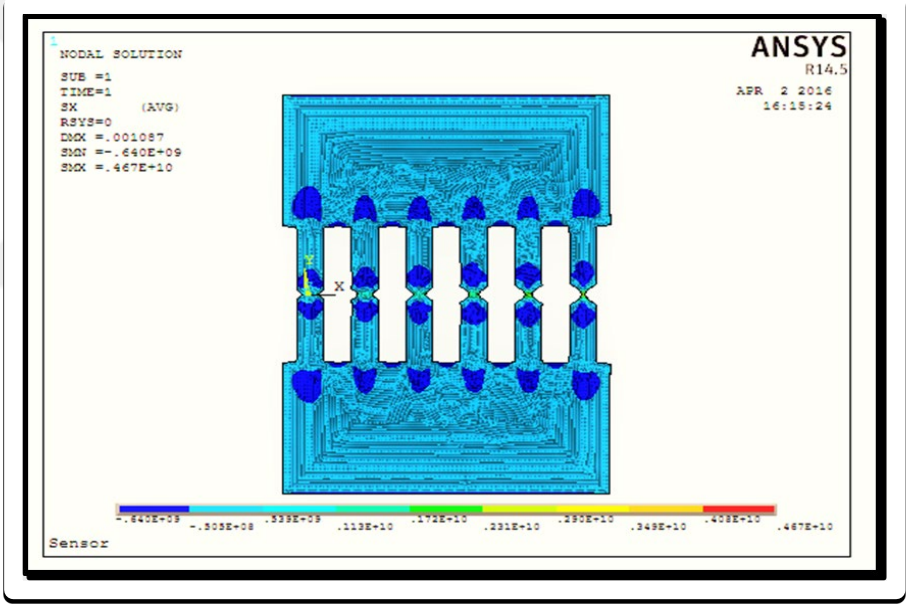

Figure 5.2. Nodal solution for V-notch fatigue sensor stress in the x-direction.

Stress concentration increases with increasing geometry, depth and angle. These two main parameters affect fatigue failure, shown in Figures 5.1 and 5.2 starting from Sensors Arm number 6 to Sensor Arm number 1 with different stresses termed as $SMN - SMX$ values starting from the values −0.130E+10 to 0.467E+10 and −0.640E+9 to 0.647E+10 Pa.

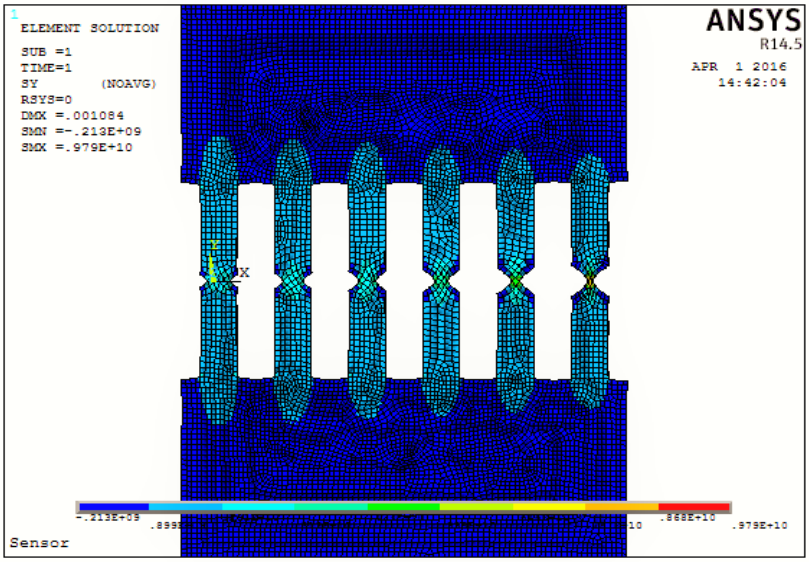

Figure 5.3. Element solution for V-notch fatigue sensor stress in the y-direction.

Figure 5.3 shows the deformation of material for six different sensors as V-shape, illustrated stress concentration in each sensor plate, focusing in the *y* direction starting with different stress values of −0.213E+09 to 0.979E+10 Pa (bridge monitoring sensors for monitoring structural integrity).

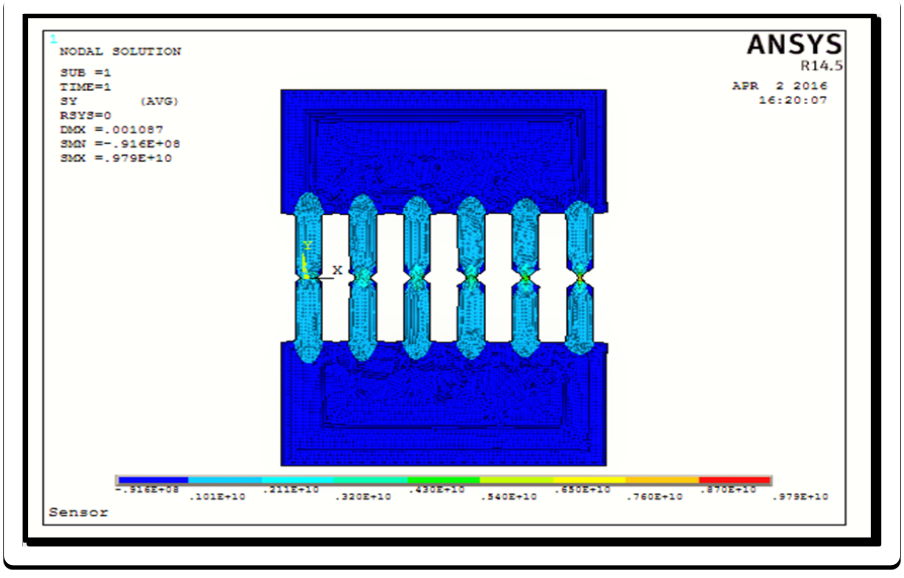

Figure 5.4. Nodal solution for V-notch fatigue sensor stress in the y-direction.

Furthermore, Figures 5.3 and 5.4 show minimum and maximum stress concentrations with element and nodal solutions. These are associated with describing the behavior of the geometry of every different arm sensor (plate) with different dimensions (depth and angle) in the y direction as SMN and SMX −0.213E+09 to 0.979E+10 and −0.916E+8 to 0.979E+10 Pa. All the data represent the stresses in the y direction, which is termed as S_y.

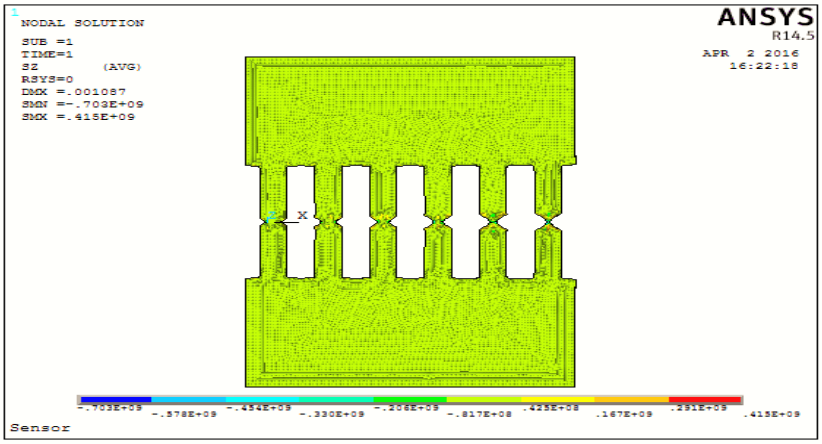

Figure 5.5. Nodal solution for V-notch fatigue sensor stress in the z direction.

Figure 5.5 shows the minimum and maximum stress concentrations, describing the behavior of geometry of every arm sensor with different dimensions related to depth and angle in the z direction as SMN & SMX −0.703E+09 to 0.415E+09. All of the data represent the stresses in the z direction, which is termed S_z, especially in the nodal solution.

5.1.1. Principle Stresses

5.1.1. 1. Element Solution of Principle Stresses

The procedure for improving the finite element model and the related information involving all dimensions and material features gained from built-shop drawings as well as actual field measurements create a standard unit system for data input as well as result output.

The shear tractions are frequently zero in a body with the principal stresses in three dimensions, which are tedious to estimate. The principle stress S_1 is a minimum stress value and principle stress S_2 is the maximum normal stress value, where all the stresses are a function of the angle.

5.1.1.2. Governing the Fatigue Failure Theory

The stress tensor (σ) assumes eigenvalues and eigenvectors. These eigenvalues are actually principal stresses which are numbered in descending order such as $\sigma_1 \geq \sigma_2 \geq \sigma_3$ to understand highest, average and low stresses, respectively. These values show the compressional stress magnitudes. $S_1 \geq S_2 \geq S_3$ are principal stresses. Eigenvector orientations are called the principal stress axes and orientation concerning principal stress, such as σ1, is termed the σ1-axis.

The principal stress planes are parallel to both stress axes or they are perpendicular to one of them. Deformation is anisotropic stress that is different from the principal stresses. The differential stress are as follows:

$$\Delta S = S_1 \_ S_3 \tag{5.1}$$

$$\Delta\sigma = \sigma_1 - \sigma_3 \tag{5.2}$$

Where S_1 = 0.103E+11 and S_2 = 0.469E+10, which means that S_1 is the minimum stress acting on the V-sensor shape. However, S_2 is the maximum principal stress acting on the same sensor, as shown in Figures 5.6 and 5.7 for element and nodal solutions.

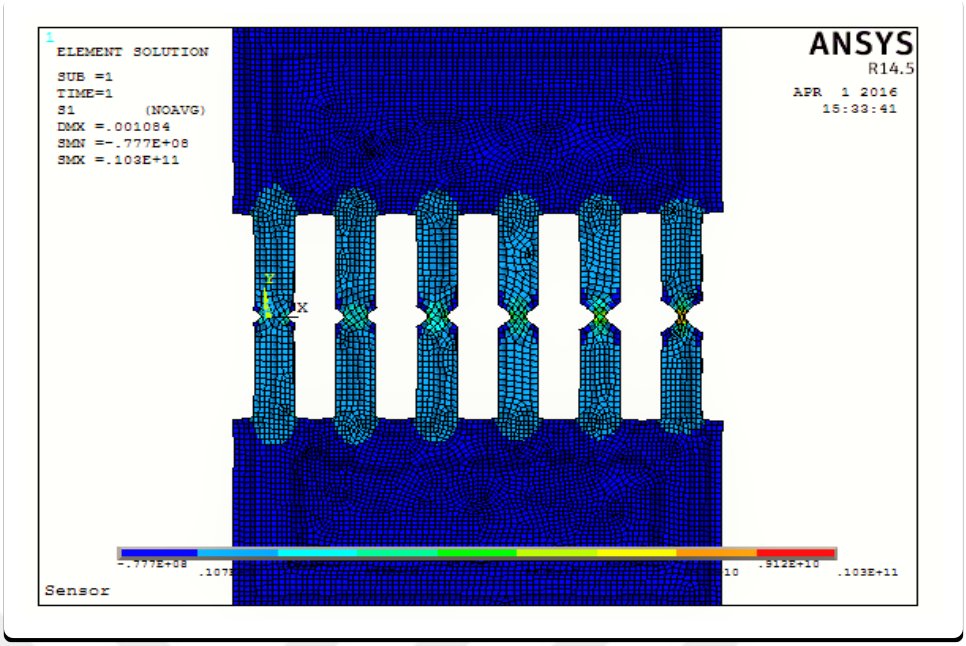

Figure 5.6. Element solution-Principle stresses S_1 for the V-notch fatigue sensor.

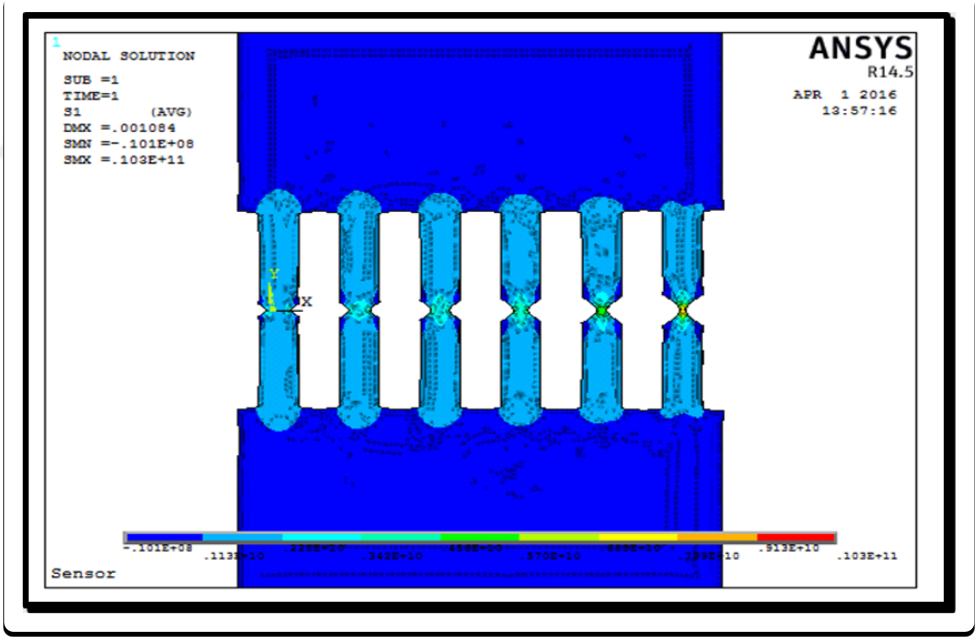

Figure 5.7. Nodal Solution-Principle Stress S_1 for the V-notch fatigue sensor.

Figure 5.8 shows the maximum principle stress in element solution S_2 acting on the fatigue sensor, which is illustrated with a value of 0.469E+10 MPa in the $X-$coordinated system, which is called SMX. Figure 5.9 shows the maximum

principle stress in nodal solution S_2 acting on the fatigue sensor, which is illustrated with a value of 0.408E+10 MPa in X-coordinated system.

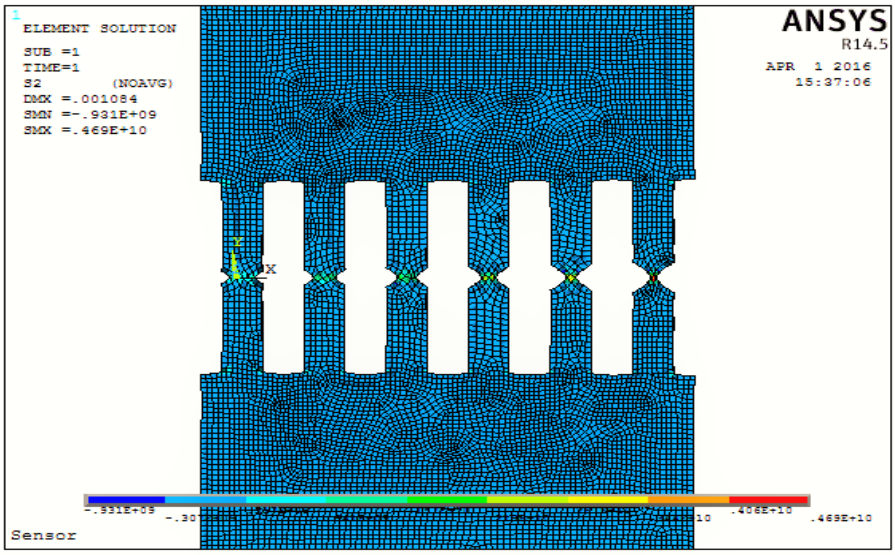

Figure 5.8. Element Solution-Principle Stress S_2 for the V-notched fatigue sensor.

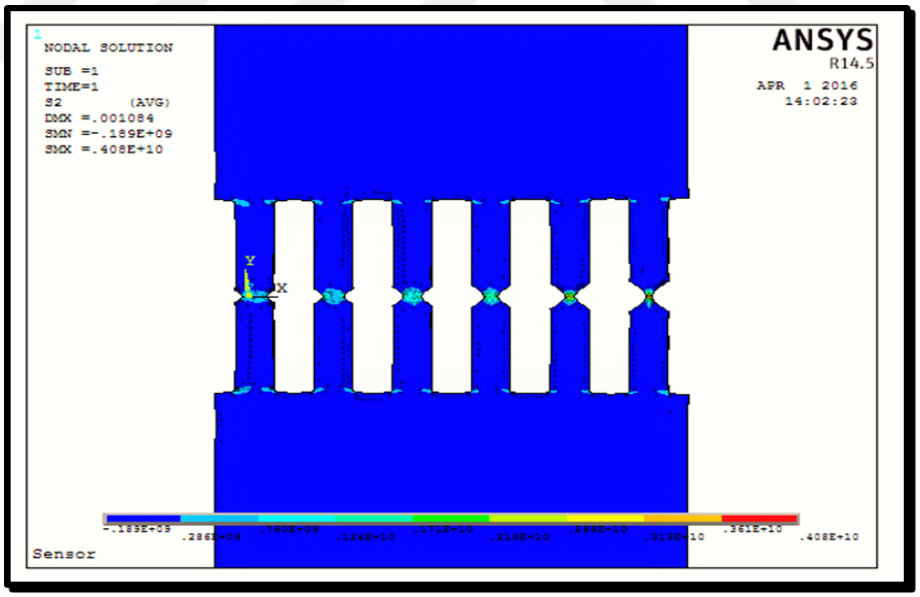

Figure 5.9. Nodal Solution of Principle Stress S_2 for the V-notched fatigue sensor.

5.1.1.3. Stress Intensity

The concept of stress intensity describes a stress field on a pointed crack/slit tip, so it is a popular topic in fracture mechanics. Here, it significantly extends into two directions. One is pointed V-notches and in this case, stress intensities depend on the angle of the notch opening.

In addition, the stress intensity factor (K) is also important in fracture mechanics because it helps in calculating the stress intensity near the crack tip, which occurs because of remote loads or residual stress. On the other hand, K has a magnitude based on simple geometry, location and crack size, the load magnitude and the modal distribution.

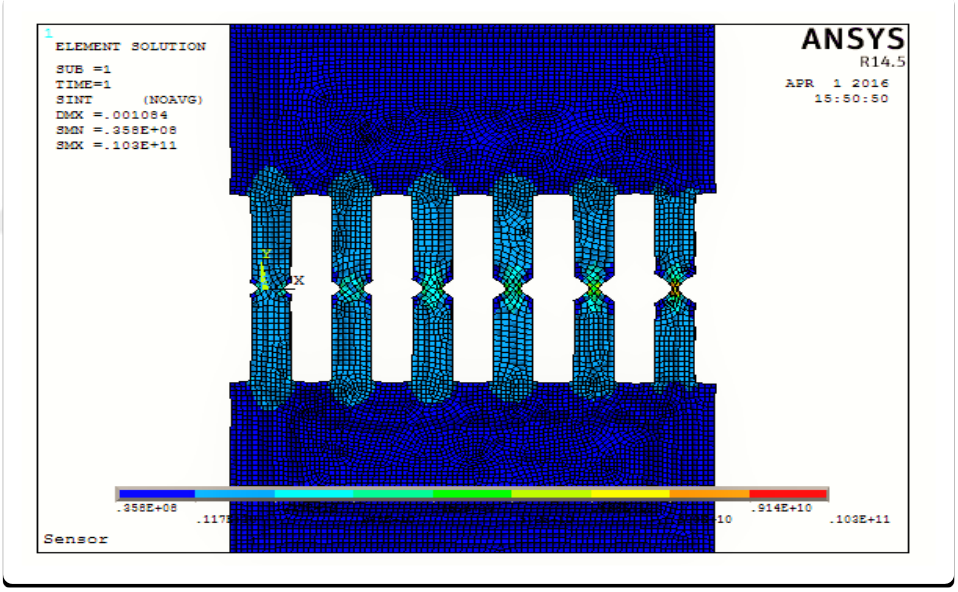

Figure 5.10. Element solution of stress intensity K for the V-notch fatigue sensor.

According to Figure 5.10 for the element solution of stress intensity in the X-direction of the six parallel beam fatigues on a V-notched sensor, the minimum stress value is 0.001084E+08 Pa, which is termed the SMN and the maximum value is 0.109E+11 Pa, which is termed SMX.

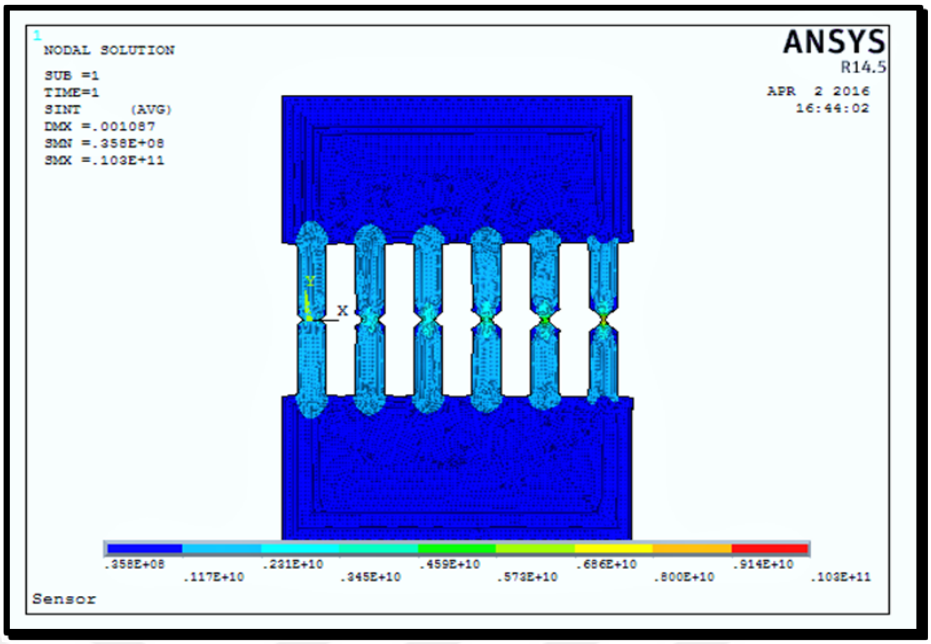

Figure 5.11. Nodal Solution of Stress Intensity K for the V-notched fatigue sensor.

5.2. Nodal Results

Tables 5.1 and 5.2 illustrate the minimum and maximum values of the principal stresses and stress intensities in addition to Von Mises stresses for different nodes along the beam sensors.

Table 5.1. Minimum values of S_1, S_2, S_3 SINT and SEQV in global coordinates.

Stress	$\mathbf{S_1}$	$\mathbf{S_2}$	$\mathbf{S_3}$	SINT	SEQV
NODE	17326	8287	17097	18428	18428
VALUE	−0.98594 E+07	−0.30615 E+09	−0.75508 E+09	0.33836 E+08	0.29331 E+08

Table 5.2. Minimum values of S_1, S_2, S_3 SINT and SEQV in global coordinates.

Stress	S_1	S_2	S_3	SINT	SEQV
NODE	17557	17557	17554	17557	17093
VALUE	0.92246 E+10	0.40052 E+10	0.26066 E+09	0.95773 E+10	0.83582 E+10

5.3. DISPLACEMENT OF THE NOTCH FATIGUE SENSOR

5.3.1. Nodal Solution Displacement

In general, displacement is highly affected only in the *y* direction. However, there is little displacement in the *x* direction, as shown in Figure 5.12, which shows a small value of *DMX* as 0.001084 mm with a minimum value *SMN* of −0.113E−03 mm and a maximum *SMX* value of 0.386E−03 mm.

This type of reading gives an indication that the effect of displacement in this direction is normal. On the other hand, the displacement is highly affected only in the *y* direction in a tension test, as shown in Figure 5.13 This is a high value as *DMX* is 0.001084 mm with a minimum value *SMN* of 0.001 mm and an *SMX* maximum value of 0.00 mm. This type of reading indicates that the effect of displacement in this direction is normal. Figure 5.14 shows us the displacement in the *z* direction with min and max readings of SMN at −0.219E-03 and SMX at 0.389E−03 mm, respectively.

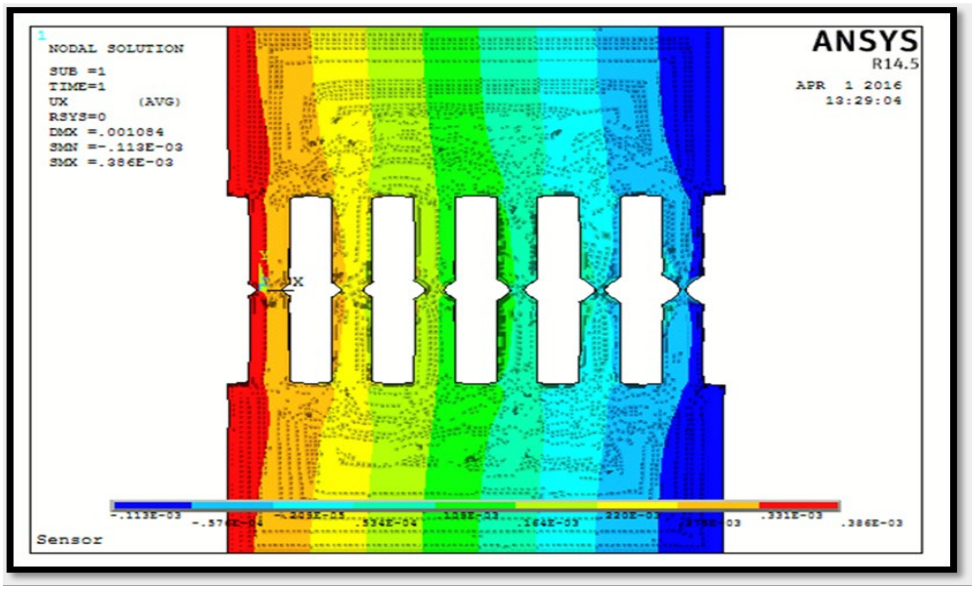

Figure 5.12. Nodal solution - horizontal displacement in the x direction of the V-notched fatigue sensor.

Figure 5.13 illustrates the sensor deformation in the *y* direction depending on the applied tension load in the same direction. There is symmetry between the upper half and the lower half. In addition, this is dependent on the V-notch parameters (angle orientation and notch depth), boundary conditions and the applied tension load on the sensor [104].

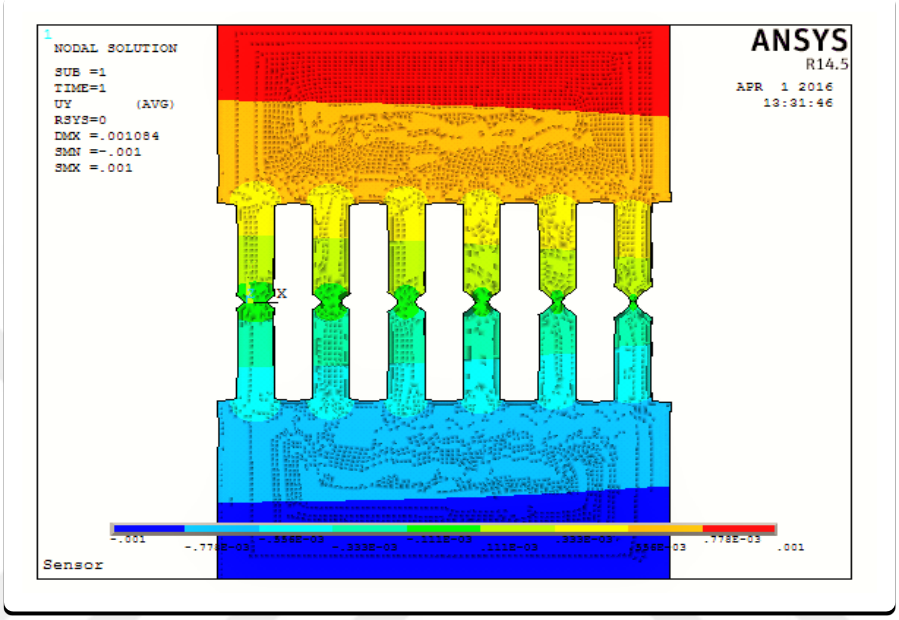

Figure 5.13. Nodal solution displacement in the y direction of the V-notch fatigue sensor.

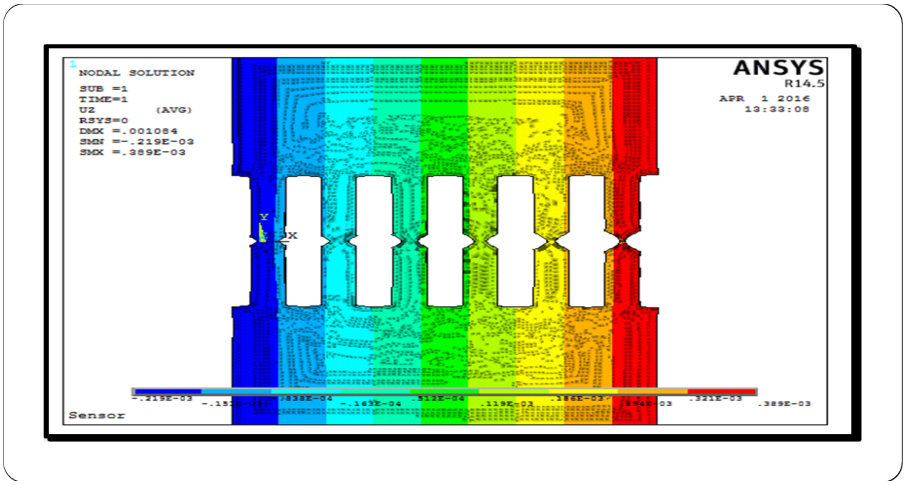

Figure 5.14. Nodal solution displacement in the z direction of the V-notch fatigue sensor.

5.4. VON MISES STRESS OF THE V-NOTCH SENSOR

There are a number of considerations before discussing Von Mises stress (VMS). Firstly, the main reason to use Von Mises stress is to determine the fatigue failure of V-notch sensors. Secondly, there is a correlation between VMS and the yield strength of steel used for sensors.

Generally, metal is claimed to begin yielding once its Von Mises stress reaches an important level referred to as its yield strength. Von Mises yields materials below a loading situation in a uniaxial tensile test. Additionally, Von Mises stress is widely utilized by designers to examine whether or not their design can bear a given load condition.

However, Von Mises stress is taken into account to be a secure haven for style engineers. Utilization of this data in nursing engineering can fail when the Von Mises stress within a material is too strong. It applies to many cases, particularly when metal is ductile. The following sections present the logic behind Von Mises stress and the reasons for its usage.

5.4.1. Results of Von Mises Stress

The higher quantities are connected with the theory of distortion, energy and failure; therefore, the conditions of failure are as follows:

In order to understand the relationship between them well, it is good to start with simplifying both. Von Mises stress helps us to discover material yields under any kind of loading condition through the outcomes of simple uniaxial tensile tests. A yield strength/point is at stress level, at which that material starts deforming plastically. Prior to the yield point, a material temporarily deforms and returns to its position when the stress is released.

The results are illustrated in Figure 5.15, which shows us the simulation of six parallel arm sensors and V-notches with different types of geometry. It starts with stress ranging from SMN = 0.0311E+8 Pa to SMX = 0.0912E+10 Pa. For the arm sensor number 6 to 1, comparing the yield strength of steel to that of ASTM-A36 used for designing a sensor, we have 250 MPa or 2.5E+08 Pa.

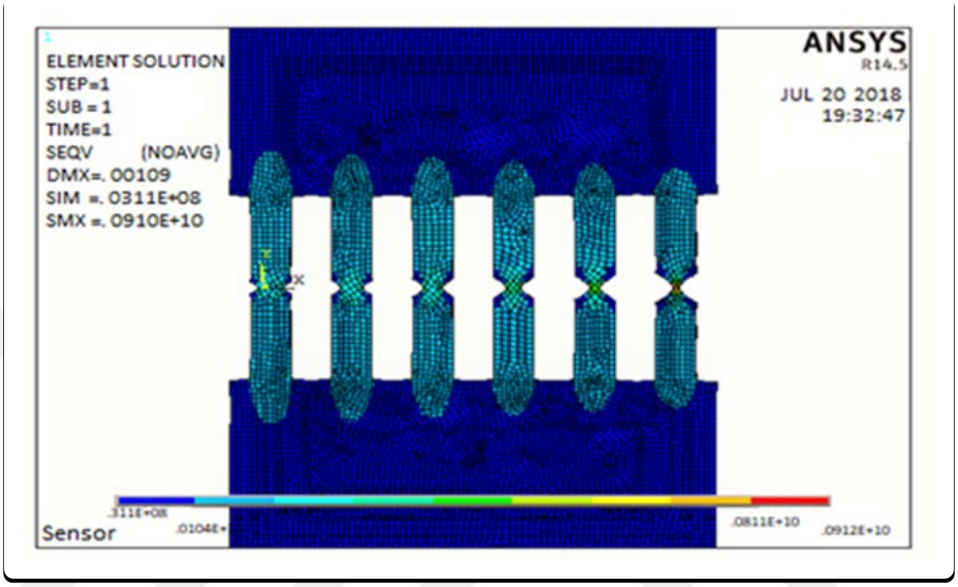

Figure 5.15. Distribution of Von – Mises stresses in the V-notch fatigue sensor.

The results of this analysis for the V-notch fatigue sensor in the Nodal Solution show the aspect ratio using isotropic materials; these were compared to the reference values. This comparison is presented in Table 5.3 below. We show a correlation of these results with Qasim Bader et al. (Effect of Stress Ratio and V-Notch Shape on Fatigue Life in Steel Beam) [9].

Table 5.3. Comparison of yield strengths for Steel A36 and Von-Mises stress with ref. [9].

Yield strength σ_y	Von-Mises stresses 1	Von-Mises stresses 2 (Ref. 2)
2.5E+8 Pa	0.0912E+10 Pa	5.953E+8 Pa

5.4.2. Comparison of Results of V.M Stresses for Six Beam Sensors

The main scope of the article using numerical solutions with ANSYS is to describe stress distribution based Von-Mises criteria. Von-Mises stress, also known as Huber stress, which accounts for six stress components of a general 3D stress state. Von-Mises stress is described with the following equation:

$$\sigma_{vm} = \sqrt{0.5[(\sigma_1 - \sigma_2)^2 + (\sigma_2 - \sigma_3)^2 + (\sigma_3 - \sigma_1)^2]} \quad (5.3)$$

The maximum Von-Mises stress failure criterion is based on the scalar-energy theory or the maximum distortion energy theory. The theory states that a ductile material starts to yield at a location when the Von-Mises stress becomes equal to the stress limit. In most cases, the yield strength is used as the stress limit. According to the Von-Mises failure criterion, the factor of safety (FOS) is expressed as:

$$\text{FOS} = \frac{\sigma_{Limit}}{\sigma_{vm}} \quad (5.4)$$

When the Von-Mises stress value of the sensor is less than the value of the yield strength of steel beam A36, which is 250 MPa, the structural design becomes safe. However, if the value of the Von-Mises stress is greater than the material's yield strength, the structural design is unsafe and failure will start at this point, as shown in Figure 5.16.

Table 5.4 illustrates the different results of Von Mises stress on ANSYS for six fatigue sensors with different geometries. They are gradually indicating the relationship between the yield strength of the material used for the sensor, which is A36 Steel and the Von Mises stress for every sensor arm as illustrated in Figure 5.5.

Table 5.4. Von-mises stress results in the sensors.

Sensor Beam.	1	2	3	4	5	6
V.M Stress (Pa)	0.031e +8	0.020e+10	0.040e+10	0.060e+10	0.071e+10	0.091e+10

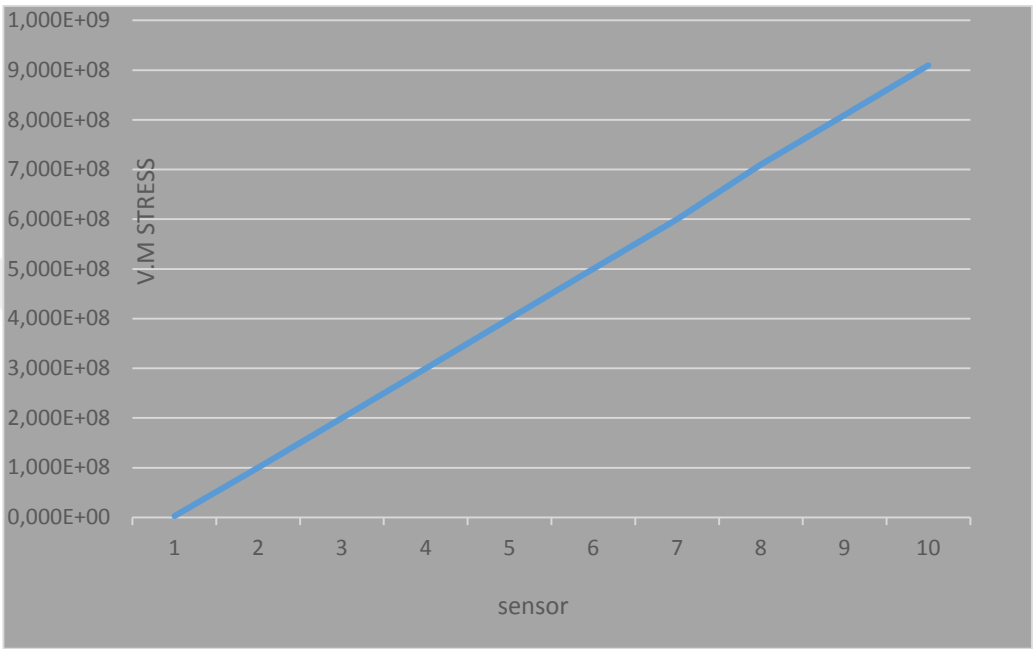

Figure 5.16. Distribution of Von – Mises stresses in beams attached to the fatigue sensor-nodal solution.

5.5. RESULTS OF DISPLACEMENT IN THE Y DIRECTION (Uy)

Table 5.5 below shows the relationship between vertical displacement in the y direction (Uy) as a result of the V-notch fatigue sensor in the nodal solution, and wisely adding a number of arm sensors, which results in a small decrease in the Von-Mises stress, as shown in Figure 5.5, and a displacement distribution, as illustrated in Figure 5.17.

Table 5.5. Effect of displacement changing the number of sensors.

No. of sensors	1	2	3	4	5	6
U_y (mm)	−0.01	−0.35E−02	−0.11E−03	−0.33E−03	−0.77E−02	0.01

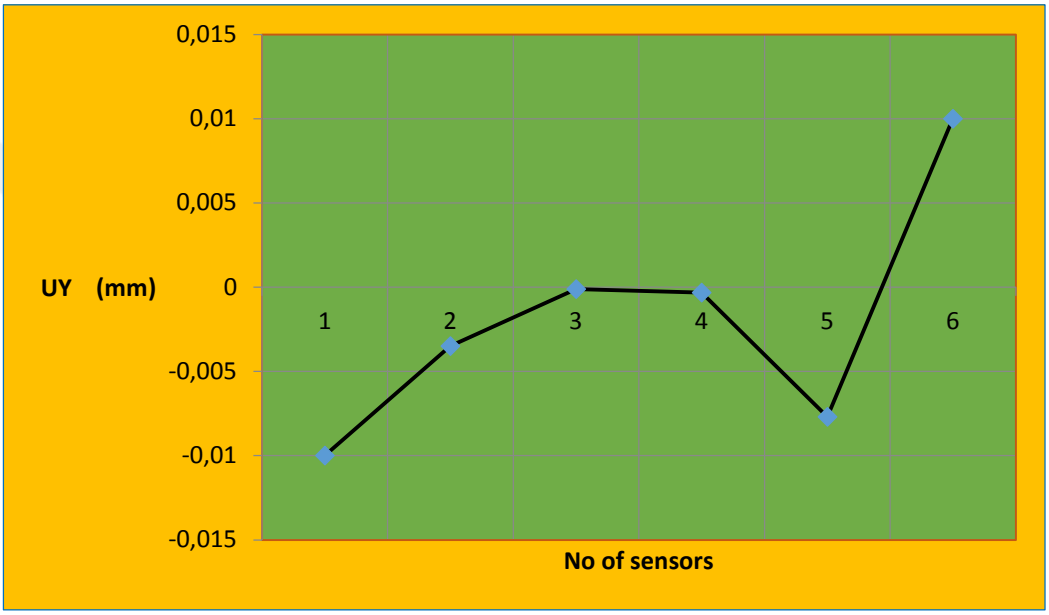

Figure 5.17. Change of the displacement effect in the sensors.

5.6. VON MISES STRESS RESULTS

The Von-Mises stress method serves as a safe process because design engineers found it helpful, and as shown in Figure 5.4 which is based on the given information, it can be predicted that the design is likely to fail when the maximum Von-Mises stress value is equal to or higher than the material's yield strength.

The greatest Von Mises stress among the six beams was found to be 0.0912E+10 Pa, which means that the first failure starts at this point due to the relationship between the yielding point and the Von Mises stress, indicating that the material transforms from the elastic region to the plastic region according to Hooks' Law.

$$F_1\sigma_1^2 + F_{22}\sigma_2^2 + F_{66}\sigma_6^2 + F_1\sigma_1 + F_2\sigma_2 + 2F_{12}\sigma_1\sigma_2 = 1 \quad (5.3)$$

Table 5.6. Safety factors for steel.

Steel Model	Von Mises Stress	Max allowable	FS
A36 Carbon Steel	12668 psi 0.0912e+10 Pa 1322744.168 psi	58000	4.58 0.0438

It can be noted that the Von Mises stress is highest on the fixed end of the beam. There, its value is 0.0912E+10 Pa, which changes to 9.12E+8 Pa. This is higher than the yield stress value of 250 MPa = 2.5E+8 Pa of carbon steel. The design can be considered unsafe, so engineers should maintain the Von Mises maximum stress value below the yield strength of the structure.

5.6.1. Sensor Deformation

As previously stated in the discussion of results for the fatigue sensor with the V-shaped A36 Carbon Steel Model, the displacement, as expected for the vertical and horizontal directions *x* and *y*, is based on the nature of the problem and how boundary conditions had been assigned. The vertical displacement is greatest at the V-shaped notch of the fatigue sensor towards the *y*-coordinate, as illustrated in Figures 5.12 and 5.13, which represent both analyses of displacement referred to as U_x and U_y.

5.6.2. Von Mises Stress on Beams

From the result of the first beam in Figure 5.18, it can be noted that they are increasing in displacement, which leads to an increase in the Von Mises stress to the maximum value. Nevertheless, the offset value lies in the range of 3.2e−2 mm. Then the value of the Von Mises stress after this point for up to 2142.977 MPa decreases. This can occur when the displacement value reaches 7.824e−2 mm. These results are related to

different geometrical V-notch parameters (angle orientation and notch depth), mechanical properties, boundary conditions and applied tension load.

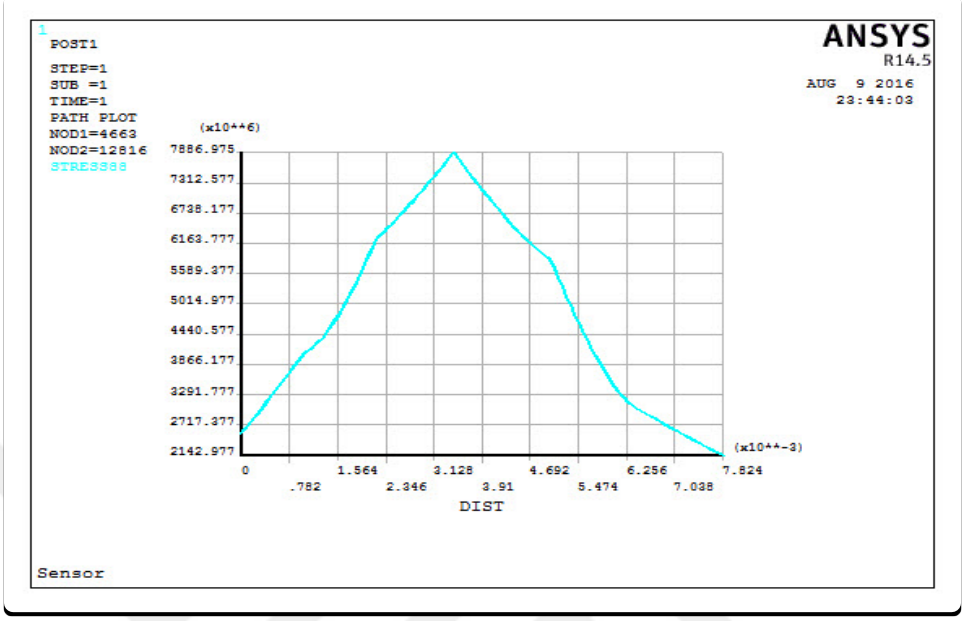

Figure 5.18. Von – Mises stress for beam 1.

In Figure 5.8, Beam 6 has lower Von Mises stress than Beam 1. According to this behavior, the failure starts on Beam 1 due to the different design geometries of the V-notch sensors. In other words, cracks on the edges are not very dangerous. The notch-opening angle provides minimum failure load that vanishes in cases of major notch depth. The findings of many researchers such as Gokanakonda et al. (2016) support this study.

However, in Figure 5.19 Beam 6 has regularly lower Von Mises stress than Beams 1-5 for the same reasons mentioned previously. Sensor mounting adjustment and a size downsizing with respect to the size of the present model sensor outline will also be necessary to attach to the structural details of the components where high-stress concentrations are possible. The findings of many researchers, such as Bader and Kadu (2014) in addition to the Von Mises stress results from the simulation of the V-notch sensor geometry agree with many research results.

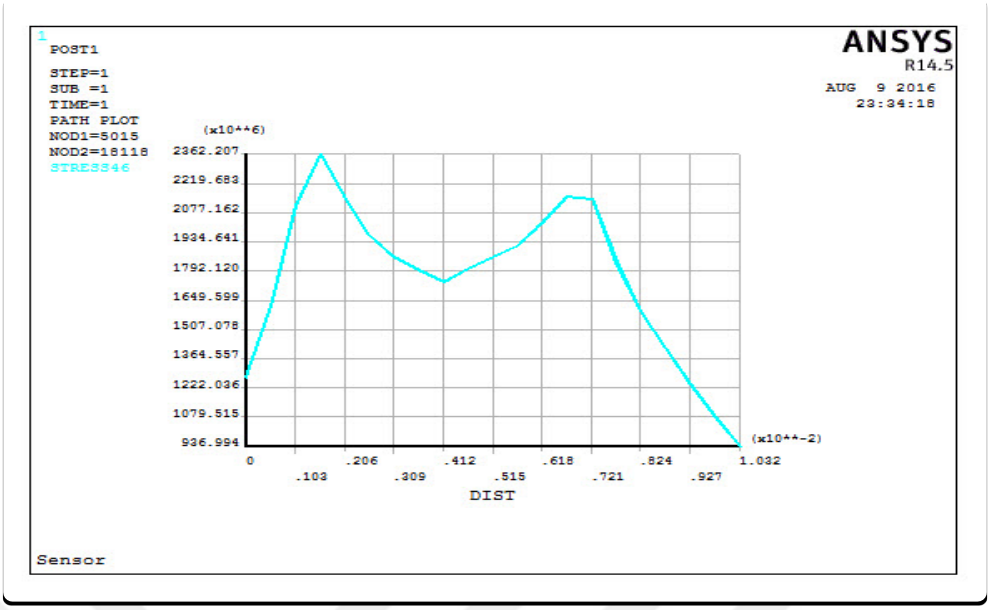

Figure 5.19. Von – Mises stress for beam 6.

Many of the studies have focused on the structural parts of bridges and they used low carbon steel as an application material. Here, we used a sensor with six beams each with a different V-notch depth with A-36 as the structural material. We used ANSYS mechanical APDL software to estimate the Von Mises stress of the fatigue sensor to provide information to engineers.

The contribution of this work to the science and technology surmised in the following items:

1. Load sensing.
2. Digitizing monitoring processes.
3. To increase efficiency, reduce costs.
4. Ensure workforce safety and match global standards.

5.7. CONCLUSION

From the numerical simulation results that we obtained from the ANSYS software, which represent different Von Mises stress values for the six beams of the sensors, it was revealed that the maximum Von Mises stress occurs on the beam that has greater depth than the other beams. This means that fatigue failure depends on the parameters of the V-notch (angle orientation and notch depth), mechanical properties, boundary conditions and applied tension. In addition, increasing the number of sensor arms can accommodate more notches, which possibly tends to lower stress ranges with a larger number of loading cycles.

It can be claimed that the simulation generated through fatigue-life analysis ANSYS software for a given specimen is usable to predict the fatigue-life of notched specimens. The obtained predictions are based on real stress developed at the notch tips. Based on numerical simulation outcomes, the following points can be concluded:

1. The ANSYS process based on the simulation of Von-Mises stress gives a good prediction of the notch effect.
2. The depth and position of the notch affect fatigue life.
3. The temperature variation at the fracture position provides a good prediction to find the position of the fracture before it occurs.
4. Stress analysis through ANSYS shows that the maximum stress value occurs in the vicinity of the change in cross section of the beam.

Based on the outcomes, Von - Mises stress increases with the notch depth of the beam. This means that the failure depends on the mechanical properties of the material, applied tension loads, boundary conditions and V-notch parameters, such as angle orientation and notch depth.

On the other hand, in composite bridges with welds connected with a series of vertical web stiffeners towards the top of the main girders, the rotation of the concrete deck

can induce fatigue cracks in the welds. Since all of them have residual stresses, both positive and negative rotations can add to the cumulative damage of the welds.

REFERENCES

[1] S. Beretta and P. Clerici, "Microcrack propagation and microstructural parameters of fatigue damage**,"** ***Fatigue & Fracture of Engineering Materials & Structures,*** vol. 19, pp. 1107-1115, (1996).

[2] K. Miller and M. Ibrahim, "Damage accumulation during initiation and short crack growth regimes**,"** ***Fatigue & Fracture of Engineering Materials & Structures,*** vol. 4, pp. 263-277, (1981).

[3] I. C. Cuthill and A. T. Bennett, "Mimicry and the eye of the beholder**,"** ***Proc. R. Soc. Lond. B,*** vol. 253, pp. 203-204, (1993).

[4] A. L. Gama and S. R. K. Morikawa, "Monitoring Fatigue Crack Growth in Fracture Mechanics Specimens with Piezoelectric Sensors," **in** ***Materials Science Forum***, (2013), pp. 83-88.

[5] K. James, "Signal Conditioning Piezoelectric Sensors," ***Application Report SLoA033A. Texas Instruments,*** (2000).

[6] R. Song, W. Dietzel, B. Zhang, W. Liu, M. Tseng, and A. Atrens, "Stress corrosion cracking and hydrogen embrittlement of an Al–Zn–Mg–Cu alloy," ***Acta Materialia,*** vol. 52, pp. 4727-4743, (2004).

[7] C. Boller and N. Meyendorf, "State-of-the-art in Structural Health monitoring for aeronautics," **in** ***Proceedings of the International Symposium on NDT in Aerospace*****,** (2008).

[8] W. H. Duan, Q. Wang, and S. T. Quek, "Applications of piezoelectric materials in structural health monitoring and repair: ***Selected research examples," Materials,*** vol. 3, pp. 5169-5194, (2010).

[9] Q. Bader and E. K. Njim, "Effect of stress ratio and v notch shape on fatigue life in steel beam**,"** ***International Journal of Scientific & Engineering Research,*** vol. 5, pp. 1145-1154, (2014).

[10] O. Fadare, A. Okoronkwo, and E. Olasehinde, "Assessment of anti-corrosion potentials of extract of Ficus asperifolia-Miq (Moraceae) on mild steel in acidic medium**,"** ***African Journal of Pure and Applied Chemistry,*** vol. 10, pp. 8-22, (2016).

[11] R. Baldwin, R. Forslid, P. Martin, G. Ottaviano, and F. Robert-Nicoud, ***Economic geography and public policy***: Princeton University Press, 2011.

[12] M. H. Hodge, "Structural monitoring sensor system," ed: ***Google Patents,*** (2000).

[13] K. Rutherford, J. Parkhill, J. Crook, T. Horsnell, P. Rice, M.-A. Rajandream*, et al.*, "Artemis: sequence visualization and annotation**,"** ***Bioinformatics,*** vol. 16, pp. 944-945, (2000).

[14] L. Yu, S. Momeni, V. Godinez, V. Giurgiutiu, P. Ziehl, and J. Yu, "Dual mode sensing with low-profile piezoelectric thin wafer sensors for steel bridge crack detection and diagnosis**,"** ***Advances in civil Engineering****,* vol. 2012, (2011).

[15] B. P. Wijesinghe, S. A. Zacharie, K. D. Mish, and J. D. Baldwin, "Design and development of in situ fatigue sensors for structural health monitoring of highway bridges**,"** ***Journal of Bridge Engineering****,* vol. 18, pp. 297-307, (2011).

[16] A. Carpinteri, P. Cornetti, N. Pugno, and A. Sapora, "On the most dangerous V-notch**,"** ***International Journal of Solids and Structures****,* vol. 47, pp. 887-893, (2010).

[17] B. Glišić, Y. Yao, S.-T. E. Tung, S. Wagner, J. C. Sturm, and N. Verma, "Strain Sensing Sheets for Structural Health Monitoring Based on Large-Area Electronics and Integrated Circuits," ***Proceedings of the IEEE****,* vol. 104, pp. 1513-1528, (2016).

[18] C. Varsakelis and M. V. Papalexandris, "Numerical simulation of unsteady chute flows of two-phase granular mixtures," ***Bulletin of the American Physical Society,*** vol. 58, (2013).

[19] E. Koston, "Fatigue crack monitoring in multi-layered aircraft structures using guided ultrasonic waves," UCL (University College London), (2010).

[20] S. Ignatovich, A. Menou, M. Karuskevich, and P. Maruschak, "Fatigue damage and sensor development for aircraft structural health monitoring," ***Theoretical and Applied Fracture Mechanics****,* vol. 65, pp. 23-27, (2013).

[21] S. LeClair and A. Jackson, "Work Unit Directive (WUD54) Amendment-Materials Process Design," ***Wright Lab Wright-Patterson Afb Oh Materials Directorate*** (1996)**.**

[22] S. Suresh, ***Fatigue of materials***: Cambridge university press, (1998).

[23] M. Balda, "Identification of low cycle fatigue parameters," ***Applied and Computational Mechanics,*** vol. 3, (2010).

[24] P. S. Veers, T. D. Ashwill, H. J. Sutherland, D. L. Laird, D. W. Lobitz, D. A. Griffin*, et al.*, "Trends in the design, manufacture and evaluation of wind turbine blades," ***Wind Energy****,* vol. 6, pp. 245-259, (2003).

[25] C. C. Ciang, J.-R. Lee, and H.-J. Bang, "Structural health monitoring for a wind turbine system: a review of damage detection methods," ***Measurement Science and Technology,*** vol. 19, p. 122001, (2008).

[26] A. Khan and S. Zafar, "Structural health monitoring: trends, challenges and recent advancement in aerospace," **in *Conference Paper*,** (2014).

[27] R. A. Hardin and C. Beckermann, "Prediction of the fatigue life of cast steel containing shrinkage porosity," ***Metallurgical and Materials Transactions*** *A,* vol. 40, p. 581, (2009).

[28] R. Haghani, M. Al-Emrani, and M. Heshmati, ***"Fatigue-prone details in steel bridges," Buildings,*** vol. 2, pp. 456-476, (2012).

[29] M. Al-Emrani and R. Kliger, "Fatigue prone details in steel bridges," **in *Nordic Steel Construction Conference***, (2009).

[30] I. Smith, E. Landis, and M. Gong, ***Fracture and fatigue in wood***: John Wiley & Sons, (2003).

[31] K. Reifsnider, "Fatigue behavior of composite materials," ***International Journal of Fracture,*** vol. 16, pp. 563-583, (1980).

[32] Z. Su and L. Ye, *Identification of damage using Lamb waves:* ***from fundamentals to applications*** vol. 48: Springer Science & Business Media, (2009).

[33] K. Kuang, W. Cantwell, and C. Thomas, "Crack detection and vertical deflection monitoring in concrete beams using plastic optical fibre sensors," ***Measurement Science and Technology,*** vol. 14, p. 205, (2003).

[34] B. M. Phares, "The Electrochemical Fatigue Sensor: A Novel Sensor for Active Fatigue Crack Detection and Characterization Material Technologies," **in *International Conference on Structural Health Monitoring & Intelligent Infrastructure*,** Ankeny, IA USA, (2007), p. 126.

[35] H. Kaplan and T. Ozkul, "A novel smart fatigue damage sensor for structural health monitoring of critical components of structures," in *Industrial Informatics and Computer Systems (CIICS),* (*2016*)***International Conference on*,** 2016, pp. 1-5.

[36] Z. A. Chaudhry, T. Joseph, F. P. Sun, and C. A. Rogers, "Local-area health monitoring of aircraft via piezoelectric actuator/sensor patches," **in *Smart Structures & Materials' 95***, (1995), pp. 268-276.

[37] J. D. Baldwin, P. Wijesinghe, S. ZACHARIE, and K. D. Mish, "***Development of an In Situ Fatigue Sensor***," (2011).

[38] M. Enckell, "***Lessons learned in structural health monitoring of bridges using advanced sensor technology***," (2011).

[39] T. Ozkul, H. Kaplan, and M. Dolen, "Wireless enabled fatigue sensor for structural health monitoring," ed: ***Google Patents***, (2014).

[40] S. Gokanakonda, M. K. Ghantasala, and D. Kujawski, "Fatigue sensor for structural health monitoring: Design, fabrication and experimental testing of a prototype sensor," ***Structural Control and Health Monitoring,*** vol. 23, pp. 237-251, (2016).

[41] G. Majzoobi and N. Daemi, "The effects of notch geometry on fatigue life using notch sensitivity factor," ***Transactions of the Indian Institute of Metals,*** vol. 63, pp. 547-552, (2010).

[42] C. P. Townsend and S. W. Arms, "System for remote powering and communication with a network of addressable, multichannel sensing modules," ed: ***Google Patents***, (2003).

[43] H. W. Smith, "Fatigue damage indicator," ed: ***Google Patents***, (1976).

[44] W. Wu, H. Liou, and H. Tse, "Estimation of fatigue damage and fatigue life of components under random loading," ***International journal of pressure vessels and piping,*** vol. 72, pp. 243-249, (1997).

[45] G. Mesmacque, S. Garcia, A. Amrouche, and C. Rubio-Gonzalez, "Sequential law in multiaxial fatigue, a new damage indicator," ***International Journal of Fatigue,*** vol. 27, pp. 461-467, (2005).

[46] B. Pyttel, D. Schwerdt, and C. Berger, "Very high cycle fatigue–is there a fatigue limit?," ***International Journal of fatigue,*** vol. 33, pp. 49-58, (2011).

[47] J. M. Papazian, J. Nardiello, R. P. Silberstein, G. Welsh, D. Grundy, C. Craven, *et al.*, "Sensors for monitoring early stage fatigue cracking," ***International journal of fatigue,*** vol. 29, pp. 1668-1680, (2007).

[48] Q. Lei, Y. Shenfang, W. Qiang, S. Yajie, and Y. Weiwei, "Design and experiment of PZT network-based structural health monitoring scanning system," ***Chinese Journal of Aeronautics,*** vol. 22, pp. 505-512, (2009).

[49] R. O. Ritchie, "Mechanisms of fatigue-crack propagation in ductile and brittle solids," ***International Journal of Fracture,*** vol. 100, pp. 55-83, (1999).

[50] R. I. Stephens, A. Fatemi, R. R. Stephens, and H. O. Fuchs, ***Metal fatigue in engineering***: John Wiley & Sons, (2000).

[51] P. TEED, "III. FATIGUE," ***Journal of the Royal Society of Arts,*** vol. 103, pp. 503-524, (1955).

[52] A. Wohler, "Wohler's Experiments on the Strength of Metals," ***Engineering,*** vol. 4, pp. 160-161, (1867).

[53] J. M. Naser and F. Serrano Toledano, "***Analysis of vibration-induced fatique cracking in steel bridges***," (2011).

[54] R. L. Norton, "***Machine design***: an integrated approach, 1996," ed: Prentice-Hall Inc: NJ, USA, (1996).

[55] J. E. Shigley, ***Shigley's mechanical engineering design***: Tata McGraw-Hill Education, (2011).

[56] L. Pook, ***Why Metal Fatigue Matters***: Springer, (2007).

[57] S. Gokanakonda, ***Fabrication, testing and analysis of a fatigue sensor for structural health monitoring*:** Western Michigan University, (2014).

[58] A. Niesłony, "Determination of fragments of multiaxial service loading strongly influencing the fatigue of machine components," ***Mechanical Systems and Signal Processing,*** vol. 23, pp. 2712-2721, (2009).

[59] S. Chandrasekaran, "***Course Contents."***

[60] G. Kirsch, "Die theorie der eiastizi~ t und die bed/irfnisse der festigkeislehre," ***Zantralblatt Verlin Deutscher Ingenieure,*** pp. 42-1898, (1898).

[61] H. J. Grover, "Fatigue of aircraft structures," ***Battelle Memorial Inst Columbus Oh***(1966).

[62] K. C. Creager, L. Y. Chiao, J. P. Winchester, and E. R. Engdahl, "Membrane strain rates in the subducting plate beneath South America," ***Geophysical research letters,*** vol. 22, pp. 2321-2324, (1995).

[63] A. Abass, "***Fatigue Failure And Testing Methods***," (2013).

[64] T. Li, J. Morris Jr, N. Nagasako, S. Kuramoto, and D. Chrzan, "'Ideal" engineering alloys," ***Physical review letters,*** vol. 98, p. 105503, (2007).

[65] H. F. HO and R. Stephens, "***Metal fatigue in engineering***," ed: John Wiley & Sons, New York, (1980).

[66] H. Zenner and K. Hinkelmann, "Fatigue of components–August Wöhler (1819–1914)," *DVM–**Special Publication,*** vol. 220, p. 13, (2017).

[67] A. Milton, "Miner: Cumulative damage in fatigue Journal of Appl," ed: Mech, (1945).

[68] D. W. Whitley, "***Interacting stress concentration factors and their effect on fatigue of metallic aerostructures***," (2013).

[69] E. N. Farsangi, "Connections behaviour in precast concrete structures due to seismic loading," ***Gazi University Journal of Science,*** vol. 23, pp. 315-325, (2010).

[70] R. H. Falen, "***Effect of stress concentrations on fatigue of composite and metallic structure***s," (2014).

[71] M. S. Duraisivam and E. Jamuna, "***Development and Fabrication of Bagasse & Palmyra Fibers Reinforced Epoxy Composite Material Spur Gear for Sugar Cane Juice Machine."***

[72] C.-C. Chu, "Comparison of mean stress correction methods for fatigue life prediction," ***SAE Technical Paper*** 0148-7191, (2000).

[73] J. Kruzic, D. Kim, K. Koester, and R. Ritchie, "Indentation techniques for evaluating the fracture toughness of biomaterials and hard tissues," ***Journal of the mechanical behavior of biomedical materials,*** vol. 2, pp. 384-395, ()2009.

[74] D. Duman, "Titanyum Talaşından Titanyum Karbür Üretimi Ve Sert Metal Üretiminde Kullanımı," ***Fen Bilimleri Enstitüsü***, (2010).

[75] M. A. Maleque and M. S. Salit, ***Materials selection and design***: Springer, (2013).

[76] J. H. Fendler, ***Membrane mimetic chemistry: characterizations and applications of micelles, microemulsions, monolayers, bilayers, vesicles, host-guest systems, and polyions*****:** John Wiley & Sons Inc, (1982).

[77] Z. N. Haji, "Low cycle fatigue behavior of aluminum alloys AA2024-T6 and AA7020-T6," ***Diyala Journal of Engineering Sciences,*** pp. 127-137, (2010).

[78] S. Bhat and R. Patibandla, ***Metal fatigue and basic theoretical models: a review*****:** INTECH Open Access Publisher, (2011).

[79] S. Subramanya and M. A. Prasad, "MEMS and MEMS based strain gauge load cells—A review," **in** ***Research & Technology in the Coming Decades (CRT 2013), National Conference on Challenges in***, (2013), pp. 1-6.

[80] H. Patni, C. Henson, and A. Sheth, "Linked sensor data," in *Collaborative Technologies and Systems (CTS), 2010* ***International Symposium on***, (2010), pp. 362-370.

[81] A. Nwosu and V. Eke, "Fundamentals and Applications of Transducers Technology and Sensors in Measuring Methodology," ***International Journal of Scientific Engineering and Technology,*** vol. 4, (2015).

[82] Y. Yao and B. Glisic, "Detection of steel fatigue cracks with strain sensing sheets based on large area electronics," ***Sensors,*** vol. 15, pp. 8088-8108, (2015).

[83] D. P. Henkel, "Remote and powerless miniature fatigue monitor and method," ed: ***Google Patents***, (1996).

[84] N. Crites and S. Chambers, "Indicating coating for locating fatigue cracks," ed: ***Google Patents***, (1974).

[85] R. Fussinger, "Apparatus for monitoring the fatigue strength of structures," ed: ***Google Patents***, (1996).

[86] M. A. Brull, "Method of making a device for monitoring fatigue life," ed: ***Google Patents***, (1987).

[87] M. Creager, "Device for monitoring the fatigue life of a structural member and a method of making same," ed: ***Google Patents***, (1995).

[88] Y. W. Kwon, "Fatigue measurement device and method," ed: ***Google Patents***, (2006).

[89] J. Sirohi and I. Chopra, "Fundamental understanding of piezoelectric strain sensors," ***Journal of intelligent material systems and structures,*** vol. 11, pp. 246-257, (2000).

[90] J.-B. Ihn and F.-K. Chang, "Detection and monitoring of hidden fatigue crack growth using a built-in piezoelectric sensor/actuator network: I. Diagnostics," ***Smart materials and structures,*** vol. 13, p. 609, (2004).

[91] G. Park, H. H. Cudney, and D. J. Inman, "Impedance-based health monitoring of civil structural components," ***Journal of infrastructure systems,*** vol. 6, pp. 153-160, (2000).

[92] Y. Zhang, "In situ fatigue crack detection using piezoelectric paint sensor," ***Journal of Intelligent Material Systems and Structures,*** vol. 17, pp. 843-852, (2006).

[93] M. Moore, B. M. Phares, B. Graybeal, D. Rolander, and G. Washer, "Reliability of visual inspection for highway bridges, volume I," (2001).

[94] N. Goldfine, V. Zilberstein, A. Washabaugh, V. Weiss, and D. Grundy, "The use of fatigue monitoring MWM-Arrays in production of NDI standards with real fatigue cracks for reliability studies," **in** ***16th world conference on nondestructive testing, Montreal, Canada***, (2004).

[95] B. Mi, J. E. Michaels, and T. E. Michaels, "An ultrasonic method for dynamic monitoring of fatigue crack initiation and growth," ***The Journal of the Acoustical Society of America,*** vol. 119, pp. 74-85, (2006).

[96] M. Kuroda, S. Yamanaka, K. Yamada, and Y. Isobe, "Detection of plastic deformation and fatigue damage in pressure vessel steel by leakage magnetic flux sensors," ***Journal of the Society of Materials Science, Japan****,* vol. 50, pp. 213-218, (2001).

[97] C. R. Farrar and K. Worden, "An introduction to structural health monitoring," ***Philosophical Transactions of the Royal Society of London A: Mathematical, Physical and Engineering Sciences****,* vol. 365, pp. 303-315, (2007).

[98] B. Glisic, J. Chen, and D. Hubbell, "Streicker Bridge: A comparison between Bragg-grating long-gauge strain and temperature sensors and Brillouin scattering-based distributed strain and temperature sensors," **in** ***Sensors and Smart Structures Technologies for Civil, Mechanical, and Aerospace Systems*** (2011), p. 79812C.

[99] N. S. Gokhale, *Practical finite element analysis*: Finite to infinite, 2008.

[100] G. Tsinker, ***Handbook of port and harbor engineering: geotechnical and structural aspects***: Springer, (2014).

[101] D. A. Hancq, "Fatigue analysis using Ansys," ***ANSYS inc,(*** 2003).

[102] R. W. Beegle, R. W. Brocato, and R. W. Grant, "IMEMS accelerometer testing-test laboratory development and usage," **in** ***Test Conference, 1999. Proceedings. International***, (1999), pp. 338-347.

[103] G. Faltin, *Kopf schlägt Kapital:* ***Die ganz andere Art, ein Unternehmen zu gründen-Von der Lust, ein Entrepreneur zu sein***: Carl Hanser Verlag GmbH Co KG, (2012).

[104] X. Li, "***Fatigue Failure Evaluation of Tie Plates due to Secondary Deformations on Steel Plate Girder Bridges***," (2012).

[105] Q. M. Doos, M. J. Jweeg, and S. D. Ridha, "Analysis of friction stir welds. Part I: Transient thermal simulation using moving heat source," ***Alnahrain Journal for Engineering Sciences****,* vol. 11, pp. 429-437, (2008).

RESUME

Ahmed Elbarouni Hadyia was born in Tripoli, Libya in 1964 where he accomplished his elementary education. He completed high school education in Suk aljmaa High School, after that, he started the undergraduate program at Bright Star University, Department of Metallurgical And Material Engineering in 1985. In 1994, he started assignment as a Research Assistant at Strathclyde University, Department of Metallurgical And Material Engineering to complete M.Sc.degree. Later, He moved to Karabük University, where he has been still working as a Ph.D. student.

In addition to his academic career, he has gained substantial experience while working for Misrata complex steel plant as the supervisor in factory TS-4, Tripoli research development center as the material inspector (welding, material selection and heat treatment), the Higher Institute of Comprehensive Careers Azizia, Libya.

CONTACT INFORMATION

Address : Karabük University
Graduate School of Natural & Applied Science
E-mail : ahmed.barouni@yahoo.com